An-Najah National University

Faculty of Graduate Studies

SYNTHESIS OF CARBON NANODOTS FROM VARIOUS TYPES OF SUGARS FOR BIOMEDICAL APPLICATIONS

By

Samah Gazi Qassim

Supervisors

Dr. Mohyeddin Assali

Dr. Shadi Sawalha

This Thesis is Submitted in Partial Fulfillment of the Requirements for the Degree of Master of Pharmaceutical Sciences, Faculty of Graduate Studies, An-Najah National University, Nablus - Palestine.

2025

SYNTHESIS OF CARBON NANODOTS FROM VARIOUS TYPES OF SUGARS FOR BIOMEDICAL APPLICATIONS

By

Samah Gazi Qassim

This Thesis was Defended Successfully on 26/05/2025 and approved by

Dr. Mohyeddin Assali	
Supervisor	Signature
Dr. Shadi sawalha	
Co-Supervisor	Signature
Dr. Sami Makharza	
External Examiner	Signature
Dr. Mohamed Hawash	
Internal Examiner	Signature

Dedication

I dedicate this dissertation to Allah Almighty, my source of strength, inspiration, wisdom, and knowledge.

To my beloved mother, the most affectionate person in the world, who is encouraging, helping, and strengthening me to fight hard to make my dreams come true. Mom I will always wish God give you good health.

To my lovely father, the source of power and support who raised me until I became what I am today.

To the other half of my heart, my beloved husband Dr. Wajdi Sharif, your support, encouragement, enthusiasm, love and understanding are the secret of my success, and you are the greatest gift of my life.

To my soul, my children Hadi, Sarah and Celia, you will always be my hope, purity and all of the beautiful things in this world.

To my lovely brothers Dr. Shadi and Alaa, for being beside me and supporting me.

For the soul of my dear brother Abd. You were always there for me—supporting, encouraging, and taking pride in my achievements. Your greatest wish was to see me fulfill my dreams, and now, I am about to achieve one of my biggest dreams. But sadly, it will be without you by my side.

To my husband's family for their everlasting support and help.

I dedicate my thesis with big love.

Samah

Acknowledgements

Primarily, I am thankful to the holy god for giving me the strength, ability, and patience to successfully complete this prestigious research.

Secondly, my deepest appreciation & thanks to those who have the utmost credit, my dear supervisors, Dr. Mohyeddin Assali and Dr. Shadi Sawalha for everything I learned from their valuable experience during these years, and the memories that will last forever.

I would also like to thank the respectful examination committee, who critiqued my thesis, offered insightful comments and suggestions, and provided valuable feedback.

Moreover, thanks go to the laboratory staff at the Pharmacy, Sciences, and Medicine faculties for their endless assistance and support.

Let me also share my heartwarming thanks to my friends and colleagues. Thanks to their guidance, support, and the most joyful memories we shared, I reached this milestone moment in my life.

Finally, and most importantly, no words can describe my happiness in making my family proud. I will never forget the love, support, and gratitude they have given me throughout my years of study and research.

Declaration

I, the undersigned, declare that I submitted the thesis entitled:

SYNTHESIS OF CARBON NANODOTS FROM VARIOUS TYPES OF SUGARS FOR BIOMEDICAL APPLICATIONS

I declare that the work provided in this thesis, unless otherwise referenced, is the researcher's own work, and has not been submitted elsewhere for any other degree or qualification.

Student's Name: **Samah Gazi Qassim**

Signature: 

Date: **26/05/2025**

List of Contents

List of Tables

List of Figures

List of Schemes

SYNTHESIS OF CARBON NANODOTS FROM VARIOUS TYPES OF SUGARS FOR BIOMEDICAL APPLICATIONS

By
Samah Gazi Qassim
Supervisors
Dr. Mohyeddin Assali Main
Dr. Shadi Sawalha

Abstract

In the world, cancer ranks second among the leading causes of death, prompting the exploration of various treatment methods such as chemotherapy with or without radiation and surgery, as well as biological and gene therapy. Due to the significant side effects of traditional therapies, alternative treatments are in high demand. Modern medical research has turned to nanotechnology, particularly nanoparticles ranging from 1–100 nanometers, to develop new cancer therapies. Carbon nanodots (CNDs) are highlighted for their unique physical, chemical, electrical, mechanical, and optical properties, making them a promising option in cancer treatment.

This project aimed to employ a green and simple hydrothermal route as a bottom-up approach to producing carbon nanodots from various types of sugars (glucose, galactose, fructose, sucrose, lactose, and maltose). The synthesis process is achieved by carbonizing the sugars in an autoclave at 200 °C for 24 hours.

The prepared CNDs were characterized by different techniques, including AFM, FT-XPS, UV-Vis, and fluorescence spectroscopy. The characterization of the CNDs confirms their solubility in water, their tiny size, and their luminescence. According to the findings, they pose particle size range of 2.7-4.5 nm, an average quantum yield of 2.35%, an average product yield of 15% and they are soluble in water with an average ζ potential of -24.08 mV.

Consequently, the prepared CNDs were exposed to two classes of cell lines, including: hepatocellular carcinoma Hep3B and Non-cancerous LX-2 hepatic stellate cells served as a comparative model to evaluate the selectivity of CNDs against hepatocarcinoma cells. The exposure of the cells resulted in an anticancer activity against the Hep3B cells, while the LX2 cells remained unaffected. The selectivity index (SI) analysis revealed that glucose- and maltose-derived CNDs exhibited the most favorable selectivity toward

hepatocellular carcinoma cells, with SI values of 2.69 and 2.55, respectively. These results indicate that certain sugar-derived CNDs can effectively target cancer cells while minimizing harm to normal hepatic cells, supporting their potential as selective anticancer agents. The supportive explanation of the anticancer activity is the generation of small reactive oxygen species ROS, indicating the specificity of the CNDs against only abnormal cells. These results support the therapeutic potential of structurally optimized, sugar-derived CNDs for the targeted treatment of hepatocellular carcinoma, demonstrating favorable selectivity indices.

Keyword: Carbon Nanodots (Cnds); Liver Cancer (Hepatocarcinoma); Nanoparticles; Carbohydrates.

Chapter One

Introduction

1.1 Cancer Disease

Based on statistics provided by the World Health Organization (WHO), cancer is the second leading cause of death worldwide., with 9.6 million deaths from the disease in 2017. It is estimated that one in thirteen men and one in sixteen women will develop cancer in their lifetimes, and that one in eight men and one in eleven women will pass away from the disease. Given that there would likely be a 70% increase in new cancer cases over the next 20 years, these figures are expected to rise even higher. Data on cancer indicate that it is a potentially fatal disease that has a lasting impact on human society, ranking second in terms of causes of death behind heart disease. (1)

Although the exact cause of cancer is still unknown, several factors may be involved, despite the persistent efforts of scientists. The following are risk factors for cancer: genetics, smoking, jobs, nutrition, environment, and infectious agents. (2)

The ability of cancer to evade programmed cell death (apoptosis), proliferate biologically and colonize distant regions, and form regions with metastatic lesions—the primary cause of cancer-related death—are just a few of the many biological components required for cancer growth and spread. To survive and proliferate, cancer cells need nourishment just like any other type of cell. However, the cellular process by which new blood vessels are generated from pre-existing ones is called angiogenesis, and it allows for this. Abnormal blood arteries that are disordered, permeable, and immature develop because of the pro-angiogenic substances secreted by high quantities of cancer cells. As they eliminate waste items and supply oxygen and nutrients, these blood vessels' growth is essential to the development of cancer. As a result, cancer cells undergo a multistage process that involves the fast division of aberrant cells and their dissemination to many body parts; at this step, the cancer has already metastasized. (3, 4)

Nonetheless, the blood vessels found in tumor cells are not like those found in healthy cells. The vascular wall is atypical, the endothelial cells that line the inside are irregular, and they multiply more quickly. A porous structure and immature phase characterize them, a phenomenon known as enhanced permeability and retention effect (EPR), as

shown in Scheme 1.1. As a result, this impact causes a large-scale leakage of blood plasma constituents into the cancerous cells, including lipid particles, macromolecules, and nanoparticles. Similarly, the cancer cells poor lymphatic clearance and delayed venous return show that macromolecules are being retained inside the cell, even as extravasation into the cancer cells interstitial persists . (5, 6)

Scheme 1.1

Schematic showing the enhanced permeability and retention (EPR) effect (6)

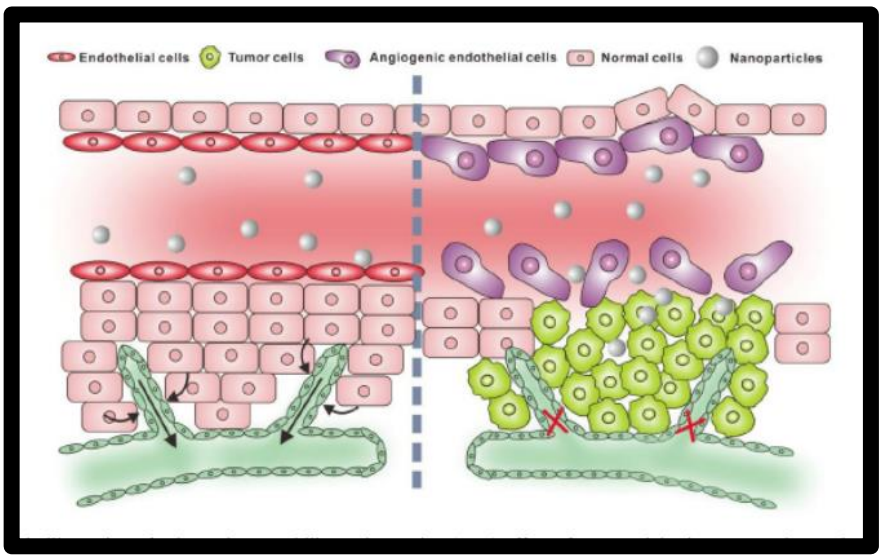

To cure this sickness, early diagnosis and detection is crucial as well as effective cancer therapy alone or in combination are essential too. Even yet, conventional medicines lack specificity and may have systemic side effects. Surgery is frequently used to remove tumors and malignant tissues, while chemotherapy and radiation therapy are used to kill or eradicate cancer cells or diseased tissues. Even though these methods cause severe pain for cancer patients, they frequently fail to obtain an effective treatment because of the numerous adverse effects that can arise from them, including fatigue, loss of appetite, vertigo, gastrointestinal (GI) issues, hair loss, pale skin, and an increased risk of infections or other forms of malignancy. (7)

Liver cancer, particularly hepatocellular carcinoma (HCC), represents one of the most prevalent and deadly forms of cancer globally. HCC accounts for most primary liver cancers and is often associated with chronic liver diseases, including hepatitis B and C infections, alcohol-induced liver damage, and non-alcoholic fatty liver disease. The global burden of HCC is increasing, especially in regions with high prevalence of viral hepatitis. Early detection remains challenging due to the asymptomatic nature of the

disease in its initial stages, and treatment options for advanced stages are often limited. This has driven interest in developing nanotechnology-based approaches for improved diagnosis and treatment.

Carbon nanodots (CNDs) have shown potential as a theranostic platform for HCC. Their small size, surface functionality, and inherent fluorescence allow for targeted drug delivery and real-time imaging of tumor sites. Additionally, functionalized CNDs can exploit liver-specific receptors to enhance selective accumulation in hepatic tumors while minimizing systemic toxicity. These properties underscore the potential of sugar-derived CNDs for addressing current limitations in liver cancer therapy. (8)

1.2 Definition of Nanotechnology

Nanotechnology is a branch of science and engineering which refers to the understanding, controlling, design and manufacturing of matters at the nanoscale which deals with dimensions ranging from 1-100 nanometers. (9)

However, the concept of nanomaterial size is brought as close to our minds as possible by a variety of commonplace products with a nanoscale. For instance, a water molecule is just approximately 0.13 nm in size, yet a white blood cell is over 10,000 nm long (10). Scheme 1.2 illustrates where nanoparticles lie on the nanometer scale.

Scheme 1.2

Nanometer-scale (5)

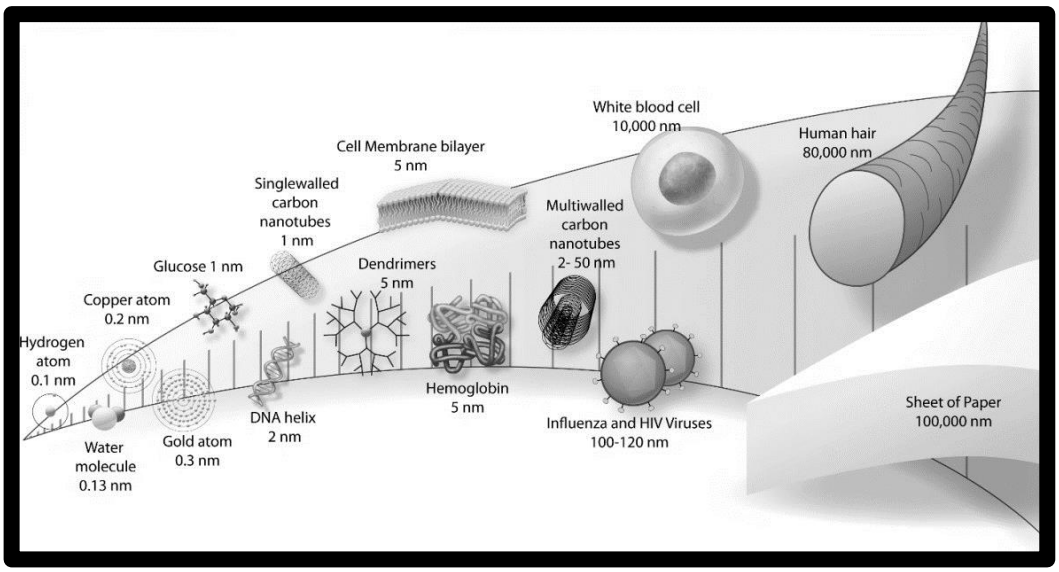

Nanomaterial synthesis, engineering, and application are included in the realm area of study known as nanotechnology. Over time, nanotechnology has gained a lot of attention because of the fascinating and inventive uses of nanomaterials for the upcoming industrial revolution. (11)

As a result, the term "nanotechnology" is defined by numerous agencies. Nanotechnology was characterized by the U.S. Environmental Protection Agency (EPA) as "the invention and utilization of structures, technologies and systems that have unique qualities and functionalities because of their tiny size". (9)

whereas, the National Nanotechnology Initiative (NNI), define nanotechnology as, " the investigation and manipulation of matter at dimensions ranging from 1-100nm, where unique phenomena enable new applications".(12)

The small size of nanoparticles produces certain advantageous qualities, such as a bigger surface area to which various parts can link, which produces materials that are lighter or stronger. They also behave differently from the typical larger units of substances and display an amazing range of traits. (11, 13)

1.3 History of Nanotechnology

The origins of nanotechnology can be traced back to Nobel Laureate Richard P. Feynman, who, in 1959, delivered his seminal lecture, "There's Plenty of Room at the Bottom," at the annual American Physical Society conference held at the California Institute of Technology. In his speech, he explored the challenges associated with manipulating and controlling matter at a minuscule scale. (14)

Years later, in 1974, Norio Taniguchi introduced the term "nanotechnology" to characterize the fabrication of materials with tolerances below one micrometer, defining it as the processing, manipulation, accumulation, and modification of substances at the atomic or molecular level. (15)

But in contrast, the current nanotechnology revolution is credited to Eric Drexler's Book "Engine of creation" published in 1986. (16)

Nonetheless, the discovery of the Atomic Force Microscopy (AFM) in 1986 and the Scanning Tunneling Microscope (STM) in 1982 by Binning, Quate Gerber, and Heinrich

Rohrer at the IBM Zurich research laboratory signaled the advent of nanotechnology science. (17)

1.4 Nanomaterials (NMs) and their classifications

According to the European Commission, a nanomaterial is a substance that can be naturally occurring, accidentally created, or purposefully engineered. It is made up of particles that can be found alone or grouped together. One of the criteria is that at least half of the particles must have at least one external dimension in the 1–100 nm range, based on their numerical size distribution. (18)

Consequently, Nanomaterials are utilized across a diverse range of industries and applications, owing to their unique physicochemical properties and nanoscale dimensions, and are now essential to many aspects of daily life as well as several fields, such as biology, engineering, chemistry, physics, computer science, medicine, and many more. Their better performance over their bulk materials can also be attributed to their diverse physiochemical properties, such as their electrical and heat conductivity, wettability, catalytic action, absorption of light and dispersion, and melting point. (10, 19)

However, as nanoparticles become increasingly prevalent in technological advancement, it is possible to vary the structure, size, and internal organization of the substances to change their attributes, including electrical conductivity, elasticity, chemical reactivity, color and others. In addition, these particles could also be round, tubular, or irregular in shape. Nanoparticles may be split into two main categories: artificial and natural. Each of these groupings is additionally subdivided into organic and inorganic (mineral) subgroups by the nanoparticles chemistry. (10, 20)

Nonetheless, nanoparticles can be generically divided into four groups based on their structural constitution: organic, inorganic, carbon-based, and composite nanomaterials, as shown in Scheme 1.3. (11)

Scheme 1.3

Classification of nanomaterials (13)

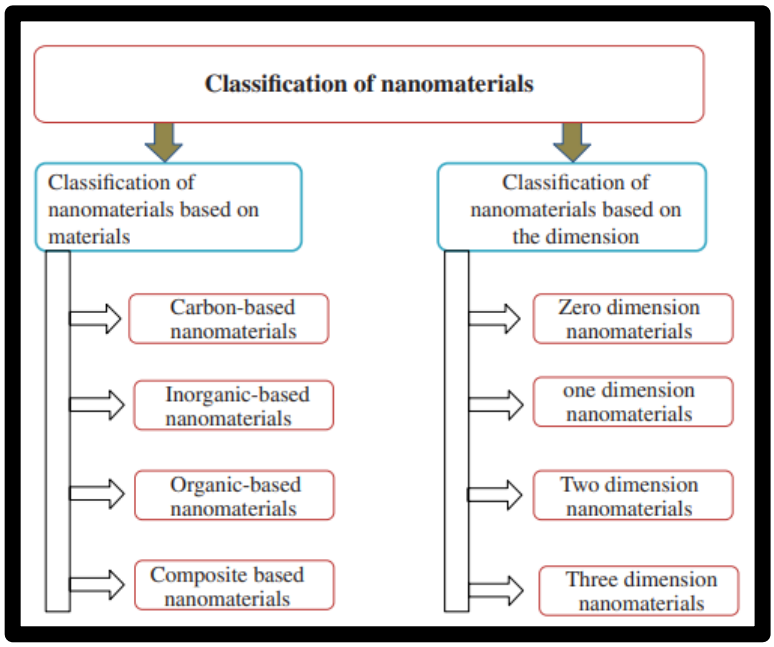

Organic molecules become organic nanoparticles at the nanoscale. Liposomes, micelles, dendrimers, and ferritin are a few instances of nanoparticles.

As seen in Scheme 1.4, liposomes and micelles are non-toxic, biodegradable nanoparticles with hollow interiors that make them susceptible to heat, light, and electromagnetic radiation. On the other hand, inorganic nanoparticles consist of components other than carbon. Based on metals or metal oxides, inorganic nanoparticles are frequently classified as nanomaterials. While composite nanomaterials are made up of an extra layer of nanoparticles, carbon-based nanomaterials are made up of the element carbon. These nanomaterials are combined with bulk materials, more nanoparticles, or more complex materials like metal frames. A wide range of materials, such as bulky polymers, metals, ceramics, and organic and inorganic compounds based on carbon, can be included in the composites. (11)

Scheme 1.4

examples of organic nanomaterials

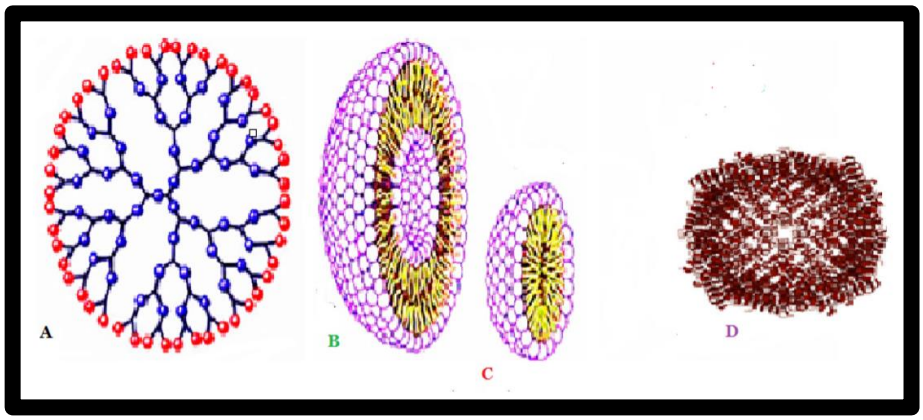

Note: *A) dendrimers,, B) liposomes, C) micelles and, D) ferritin.*

Based on the number of dimensions, nanomaterials can be further classified into 4 types: zero-dimensional (0D), one-dimensional (1D), two-dimensional (2D), and three-dimensional nanomaterials (3D). (11)

1.5 Carbon Nano Allotropes

1.5.1 carbon

Carbon is probably derived from the Latin word carbon referring to "coal", "charcoal" or "ember". It was discovered by the first person who treated charcoal made by fire; as a result, carbon was of a small group of elements that were well-known in antiquity. However, carbon is one of the major plentiful elements on the planet. It happens naturally as an overall large quantity of organic substances and may be present in the atmosphere as a form of carbon dioxide. Pure carbon may be exist in nature in a variety of crystallographic forms, including graphite and diamond. It is the fifteenth most widespread element on Earth crust, the fourth most abundant element in the entire universe and it makes up around 18.5% of the total mass of the human body. (21-23)

Furthermore, carbon can be found in every organic material, including all plant and animal cells as well as proteins, carbohydrates, and lipids. Chemistry literature has identified over a million carbon compounds. Additionally, every year, scientists produce a huge number of new carbon-based molecules. (24)

Since the ability of carbon atoms to make bonds with each other in different chemical structures, 3D forms and even to link with other different atoms, is largely responsible for the variety and complexity of organic structures. (25)

Carbon may be sp, sp2 and sp3 hybridized. This notable capability to form powerful covalent bonds with another atoms of carbon permits them to produce a broad range of nano and large structures. To emphasize carbon's valency, it may occur in many allotropes (different structural forms of the same element). They may exist in both amorphous and crystalline forms, diamond and graphite are the most two widespread natural allotropes forms of carbon. (25)

The allotropes possess remarkably different chemical and physical characteristics, such as stability, structure, optical, mechanical, and electrical features; these properties enable them to be essential building blocks for many applications in the science of materials and nanotechnology. (26)

1.5.2 Classification of Carbon Nano Allotropes

Recently, carbon-based nanomaterials have been extensively studied due to their remarkable potential for advancing innovation and enhancing applications across various fields, particularly in biomedicine.(24)

Allotropes of carbon can be classified based on their dimensional characteristics. Scheme 1.5 illustrates that the primary determinant of their classification is their size, which specifically ranges between 1 and 100 nm in at least one dimension. Consequently, they can be further divided into four distinct categories. Zero-dimensional (0D) nanomaterials are characterized by having all three dimensions at the nanoscale, measuring less than 100 nm. In this group are metals, hollow spheres, core-shell nanomaterials (NMs), spherical nanomaterials, nanocubes, nanorods, polyhedral structures, and carbon nanodots (CNDs). One-dimensional (1D) nanomaterials, on the other hand, possess one dimension that extends beyond the nanoscale, while the remaining two remain confined within it. Examples of 1D materials include metallic, polymeric, and ceramic structures like nanotubes, nanowires, nanofibers, and nanorod filaments. Two-dimensional (2D) nanomaterials exhibit only one dimension at the nanoscale, whereas the other two exceed this limit. This category encompasses thin films, nanoplates, and nanocoating, which may be single-layered or multilayered, as well as crystalline or amorphous in structure. Lastly,

three-dimensional (3D) materials extend beyond 100 nm in all three dimensions, with common examples including polycrystals, diamond, and graphite. (25)

Scheme 1.5

Different carbon allotropes (19)

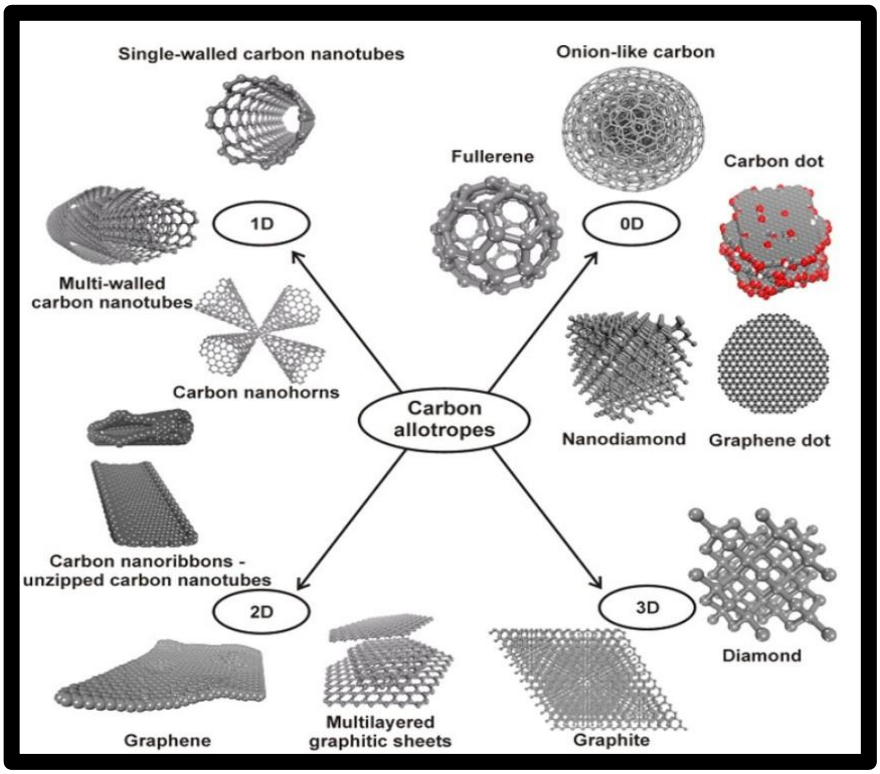

1.5.3 Three-Dimensional (3D) carbon allotropes

1.5.3.1 Diamond

The most powerful known natural mineral is diamond, a well-known carbon allotrope. Because of its broad light dispersion, high refractive index (RI), and toughness, it is ideal for industrial applications. In addition, one of the costliest elements in diamond form is carbon. Each unit cell in the face-centered cubic lattice consists of eight atoms, that make up the crystal structure of diamonds. The diamond's cubic shape originates from this lattice. The atoms in diamond form tetrahedrons with their four closest neighbors and exhibit sp3 bonding. Diamond has the highest number of atoms per unit volume of all recognized solids, making it the least compressible and most rigid solid. Tetrahedrons are also strong and have strong bonding. (27)

1.5.3.2 Graphite

One crystalline form of carbon is graphite. Layers of graphene are stacked to form the structure. Under normal circumstances, graphite, a naturally occurring chemical, is the mostly stable format of carbon. Both natural and synthetic graphite are widely used to make electrodes, lubricants, and pencils. It turns into diamond when the temperature and pressure are raised. Its electrical and thermal conductivity are adequate(28).

1.5.4 Two Dimension (2D) Carbon Nano allotropes

1.5.4.1 Graphene

A two-dimensional monolayer with a hexagonal structure made of covalently bonded sp2 hybridized carbon atoms is called graphene. It is an essential constituent of every other dimensional carbon compound, including 1D-carbon nanotubes, 3D graphite, 0D Bucky balls, and graphene quantum dots (GQDs). By using scotch tape that adhered to layers of graphene particles, Geim and Novoselov were able to mechanically separate graphene from graphite in the beginning. Graphene's derivatives, such as thermally reduced graphene oxide (TRG), reduced graphene oxide (rGO), and graphene oxide (GO), graphene possess remarkable electrical, mechanical, and optical features that makes them attractive for usage in the electronic, optoelectronic, and aerospace industries (26, 29).

1.5.5 One Dimension (1D) Carbon Nano allotropes

1.5.5.1 Carbon Nanotubes (CNTs)

Carbon nanotubes (CNTs) were a by-product of fullerene synthesis that Ijima discovered in 1991. They are now acknowledged as a valuable resource for improving biological approaches to the management and treatment of a range of illnesses(30). CNTs possess a remarkable capacity for cell membrane penetration, due to the sp2 hybridization of their carbon atoms. This unique structural feature facilitates the functionalization of CNTs with a wide range of biomolecules and compounds, enabling them to selectively target cells and effectively deliver therapeutic agents in response to certain triggers. (31)

CNTs are cylindrical structures composed of a single sheet of graphene that has been wrapped up. The CNTs under consideration are categorized based on the number of wall sheets in their structure. Specifically, there are single-walled carbon nanotubes (SWCNTs), which consist of a solitary graphene sheet with a diameter typically ranging

from 0.4 to 40 nm. Additionally, there are multi-walled carbon nanotubes (MWCNTs), which comprise multiple sheets arranged in concentric cylinders. (32)

However, the interlayer distance between these sheets is approximately 0.35 nm, like the separation observed in the basal plane of graphite. The diameters of MWCNTs vary from (2-100 nm). (33)

1.5.5.2 Single Walled Carbon Nano-horns (SWCNHs)

Single graphene layers that form cone and horn-shaped ends make up single-walled nano-horns (SWCNHs), which are carbon-based materials. The diameter and length of each conical nanostructure are 2–5 nm and 40–50 nm, respectively. Furthermore, through synthesis, they typically form 2000 cone aggregates with a diameter of around 100 nm. Because of its conical form and surface chemical composition, which allow drug loading and targeted release, SWCNH offer unique features. Furthermore, the conical shape may help trap drugs or other substances inside the structure, and the tip of the structure may be chemically functionalized by adhering to specific molecules. These characteristics make SWCNH a desirable substitute for graphene oxide and carbon nanotubes in a broad variety of biological applications. (34)

1.5.6 Zero-dimension (0D) carbon nano allotropes

1.5.6.1 Fullerenes

A fullerene is characterized as a 60-carbon (C60) molecule acceded by single and double bonds to make a spherical hollow that has a diameter of 1 nm and resembles a soccer or football ball. The field of carbon nanostructure research began with the discovery of fullerenes. Typically, fullerenes are sealed hollow structures made of sp2-hybridized carbon atoms arranged in several hexagons and 12 pentagons, according to the total number of carbon atoms. (35)

Fullerene, on the other hand, has 20, 40, 60, 70, or 84 carbon atoms. C60 is the most often used. (36)

1.5.6.2 Onion-like Carbons (OLCs)

They are quasi-spherical nanoparticles made up of fullerene-like carbon layers encased in cylindrical graphitic shells. Due to their extremely symmetric structure, they are projected to have characteristics that distinguish them from different carbon nanostructures like graphite, nanodiamonds, or nanotubes and may find utility in a variety of applications. (37)

However, they can vary in size, shape, and core type, which affects their physicochemical characteristics. The exterior graphite layers of carbon onions can even be used as Nano capsules for drug delivery systems, protecting the chemicals they contain and acting as a foundation for the binding of appropriate functional groups(38).

1.5.6.3 Carbon Nano Dots (CNDs)

Carbon Nano dots are the most common class of Nano dots. CNDs are nanoparticles with particles less than 10nm. They exhibit facile and economic synthesis, high water solubility, negligible toxicity, excellent photo stability, good biocompatibility, high quantum yield (QY), as well as increased selectivity and sensitivity(39, 40). Synthesis approaches, applications and properties of CNDs will be discussed in detail later.

1.5.6.4 Graphene Quantum Dots (GQDs)

Graphene quantum dots (GQDs) refer to nanoparticles composed of graphene material, characterized by their dimensions being less than 100 nm. GQDs are referred to a promised material for many applications in the fields of biology, optoelectronics, energy, and the environment, owing to their remarkable characteristics such as low toxicity, sustained photoluminescence, chemical stability, and significant quantum confinement effect. (41)

Additionally, these entities exhibit chemical and physical stability, possess a significant surface area relative to their mass, and may readily disperse in water owing to the existence of functional groups lies at their peripheries. (42)

However, the fluorescence emission of graphene quantum dots (GQDs) exhibits a wide spectrum range including ultraviolet (UV), visible, and infrared (IR) wavelengths. (29)

1.5.6.5 Nano diamonds (NDs)

Nano diamonds, also known as diamond nanoparticles, are diamonds smaller than 100 nanometers in size. (43)

Nano diamonds have extraordinary mechanical and optical properties. They have larger surface areas and tunable surface topologies. Their remarkable biocompatibility, surface functionalization ability, and ease of production have led to their considerable interest in the fields of biological and electrical applications. They are also non-toxic materials, which makes them ideal for use in biomedical applications. Synthetic methods of NDs include laser ablation, autoclave synthesis from super critical fluids, chlorination of carbides, ion irradiation of graphite, and detonation technique. (44)

1.6 Carbon Nano Dots (CNDs)

1.6.1 Introduction

Carbon nanodots (CNDs), a novel zero-dimensional member of the carbon family, are spherical particles that are small in size, with a diameter of less than 10 nanometers.(45) Their structure is sp2 hybridized and incorporates oxygen in the way of different oxygen-containing groups, including hydroxyl (–OH), carboxyl (–COOH), and aldehyde (–CHO) groups; which account for their high water solubility, high biological activity, and their ability to form covalent bonds, hydrogen bonds and electrostatic interactions with a broad variety of inorganic and organic materials.(46) CNDs were accidentally discovered in 2004 during the isolation and purification of single-walled carbon nanotubes (SWCNTs) by Xu et al.(47) In 2006, Sun et al. suggested a synthetic method to produce fluorescent carbon nano particles (CNPs) with improved fluorescence emissions through surface passivation. Subsequently, scientists referred to these CNPs as carbon quantum dots (CQDs). (48) in addition to their high aspect ratio, CNDs are composed of carbon atoms that are exceptionally organized and have a large surface area, drug loading capacity, and superior thermal and chemical stabilities in comparison to larger particles like quantum dots QDs. (49) So far, CNDs have shown several unique characteristics, including facile and economic synthesis, water-solubility, negligible toxicity, excellent photostability, good conductivity, ease of functionalization, good biocompatibility, viability of large-scale production, environmental friendliness, high quantum yield (QY), marked electron-donating and accepting capabilities, tunable photoluminescence (PL) and dispersibility, as well as increased selectivity and sensitivity. (39)

These properties encourage the numerous uses of CNDs in bio-imaging, biosensors, cancer therapy, gene transmission, drug carriers, optoelectronic devices, catalysis, functional materials, and agriculture. (50, 51)

CNDs possess special PL properties that are influenced by a variety of parameters, like: 1) surface compound occurrence, which also affects radiation intensity; 2) particle size and uniformity of the particle size distribution; and 3) organic molecule surface functionalization to provide greater control over the radiation wavelength. Depending on the necessary PL circumstances, CNDs are a promising material in a diversity of applications due to the ability to alter the PL parameters (wavelength, radiation intensity, and quantum yield) with simple modifications to the synthesis requirements. (52)

Depending on the nature of the surface states, some CNDs have also been reported to exhibit excitation-dependent PL characteristics, whereas other CNDs have been reported to exhibit excitation wavelength independence. (53-55)

However, it is generally agreed that surface passivation with functional groups not only creates surface defects that cause fluorescence emission, but it also creates possible reactive sites for specific functional modifications. These reactive groups also make it possible for different organic, polymeric, inorganic, or biological materials to stick to the surfaces of carbon nanodots (CNDs) through covalent bonding, hydrogen bonding, and electrostatic interactions. This functionalization allows CNDs to serve as versatile platforms for applications such as targeted sensing, drug delivery, and other specialized tasks. (56)

Typically, CNDs show two distinct absorption peaks in their UV/Vis spectra, one at around 240 nm (the sp2 -carbon network) and the other at approximately 350 nm (the n-π^* transition of surface carbonyl groups). A few samples exhibit a shoulder peak at about 450 nm that is connected to the lower energy states because of the carboxylic acid groups in CNDs (57-59). As a result of the many surface states that correlate to a narrow band gap, absorbance over 450 nm has also recently been reported(60, 61). The photocatalytic systems efficiency in UV and visible light has an impact on these broad spectrum. In addition, charge separation in CNDs happens upon irradiation, and this is succeeded by quick charge recombination, resulting in the distinctive PL features. Under UV and visible light exposure, most CNDs generally generate blue PL emission. (57, 62)

However, longer wavelength CNDs have been developed in order to enable CNDs to be used in more applications. Yellow, green and red CNDs emission have been reported based on the types of precursors. Qu and collageuse, for instance, observed orange emission (QY = 46%) from CNDs made from citric acid and urea prepared by solvothermal reactions in the presence of Dimethylformamide (DMF)(63). Additionally, Li and others used 1,3-dihydroxynaphthalene and KIO4 in ethanol solution to improve the quantum yeild (QY) to 53% for the red emission of CNDs. This was made possible by the large-sized conjugated sp2 -clusters with evenly distributed hydroxyl groups on the surface. (64)

Unlike other fluorescent materials that often require costly precursors or intricate fabrication processes involving specialized equipment, carbon nanodots (CNDs) can be synthesized from readily available and inexpensive sources. These include amino acids, chitosan, and various natural substances such as orange juice, apple juice, grape peels, watermelon rinds, vegetables, and sugars. (65)

1.6.2 Synthesis Methods of CNDs

The process of synthesizing CNDs can take several different forms. Researchers can only take approaches that produce high yields in a clean and highly efficient way. The "top-down" method uses graphite materials as carbon source, and the "bottom-up" method of organic molecules as the source of carbon as in scheme 1(51, 66).

Scheme 1.6

Synthesis of graphene nanodots/carbon nanodots using

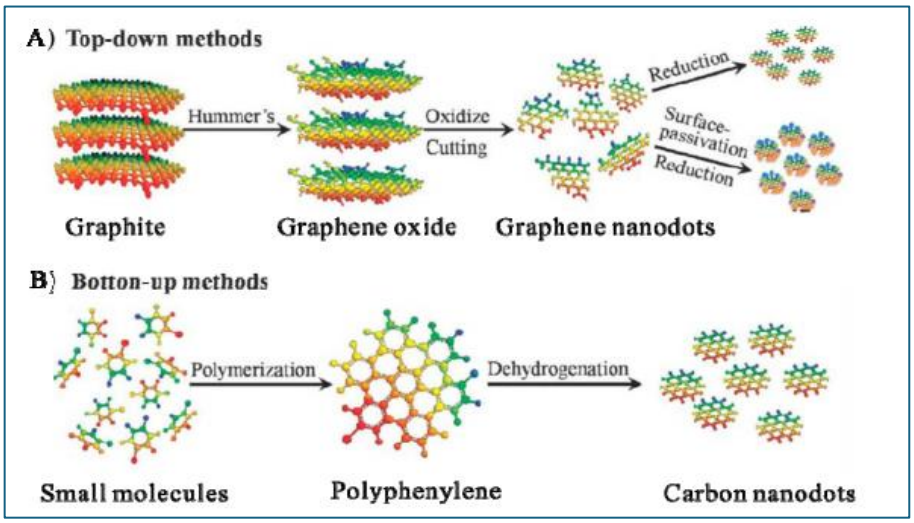

Note: (A) top-down approach, (B) bottom-up approach (3).

However, the "top-down" method is identified using bulk precursors as the initial material, which is converted to nanostructures by different techniques, for instance: electrochemistry, chemical oxidation, arc discharge, or laser ablation that removes nanoparticles from the bulk substrate. Graphite, graphene, candle soot, single- or multi-walled carbon nanotubes, and many more are examples of common substrates. (51, 66, 67)

Conversely, the "bottom-up" approach relies on applying a molecular precursor that is converted to CNDs through chemical reactions. A diversity of approaches used to facilitate conversion reactions, such as thermal destruction, chemical or hydrothermal oxidation, electrochemical, Combustion, microwaves, ultrasonic irradiation, or silica nanoparticle template synthesis. (51, 66, 67)

Moreover, compared with the top-down technique, the bottom-up approach yields multi-gram scale quantities with functional groups such as the carboxyl group, amide, and hydroxyl group, also, economical, eco-friendly, and low-cost productions. (57, 68)

Further, Bottom-up synthesized CNDs exhibit a high UV/Vis absorptivity, allowing for photo-induced charge carrier transfer and charge separation when exposed to radiation. The chemical and physical features of CD-based composites can be improved by these special qualities. (57)

However, the most common approaches in bottom-up synthesis are microwave method, which is a convenient approach for preparing CNDs within 10 minutes, and the hydrothermal approach in which the CNDs were polymerized under highly vapor pressure and highly temperature (150-200˚c) in aqueous solution using organic precursors such as, polymers, organic acids, amino acids, and carbohydrates. (51, 57, 69, 70)

1.6.2.1 Top-Down Approaches

1.6.2.1.1 Arc Discharge (AcD)

Carbon atoms are vaporized during the arc discharge procedure by the helium gas plasma that is combusted by massive currents flowing through the opposite carbon anode and cathode. The arc current produces an extremely hot plasma—approximately 4000°C—which causes the carbon precursor within the arc to supreme and form carbon nanoparticles. (71)

This process has the benefit of producing nanoparticles in a variety of gases, but it also has the drawback of requiring further purification of CNDs because of the presence of unwanted carbon material. (72)

However, the first scientists who created CNDs using the arc discharge method were Xu et al. and Bottani et al. They did that by oxidizing single-walled and multi-walled carbon nanotubes as carbon origins, respectively. Several composite segments are typically used in the arc discharge process, which presents difficulties for their purification. (73)

1.6.2.1.2 Laser Ablation (LA)

A carbon source and a laser beam are needed for the LA process. Using this technique, a laser beam is directed at a solid target that is submerged in a liquid. By increasing the temperature of the liquid-solid interface by a few kelvins, a laser beam causes the surrounding liquid to contain a plasma plume. The pressure inside the bubble can reach several gigapascals, which means that the ablated species and the gaseous medium must interact chemically. Under these conditions, nanomaterials are formed by a crystallization process. (71)

The laser ablation method has been used in many experiments to produce CNDs. For example, argon was utilized as the carrier gas to create CNDs by Sun et al., the pioneers of the laser ablation technique. The carbon of interest was produced by mixing graphite powder with exhaust cement. The laser utilized was a Q-switched Nd:YAG laser with a frequency of 10 Hz and a wavelength of 10,464 nm. A pressure of 75 kPa and a temperature of 900 C were used for the operation. After ablation, the sample was refluxed with HNO_3 for 12 hours. Subsequently, polyethylene glycol 1500N (PEG 1500N) was applied to the sample to inhibit any additional reactions. The solution was cooled and then subjected to centrifugation to create CNDs with a size smaller than 5 nanometers. (69)

Compared to CNDs generated using a single-pulsed laser beam, those made using double-beamed laser ablation offer better properties such as higher quantum yield (QY), minuscule size (~1 nm), excellent surface-to-volume ratio, improved stability, and increased homogeneity. Therefore, it is advised to use double-pulsed laser ablation to improve the catalytic and sensing properties of CNDs. (72)

1.6.2.1.3 Ultrasonic Method

Recently it has been established that ultrasonic is a useful technique for creating different kinds of CNDs. Nevertheless, in this process, carbon precursors, acid, alkali, and other oxidants are exposed to high ultrasonic vibrations, which break down carbon particles into minuscule nanoparticles. There is a persistent cavitation of the molecules. By removing the necessity for a complex post-treatment procedure, high-energy ultrasonic waves allow for the simple manufacture of smaller CNDs. (71)

Li et al. originally reported the manufacture of CNDs using ultra sonication and glucose in both basic and acidic conditions in 2011. He was able to create PL CNDs that were less than 5 nm in size. (74)

Wu et al. also created amine-functionalized CNDs using ultrasonic techniques for the detection of metal ions, such as cobalt (II) ions, nucleic acid sensing, and cell imaging. In contrast, Huang et al.'s study combined cigarette ash with polyethylene glycol (PEG) that included thiol groups in a single step using ultrasonic treatment (SH-PEG). This procedure yielded high quantum yield (QY) PEG-decorated carbon dots (CDs), which might be utilized for cell imaging. (75, 76)

1.6.2.1.4 Electrochemical/Chemical Oxidation Method

Chemical oxidation can often be used to create stable mixes of carbon-based nanomaterials in polar liquids by attaching polar functional groups containing oxygen, such as carboxyl or hydroxyl, to carbon atoms. Chemical oxidants such as hydrogen peroxide and oxidizing acids like nitric acid (HNO_3), sulfuric acid (H_2SO_4), and hydrogen peroxide (H_2O_2) can be used to break down and convert large amounts of carbon into CNDs or to help convert small organic molecules into carbonaceous materials. This process yields CNDs with high QY and is incredibly quick, inexpensive, and repeatable. It also makes adjusting CNDs sizes simple. (76)

Using oxidation-reduction reactions, CNDs are electrochemically synthesized at room temperature and pressure. Graphite, carbon nanotubes, and carbon fiber electrodes are examples of bulk carbon materials that must be chopped in order to use the electrochemical process. By managing redox processes and electrolyte components, hydrophilic groups such as NH2, -COOH, -OH, etc., can be added to CNDs surfaces. Because the electrolytes and electrode materials can produce CNDs with unique

properties concerning of luminescence, cytotoxicity, and surface changes, they are essential. (77)

A simple technique for creating CNDs was presented by Liu et al. These CNDs might be utilized for bioimaging and ferric ion (Fe^{3+}) detection in water samples. In this work, graphite was oxidized in alkaline alcohols to successfully electrochemically create CNDs with a significant level of crystallinity and an average size of about 4 nm. (78)

1.6.2.2 Bottom-Up Approaches

1.6.2.2.1 Hydrothermal

The hydrothermal route is a widely utilized technique for synthesizing novel carbon-based nanomaterials from various primary raw materials. This method is particularly advantageous due to its one-step nature, cost-effectiveness, environmental friendliness, non-toxicity, and low susceptibility to photobleaching. The process yields carbon nanodots (CNDs) that exhibit high luminescence and maintain a nearly uniform size distribution. Traditionally, this approach involves dissolving organic precursors in a solvent, which is then transferred into a Teflon-lined stainless-steel reactor. By heating the reaction mixture above room temperature for several hours, the precursors can fuse more easily, which creates carbon cores. These cores subsequently evolve into CNDs with particle diameters typically below 10 nm. (47)

Up to now, varieties of chemicals have been used as precursors in the creation of CNDs, such as amino acids and citric acids. However, wasteful spending and excessive resource use could enhance the creation of these compounds. Lately, the most effective method to produce CNDs is "green chemistry," which involves the hydrothermal processing of renewable materials. Renewable resources like aloe, lychee peel, bombyx mori silk, and sweet pepper were hydrothermally treated to create CNDs (79-81). Zhu et al. utilized a hydrothermal method to synthesize carbon dots (CDs) derived from citric acid and dope with nitrogen. In their approach, citric acid and ethylenediamine were dissolved in deionized water within a Teflon-lined autoclave and heated to 200°C for five hours. The reaction started with citric acid and ethylenediamine coming together, which led to the formation of polymer-like aggregates. These aggregates subsequently underwent carbonization, resulting in the formation of CDs. The nitrogen-doped carbon nanodots

(N-CNDs) had an 80.6% quantum yield (QY) at a wavelength of 360 nm, which is about the same as most semiconductor quantum dots (QDs) and fluorescent dyes. (53)

Lu et al. recently used a one-step hydrothermal process to make nitrogen-doped carbon nanodots (N-CNDs) with an average diameter of 2.6 nm. In this method, citric acid was used as the carbon precursor, and polyethyleneimine (PEI) did two things at once: it added nitrogen and protected the surface. The resulting N-CNDs exhibited blue luminescence with a quantum yield (QY) of 51%. These nanodots have a lot of potential as optical nanoprobes for real-time live-cell imaging because they are very stable under light and don't hurt cells. Also, PEI's small size and positively charged surface make it easier for N-CNDs to cross the blood-brain barrier (BBB). This makes them good candidates for targeted drug delivery in neurological disorders. (82)

1.6.2.2.2 Solvothermal

Like the hydrothermal technique, the Solvothermal method preparation of CNDs includes heating organic compounds in an organic solvent. CNDs synthesis is a simple method that applies to the "bottom-up" principles through the carbonization and polymerization of precursors. (71)

A variety of organic compounds are used to treat CNDs via Solvothermal methods. For instance, Wu et al. produced CNDs via Solvothermal treating vitamin C and ethylene glycol. Additionally, Zhang et al. used the Solvothermal approach to create N-doped carbon nanoparticles in their study by using carbon tetrachloride (CCl_4) as a carbon source and $NaNH_2$ as a nitrogen source. As a result, an extraordinary 3.3 nm-sized carbon dot with a height that ranged from 0.5 to 5 nm was created. (83, 84)

In a related study, Qian et al. used SiCl4 and hydroquinone in Solvothermal synthesis to create Si-doped CNDs. The researcher used a typical stainless-steel autoclave with acetone as the solvent. They combined hydroquinone and SiCl4 in an autoclave and cooked the mixture for 120 minutes at 200 ◦C. As a result, 7 ± 2 nm-long Si-doped carbon nanoparticles were generated (85). However, this approach is limited by the elevated reaction temperature and the poisonous nature of organic solvents, despite its simple operation. (71)

1.6.2.2.3 Microwave-Assisted Method

The elevated reaction temperature and the poisonous nature of organic solvents, despite their simple operation, limit this approach. Microwave assistance for the synthesis of CNDs is a simple and low-cost process that involves exposing the precursor molecules to electromagnetic radiation at wavelengths ranging from 1 mm to 1 m. The main benefit of the microwave-assisted procedure is that it saves time. The microwave-assisted approach is relatively simple, inexpensive, and relatively quick, with shorter reaction times. It generates homogenous heat for the uniform dispersion of CNDs. (76, 86)

Zhu et al. produced fluorescent CNDs with a diameter of 3.7 nm on their first attempt at microwave irradiation. They heated aqueous saccharides and polyethylene glycol solution in a 500 W microwave oven for nearly three minutes. (87)

Furthermore, Wang and colleagues made water-soluble CNDs by pyrolyzing citric acid with the use of a single-step microwave. as a passivation nitrogen source, they used tryptophan (Tarp). Then, the liquid solution of citrate and L-Tarp was heated in a 700 W microwave oven for three minutes to produce CNDs smaller than 2.6 nm. The large pieces were then purified by high-speed centrifugation at 10,000 rpm. (88)

Cao and colleagues carried out an experiment in which they created CNDs using a 700 W microwave for around ten minutes, an aqueous solution comprising glucose and arginine was used for pyrolysis. The CNDs measured size was 7 nm. (71)

1.6.2.2.4 Thermal Decomposition

Thermal decomposition is among the best approaches for producing CNDs. This involves heating the large carbonaceous precursors at a high temperature. The thermal processes that take place during decomposition are often endothermic. Benefits of this technology include solvent-free processes, large-scale production, low cost, and less time investment. On the other hand, thermal procedure parameters such as reaction-mix pH, reflux time, and reaction temperature can be adjusted to improve the luminous properties of CNDs. (76, 89)

Wang and his colleagues presented a unique technique using extremely luminous CNDs as a passivation agent. Citric acid was utilized as the carbon source and was thermally decomposed to create CNDs. N-(β-aminoethyl)-γ-aminopropyl methyl dimethoxy silane

(AEAPMS), an organ silane molecule, was used in the synthesis procedure. After that, the reaction mixture was heated for one minute at 240 °C, which caused the diameter of the CNDs to become visible, which was about 0.9 nm. (90)

Additionally, Wang et al. created CNDs at 240 °C by breaking down l-cysteine and 1-butyl 3-methyl bromide imidazolium. The AFM investigation showed that the height of the CNDs varied from 1.0 to 3.5 nm. (71)

1.6.2.2.5 Pyrolysis Synthesis Method

One example of nearly irreversible thermal deposition is pyrolysis, which is the breakdown of organic substances in inert environments. Under the inert atmosphere, the organic material undergoes physical and chemical transformations that produce carbonaceous solid residues. Pyrolysis hence often uses very high temperatures and regulated pressures. Feng et al., for instance, used the pyrolysis process to create carbon nanoparticles from citric acid. Utilizing transmission electron microscopy (TEM) analysis, they created CNDs measuring 5–8 nm throughout this process by utilizing diethyl-ene-triamine. (91, 92)

1.6.2.2.6 Carbonization Synthesis

Carbonization is a chemical process that is environmentally inert and involves the continuous pyrolysis of organic compounds to produce solids that contain a higher concentration of carbon. This is one of the simplest, most popular, and fastest, most affordable and single-step methods for making CNDs. Wei et al. produced N-doped -CNDs utilizing this ultrafast carbonization technique. The synthetic carbon dot's diameters were measured to be between 1 and 7 nm, yielding 48% of QY. (93, 94)

1.6.3 Surface Functionalization, Element Doping and CNDs Nano Hybrids

Carbon and oxygen make up CNDs, which can be created via hydrothermal, microwave methods from a variety of natural resources, or manufactured organic compounds. Nonetheless, CNDs surface functional groups are often homogeneous, thus additional active sites can be needed for purposes. One useful method for improving CNDs photo-physical and luminescence capabilities is to functionalize them with certain groups. (56)

The two main types of functionalization are surface modification and doping. The covalent or non-covalent change of CNDs surface chemical structure is possible by the

functionalization approach known as surface modification, which is widely employed. This enables CNDs to have their selectivity and sensitivity gradually increased. Surface functional groups therefore have a significant influence on the properties of carbon dots. They can be modified covalently or non-covalently to add amino, carboxyl, and hydroxyl groups, which are frequently present. (95)

On the one hand, amide coupling reactions, sialylation, and other processes including esterification, sulfonylation, and copolymerization are responsible for the covalent changes. Conversely, π interactions, complexation/chelation, and electrostatic interactions can result in non-covalent changes. (95)

The resulting modified CNDs, however, are useful nanomaterials for medication delivery and analyte extraction and targeting. Together with the synthesis of CNDs utilizing novel precursors or partial substitution of other elements for carbon, the precise enhancement of luminescence characteristics and the creation of new applications through CNDs surface modification are expected to be critical perspectives. In addition, complexation capacity, quenching efficiency, fluorescence color, and quantum yields of fluorescence are affected by surface modification.

For instance, Dong et al. synthesized ethylenediamine (EDA)-modified CNDs-COOH (CNDs-1) through an EDC coupling reaction, using glucose as a carbon source. CNDs-COOH effectively passivates the strong linkage of amide bonds, improving QY from 1.3 to 3.0%. The unique optical properties and biocompatibility of CNDs-1, which have free amino groups attached to their surfaces, have been employed to label and image human gastric cancer cells fluorescently as shown in Scheme 1.7. (96)

Scheme 1.7

The synthesis process of CNDs-1 via amide coupling reaction

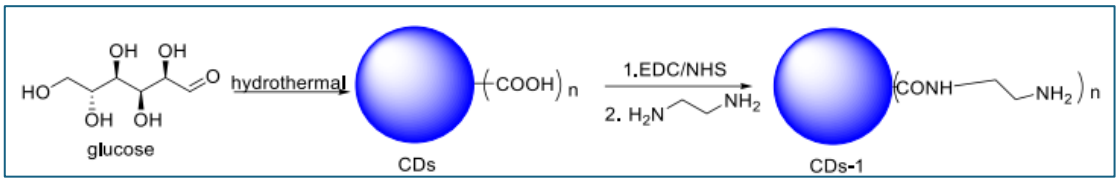

On the other hand, D'Angelis et al. used chemical oxidation to produce CNDs-COOH from cow manure. They modified CNDs-2 with EDA under nitric acid activation conditions, resulting in a high yield. The CNDs-2 exhibit a 65% increase in QY compared

to the Dong' group. CNDs-2 are biocompatible and could selectively stain the cell nuclei of the MCF-7 breast cancer cell line. they have effectively tested them as a selective live-cell fluorescence imaging assay with remarkable subcellular selectivity. (95)

Although fluorescent CNDs have greatly advanced bioanalytical applications, including optical sensing and imaging, heteroatom-doped carbon nanoparticles have emerged from recent findings. Consequently, the goal of doping CNDs with heteroatoms is to alter the electrical structures of these nanoparticles and give them unique intrinsic optoelectronic properties. Elements like phosphorous (P), sulfur (S), and nitrogen (N) might be employed for this. Nitrogen is a favored heteroatom for producing doped CNDs because of its five valence electrons and atomic size, which is similar to that of carbon. (84, 97, 98)

Moreover, new hybrids have been created using metallic nanoparticles such iron oxide, zinc oxide, silica, Titania, silver, and gold, as well as CNDs and inorganic nanoparticle cores. The resulting hybrids combine the mechanical, optical, electrical, magnetic, biological, and fluorescent properties of the oxide cores or metallic hybrid components with the fluorescence properties of the CNDs. Some hybrid technologies show great promise as highly efficient photocatalysts or as chemicals for magneto-optical biolabeling. (99)

1.6.4 Physical and Chemical Properties of CNDs

Scientists worldwide have shown significant interest in carbon nanostructures because of their remarkable qualities. CNDs have special optical, chemical, and physical properties. The chirality, UV absorbance, and photoluminescence of CNDs make their chemical properties very important. CNDs can be used as donors or acceptors of electrons. (45, 100)

1.6.4.1 Surface Elements and Structure

Sun et al. called quasi-spherical nanoparticles carbon dots. CNDs have a size below 10 nm, and some are hollow as mentioned previously. Several studies have found amorphous CNDs with sp2 and sp3 geometry in a diamond-like form. High-resolution transmission electron microscopy (TEM), scanning electron microscope (SEM), and X-ray diffraction (XRD) instruments confirmed that CNDs are circular, elliptical, quadrate, triangular, and hexagonal. Fourier Transform Infrared (FTIR) and X-ray photoelectron spectroscopy

(XPS) may use to determine the elements and functional groups on the surface of carbon dots. (101) In general, CNDs are mostly composed of C, H, and O in different ratios. However, in cases where they are synthesized from heteroatomic precursors like hair or proteins, other elements such as N and S may be present. In addition, most CNDs have complex surface groups, mainly oxygen-related functional groups like hydroxyl, epoxy/ether, carbonyl, and carboxylic acid and also it contains -NH2 (amine) groups, which result in strong biological activity, great water solubility, and the capacity to form bonds with numerous inorganic and organic compounds. (72)

1.6.4.2 Dispersibility

The processing of solutions and related applications requires CNDs dispersibility. Most CNDs have functional groups including oxygen on their surface, which makes them hydrophilic and easily dispersed in water. Related precursors combined with appropriate synthesis methods can produce hydrophobic and amphiphilic CNDs; correspondingly, hydrophilic CNDs can be modified with appropriate chemicals. (102)

1.6.4.3 Cytotoxicity and Biocompatibility

In biological applications, CNDs toxicity and biocompatibility are critical factors. CNDs are generally non-toxic at low doses (e.g., 10 μg/mL) and can be broken down or eliminated by organisms. The toxicity of CNDs varies with their size, molecular makeup, and concentration. Thus, higher concentrations could be harmful to cells and inhibit the growth of new organs. If not, they might be innocuous in the dark but produce reactive oxygen species when exposed to light, making them phototoxic. Apoptosis and autophagy may be induced by photoexcitation of CNDs, and this could be utilized in photodynamic therapy. (103)

1.6.4.4 Optical Properties

A broad spectrum of light from UV to NIR, tunable fluorescence, effective multiphoton up- and down-conversion, and the capacity to change properties through surface functionalization, size, shape, and doping using the quantum confinement effect (QCE), surface effect, and edge effect are just a few of the special qualities of CNDs. (47)

1.6.4.4.1 Absorbance

CNDs exhibit absorption in the short-wavelength region because of the π-π* double bond transition. With a tail that extends into the visible range, they frequently show high optical absorption in the UV region (260–320 nm) to the visible range (400–700 nm). They frequently process long wavelengths more effectively. (47)

The surface passivation of CNDs and the functional groups attached to them influence their absorption properties. They absorb both visible and ultraviolet light. Size-dependent absorbance is observed in top-down made CNDs between 200 and 252 nm when the diameter grows from 12 to 22 nm. While discrete absorption bands are visible in the 250–300 nm range on CNDs produced using a variety of techniques, such as hydrothermal, microwave, and ultrasonic. (76)

The shoulder peaks observed in UV absorption spectra are primarily attributed to π-π* transitions in aromatic rings and C=C double bonds. In addition, they have n-π* transitions in additional sub-fluorophore groups and C=O bonds. Following 4,7,10-trioxa-1,13-tridecanediamine (TTDDA) surface passivation, CNDs absorb more at longer wavelengths (350–550 nm). (104)

1.6.4.4.2 Photoluminescence (PL)

CNDs glow with photoluminescence, which can be observed at a wide range of wavelengths and with strong emission peaks that go from ultraviolet to visible to near infrared. We can also refer to this characteristic as an excitation-dependent luminescence spectra. Therefore, by applying the quantum confinement effect (QCE) and nanoparticle size, one can adjust the light-emitted color of CNDs based on the given excitation wavelength. The impact of quantum confinement or the occurrence linked to core emission resulting from the conjugated carbon core domains; surface states arising from the existence of carbon-backbone-linked functional assemblies; and molecular states in which the emission originates from unbound or bound fluorescent molecules.

The PL characteristics of CNDs may be modified via surface changes or electron/energy transfer. Therefore, when selecting luminous material, it's crucial to consider QY. Their starting material and manufacturing procedure mainly determine the quality of CNDs. Initially, surface engineering and element doping are effective methods for improving CNDs quality. Although nitrogen and sulfur are often utilized as doping materials, boron

has also been documented. CNDs increased QY is nonlinearly proportional to their optical characteristics. (47)

1.6.4.4.3 Up-Conversion Photoluminescence (UCPL)

Both up-conversion and down-conversion fluorescence emissions are present in certain CNDs. For in vivo bioimaging, up-conversion fluorescence emission—where the emission wavelength is shorter than the excitation wavelength, this is the best option. Longer wavelength bioimaging enhances tissue penetration and decreases background auto fluorescence, particularly in the near infrared (NIR) range. This type of emission requires a multi-photon excitation mechanism, which is most likely, what produced the up-conversion fluorescence emissions. (97)

Nonetheless, after being excited by many low-energy photons, electrons are thought to relax from a higher energy state of the p orbital (LUMO) to the s orbital, which is the origin of the effect. Similar stimulation of electrons in the s orbital can only result in the production of traditional down-conversion light. (97)

1.6.4.4.4 Photo-Induced Electron Transfer (PET)

The mechanism by which an electron in a molecule or material absorbs light and moves to another molecule or substance is known as photo-induced electron transfer. This technique is essential in many fields, including biological systems, photocatalysis, solar energy conversion, and optoelectronics. (47)

Because of CNDs exceptional properties related to photo-induced electron transport, extensive research has been conducted on this fluorescent material. They are beneficial for sensors, optoelectronics, and photovoltaics because of these features. These materials can efficiently contribute to the donation or absorption of electrons during energy transfer processes due to their electrical and optical properties. (47)

CNDs, on the other hand, have properties that make them a desirable alternative for developing state-of-the-art electronics and systems that employ photo-induced electron transfer for diverse purposes. Therefore, due to their excellent mechanical, electrical, optical, thermal, and biocompatible qualities in photo-induced electron transfer processes, CNDs have received widespread attention. (47)

Researching and comprehending the processes underlying photo-induced electron transfer in CNDs will help develop more environmentally friendly and efficient energy conversion technologies. It will also advance our knowledge of the basic mechanisms underlying the interaction of light and matter. (47)

Nonetheless, their distinct qualities make them desirable options for developing state-of-the-art electronics and photo-induced electron transfer devices. By examining the interactions of carbon quantum dots in a solid-state solution, we can improve our comprehension of the basic mechanics underlying the interaction between light and matter and create extremely efficient charge transfer systems for optoelectronic devices. (47)

1.6.5 Biological Applications of CNDs

As was previously discussed, CNDs are, naturally safe, and possess fluorescent characteristics. These features highlight the wide range of applications that CNDs can be used for, including bioimaging, drug delivery systems, medical photodynamic applications, biosensors, environmental applications, anti-microbial use, superior energy transfer, and very effective photocatalyst. (105)

For biological applications, CNDs toxicity and biocompatibility are critical considerations. Nonetheless, the toxic effect of CNDs varies according to their sizes, chemical structures, and concentrations. Growing concentrations might make cells more poisonous and hinder the growth of organs. Furthermore, CNDs may not be harmful in the dark but become hazardous when exposed to light because they release reactive oxygen species (ROS). Certain CNDs have the potential to induce photoexcitation-induced programmed cell death via autophagy and apoptosis, which could be utilized in photodynamic treatment. (50, 106-109)

1.6.5.1 Bio Imaging

A wealth of information about the distribution, cytotoxicity, and imaging capacity of sensors in cells can be obtained using in vitro imaging. A range of cell transfection imaging applications, including human neural stem cells (NSC), HepG-2, NIH-3T3, 4 T1, A549, and HeLa, have been effectively employed using CNDs. CNDs were mostly deposited in the cytoplasm of the cells after entering through endocytosis. There aren't many reports of CNDs entering the nucleus of cells. (51)

Additionally, Liu et al. discovered that 1.5–2 nm CNDs were absorbed by Escherichia and murine P19 progenitor cells, and that these images could be obtained by laser scanning confocal microscopy. The CNDs PL exhibited reduced photobleaching, no blinking, and great photostability throughout a wide wavelength range of 458–514 nm as shown in Scheme 1.8. (110)

Scheme 1.8

Confocal microscopy images of E. coli cells labeled with the CNDs

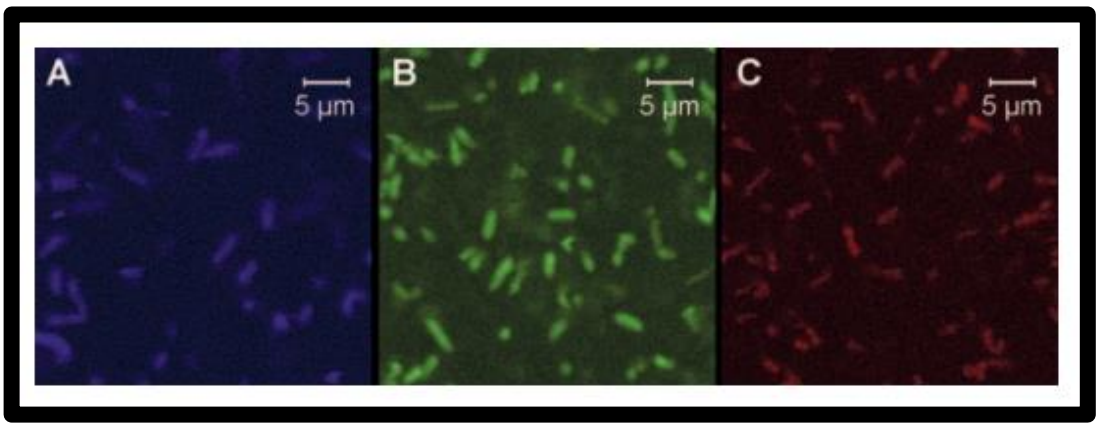

Zhu et al. used a solvothermal technique to create green fluorescent CNDs that were low cytotoxic and effectively used in cell imaging(111). Also, Tang et al. developed CNDs to specifically recognize cancer cells, transport drugs, and use fluorescence imaging by adding folic acid and doxorubicin DOX (112). However, Bhunia et al. created a range of CNDs with varying fluorescence and used folic acid to modify the CNDs surface to achieve target recognition. Choi et al. altered CNDs to include zinc phthalocyanine and folic acid to accomplish photothermal treatment and tumor targeting. Also, Dopamine's functional groups were preserved in the biomolecule-imitating CNDs that were created by neutralizing heat treating the drug. These CNDs could "trick" nuclear membranes to accomplish nuclear localization and imaging. (113-115)

Further investigation is required to gain a comprehensive understanding of the cellular uptake mechanism of CNDs., however the evidence available thus far points to an endocytosis mechanism. In the future, connecting the CNDs to facilitator peptides or proteins that more easily overcome cell membrane barriers may help improve CNDs accumulation in the cell and possibly even the nucleus. (116)

1.6.5.2 Sensing

Because CNDs are flexible, very water soluble, low toxicity, have great photo stability, and are highly biocompatible, they have also been used as biosensors. Nucleic acid, pH, glucose, cellular copper, H2O2 residual levels, and biosensors composed of CNDs materials can all be seen with the naked eye.

Because of its effective response to pH, local polarity, and metal ions in solution, CNDs fluorescence is a good choice for Nano sensing applications like pollution monitoring. Shabasy et al. and Das et al. explored carbon dots, in particular graphene and quantum dots, for sensing applications. Temperature, pH, light, phase, solvent, pressure, and multi-sensitivity have all been measured using it regularly. (47)

1.6.5.3 Drug Delivery and Gene Transfer

CNDs were applied to gene transfer and medication administration. For instance, the identification of cancer cells using folic acid-modified CNDs via amide condensation reaction offered a practical means of developing cell screening and disease recognition. (117)

Liu et al. assessed the transport capability of CNDs and discovered that in addition to having DNA transfer capabilities comparable to positively charged PEI-25K, CNDs also possessed the fluorescence property necessary to demonstrate the spreading of the plasmid DNA through the transfer process and offer comprehensive data for the study of the physiological function of plasmid DNA. The cell may be exposed to CNDs -DNA composites three hours after transfection. Upon stimulation at various wavelengths, dots retained their multicolored fluorescence properties during the transport process. (51)

Scientists altered a modification on CNDs to enhance drug delivery and gene transfer, a lot of trials were done. Hsiao et al. developed modified CNDs made of PEG and carried out the loading and delivery of doxorubicin (DOX). The release mechanism of doxorubicin in cells was demonstrated by fluorescence pictures. CNDs primarily displayed green fluorescence in the cytoplasm. In the nucleus, red fluorescence from DOX was visible. It showed that DOX enters cells and is then released into the nucleus for theraputic purposes (118). Moreover, PEI-modified CNDs were another common alteration. Because PEI-modified CNDs had a positive surface potential, they could take up negative DNA to transfer genes. (119)

While Wang and others achieved a near-infrared light/PH dual reactive hybrid gel employing the mixture of chitosan, PEG, and CNDs, others modified CNDs utilizing metal-organic frameworks. The aforementioned studies supported the clinical uses of CNDs by highlighting their potential for use in gene transfer and medication administration. (120, 121)

Ray and others used the MTT and Trypan blue assays to examine the vitality of HepG2 cells. For a CNDs exposure of less than 0.5 mg mL-1, the cell survival rate varied from 90% to 100%. The survival rate decreases to roughly 75% at CNDs doses above 0.5 mg mL-1, although the highest values tested were 10^2–10^3 times greater than required for bioimaging experiments, indicating that CNDs have little toxicity effects at practical concentrations for bioimaging. (122)

Sun and colleagues have also investigated the in vivo impacts of CNDs in addition to their in vitro cytotoxicity. After being exposed to CNDs (about 5 nm, created by laser ablation and surface passivation with PEG1500N), human breast cancer MCF7 and human colorectal carcinoma HT-29 cells underwent Trypan Blue and MTT assays to measure cell viability, proliferation, and death (123, 124). Although their findings for both cell lines were comparable to those of Ray et al., they discovered that CNDs concentrations as high as 0.1 mg mL-1 had a cell viability rate of better than 80%. Zhao and colleagues demonstrated that 293T human kidney cells exhibited cell survival above 80% when exposed to up to 400 ug mL-1 of electrochemically oxidized CNDs (in the absence of PEG passivation). (125)

Zheng et al. used L-aspartic acid and D-glucose as starting ingredients to create a straightforward thermolysis process that produced a unique fluorescence CD-Asp with self-targeting capabilities. Continuous full-color emission and great biocompatibility are displayed by the as-synthesised CD-Asp. CD-Asp exhibits a high degree of selectivity and targeting capacity toward C6 glioma cells, according to in vitro tests. The ability of CD-Asp to localize into glioma sites with significantly higher fluorescence than normal brain tissue is further confirmed by in vivo imaging studies, suggesting that CD-Asp can be employed as a targeted fluorescence imaging tool for brain gliomas. This study showed that CNDs could be a platform for the development of an intelligent nanomedicine that integrates therapeutic, targeted, and diagnostic capabilities. (126)

Cailotto et al generating CNDs via hydrothermal approach using variouse types of sbstrates (glucose, fructose, and ascorbic acid). The morphology, physicochemical, and toxologocal propereties were tested for G- CNDs, F- CNDs, and A-C CNDs. Also, the drug carrier model of the three synthesized CNDs was obtained using Dox as anti-cancer agent. The study demonstrated how the reagent selection affects the morphology, structure, and characteristics of the resulting CNDs and how these relate to the drug loading capacities. The binding trend demonstrated by the fluorescence quenching tests highlighted the significance of the graphitic core regions in attaining high CDs-DOX affinities. By using PL spectra recording and UV-vis absorption spectroscopy, the optical characteristics of the carbon dots were examined. The sp2 C=C conjugated system's π–π* transition is responsible for the shared absorption band observed in the UV-Vis spectra of the three distinct CNDs, which is located in the 225–235 nm area. The G– CNDs and F– CNDs had absorption peaks at 265 and 280 nm, accordingly, which were attributed to the C=O groups' n–π* transition on the surface. Additionally, the F- CNDs displayed an absorption peak at 360 nm for the transition linked to the surface state trapping excited-state energy. (65)

Also, Fluorescence quenching was used to quantify how the three distinct CNDs interacted with DOX. The findings unmistakably show that the addition of DOX gradually causes the fluorescence intensity to gradually diminish, which can be related to either static or dynamic interactions that occur between CNDs and DOX. (65)

However, The toxicity of the carbon nanoparticles against HeLa cells was then investigated in light of their possible application in the nanomedical industry. The vitality of the cells was assessed at various concentrations of CNDs in relation to a control solution. At every concentration that was evaluated, the G- CNDs demonstrated good viability. Rather, biocompatibility of the A- CNDs was only observed at low concentrations (< 250 μg/ml). The existence of the previously discovered carcinogenic furanics in the F- CNDs mixture explains why the F- CNDs showed substantial toxicity even at low doses. (65, 127)

In conclusion, CNDs are intriguing newcomers to the field of nanomaterials; they are intriguing luminous materials that hold great promise as future nanodevice building blocks. There is still a lot of opportunity for development, therefore creating better synthetic pathways and conducting more thorough fundamental research of their

characteristics is vital. These are intriguing nanomaterials in and of themselves, even though a complete knowledge of their photophysical characteristics is yet lacking. Not surprisingly, CNDs have exhibited substantial potential in optical imaging and related biomedical applications due to their low cost and easy scalability, superior stability chemically, biocompatibility/non-toxicity, colloidal stability, and durability of PL in vivo. Through appropriate doping, chemical processing, or as fundamental constituents of nanocomposites, they could potentially unlock an array of unanticipated uses, such as battery electrodes and contrast chemicals for magnetic resonance imaging (MRI) and magnetic data storage. Eventually, one can even imagine CNDs -based systems in advanced cancer/photodynamic therapy, organic light-emitting diodes (OLEDs), separation membranes, displays and back lights, administration of drugs, and displays. This is provided a greater understanding of their essential features is attained. Time will tell, but it looks like these emerging nanolights have a bright future. (116)

1.6.5.4 Cancer Disease

Numerous modern therapies, such as gene therapy, phototherapy, and immunotherapy, have been developed to largely overcome the limitations of existing cancer therapy approaches. However, despite their advancements, these cutting-edge modalities continue to face obstacles like systemic side effects, allergic reactions, and high specificity to cancer types, which hinder their widespread application in treatment. Furthermore, treating metastatic cancer calls for intricate, expensive, and oftentimes futile treatment choices. To improve the survival percentage of cancer patients in the final stages of the disease, innovative techniques for early cancer diagnosis, surveillance, and localized tumor management are essential. (128, 129)

The PL characteristics of carbon-based nanoparticles and their ability to act as a medium for medicine delivery while simultaneously delivering treatment make them promise for use in cancer therapy. CNDs can sense phosphorescence and fluorescence and can alter the structure of their surface. This makes imaging and detecting techniques like biosensor analysis and in-vivo tracking possible. (130)

However, the potential of CNDs treatment to induce programmed cell death is an exciting feature. Studies have demonstrated that when CNDs are subjected to photo-irradiation, they cause reactive oxygen species (ROS) to be produced in cancer cells. This could

trigger autophagy and apoptosis, leading to an extremely focused anti-cancer treatment that eliminates just abnormal cells while leaving healthy, normal cells untouched . (92)

Additionally, the physicochemical properties of CNDs have led to advancements in the treatment of numerous ailments. These particles nanoscale size enhance the surface area to volume ratio, which makes them a perfect platform for conjugating several medications needed for combination chemotherapy regimens. In cancer treatment, this selectivity will result in fewer side effects and more therapeutic efficacy. (131)

1.6.5.4.1 Photodynamic Therapy (PDT)

In recent years, more research and development of CNDs for PDT and PTT have been conducted. Nevertheless, CNDs can kill cancer cells by producing reactive oxygen species, which are created from ambient oxygen when a corresponding wavelength of light is applied. (132)

Furthermore, PDT offers minimum invasiveness and low toxicity. As a result, this treatment has become extremely important since it targets malignancies that are resistant to many drugs and may eventually replace traditional chemotherapy. Porphyrin-containing carbon dots were synthesized and demonstrated intrinsic photodynamic capacity following photoirradiation in a work by Xie et al. In addition, the porphyrin-CNDs demonstrated strong cytotoxicity, excellent photostability, high cellular uptake, and biocompatibility. Conversely, Zhou et al. produced CNDs with good biocompatibility using fresh, tender ginger juice. The CNDs produced many ROS, which indicated their specific cytotoxic effect against HepG2 cells. Even though, the normal liver cell (FL83B) and normal mammary epithelial cell (MCF-10A) lines were equally cytotoxically affected by these CNDs. According to a different study by He and colleagues, diketopyrrolopyrrole (DPP)--based fluorescent CNDs were made using a one-pot hydrothermal method using chitosan and DPP as precursors. The DPP-CNDs demonstrated excellent hydrophilic and biocompatible qualities in addition to their ability to produce singlet oxygen. Additionally, the DPP-CNDs reduced the growth of tumors both in vivo and in vitro when exposed to 540 nm laser radiation. (132-135)

1.6.5.4.2 Photothermal Therapy (PTT)

Photothermal therapy (PTT) is also referred to as thermal ablation therapy or hyperthermia from a theragnostic perspective. PTT is a diagnostic and therapeutic technique that gives high-specificity analysis with minimal invasiveness. It works by converting absorbed energy into heat using electromagnetic radiation in the infrared (IR) range. Since carbon dots have a large number of π electrons and behave similarly to the free electrons of metallic nanomaterials, they are regarded as appealing photothermal agents. (132)

However, Zheng and colleagues used a solvothermal method to create multifunctional theragnostic CNDs, or CyCNDs. Excellent PTT efficiency was demonstrated by CNDs, and in vitro experiments showed that the viabilities of HepG2 and CT26 cell lines were lowered in the presence of CyCDs. Another study by Nurunnabi et al. showed that heat (>50 °C) and decreased cell viability are produced by electron clouds formed by carboxylated photoluminescent graphene nanodots (cGDs) activated by NIR laser irradiation. 70% of MDA-MB 231 cancer cells were eliminated by heat ablation. Bao X. et al. demonstrated that following an in vivo CD injection, the PTT significantly slowed tumor growth and extended the mice's survival. Conversely, some in vitro research has shown that PTT with chemotherapy outperforms monotherapy in terms of cancer cell death. (132, 136-138)

1.7 Carbohydrates

Carbohydrates are abundant, renewable, and structurally diverse organic molecules composed of carbon, hydrogen, and oxygen. They serve as ideal green precursors for CNDs synthesis due to their high carbon content, ease of carbonization, and the presence of multiple hydroxyl groups that enhance water solubility and surface passivation. Compared to synthetic chemicals, carbohydrates offer an eco-friendly alternative for nanomaterial synthesis. Various mono-, di-, and polysaccharides have been utilized to generate CNDs with tunable optical and chemical properties, depending on the sugar type and synthesis conditions. The choice of sugar influences quantum yield, fluorescence intensity, surface functionality, and biocompatibility, which are all critical for biomedical applications including imaging, drug delivery, and photodynamic therapy.

Sugar-derived CNDs exhibit diverse physicochemical properties that are strongly influenced by the synthesis conditions and the molecular structure of the sugar precursors. The size distribution of CNDs synthesized from sugars typically ranges from 1–10 nm, and their morphology is often quasi-spherical with high monodispersity. These nanoscale dimensions allow for efficient cellular uptake and fluorescence-based bioimaging. Surface chemistry plays a critical role in determining the solubility, fluorescence, and biological interaction of CNDs. Functional groups such as hydroxyl (-OH), carboxyl (-COOH), and amino (-NH_2) are commonly found on sugar-derived CND surfaces due to incomplete carbonization and the natural chemical composition of the precursor. Hence, these groups enhance hydrophilicity and allow for further functionalization for biomedical-applications.

Synthesis parameters—including hydrothermal temperature (typically 150–250°C), reaction time, and solution pH—significantly affect the size, quantum yield, and surface charge of the resulting CNDs. For example, higher synthesis temperatures often lead to smaller and more carbonized dots with stronger fluorescence, while more acidic or basic environments can influence the type and density of surface functionalities. Control over these parameters enables the fine-tuning of optical and biocompatibility properties, which is crucial for the design of efficient theranostic agents in cancer treatment and imaging. (104, 139, 140)

1.8 Literature Review

Among the most diverse and significant families of biomolecules found in nature, carbohydrates supply well-defined chiral scaffolds that are ready for numeric position transformation as well as alcohol functions. Therefore, the quantity, heterogeneity, and availability of carbohydrates, coupled with their high water solubility, cost-effectiveness, low carbonization temperature, and generally non-toxicity, make them a highly appealing starting material for the synthesis of CNDs. With the multitude of available options for tuning CND synthesis, it is unsurprising that researchers have already recognized the advantages of carbohydrates in the development of novel fluorescent carbon dots (F-CNDs) with enhanced properties. (65)

For instance, fluorescent carbon dots (F CNDs) were generated using various methods using common disaccharides, such as sucrose, lactose, and maltose, and simple monosaccharides, such as glucose, glucosamine, mannose, fructose, and their

derivatives(141). So, It is also possible to create CNDs with a lot of carboxylic groups on their surface by using monosaccharides, such as glucose, which are inexpensive, plentiful, and biocompatible. (65)

However, glucose is considered as a biomass-derived substrate for the formation of CNDs with 7% (QY), through microwave method through oxygen groups on the surface of glucose. (61, 74, 142-144)

Nonetheless, in recent decades the hydrothermal approaches used for synthesis of suger-based CNDs (65). Because of its unique properties and viability as a model to comprehend the synthesis and source of PL in carbon-based nanostructures, CNDs derived from D-glucose, have garnered a lot of interest. One of the most utilized methods for preparing CNDs is to synthesize them in a hydrothermal environment. It's challenging to understand all of the specifics of this method. (145)

The need to discover an easily accessible, affordable, and renewable carbon source has arisen from the need to sustain CNDs sustainably; glucose, a monosaccharide, is a potential alternative. In addition to being inexpensive and widely accessible, glucose also possesses a low carbonization temperature and easily ring-opens, showing a reactive aldehyde moiety that may be utilized for conjugations, polymerizations, and (hetero)aromatic formation, all procedures that are appropriate for the production of CNDs. Since glucose has a high water solubility and low toxicity by nature, it is a perfect carbon source for CNDs production and has been employed extensively under several experimental conditions. (141)

As far as we know, Yang et al. were the first to use a microwave approach in conjunction with PEG-200 to synthesize glucose-based CNDs, as shown in scheme 1.9. (62, 141)

The team also demonstrated, remarkably, that favorable PL characteristics and QYs of up to 6.3% were possible to achieve with the application of PEG-200 as a surface passivation agent (SPA). Two common methods are used to enhance the PL features of F CNDs, and one of them is the use of SPAs. On the CNDs surface, SPAs are said to offer consistent PL trapping sites in addition to developing novel functionality that may cooperate with the core to generate fluorescence. (141)

Scheme 1.9

Microwave-driven reaction of glucose in the presence of PEG-200 to afford blue-emissive CNDs (12)

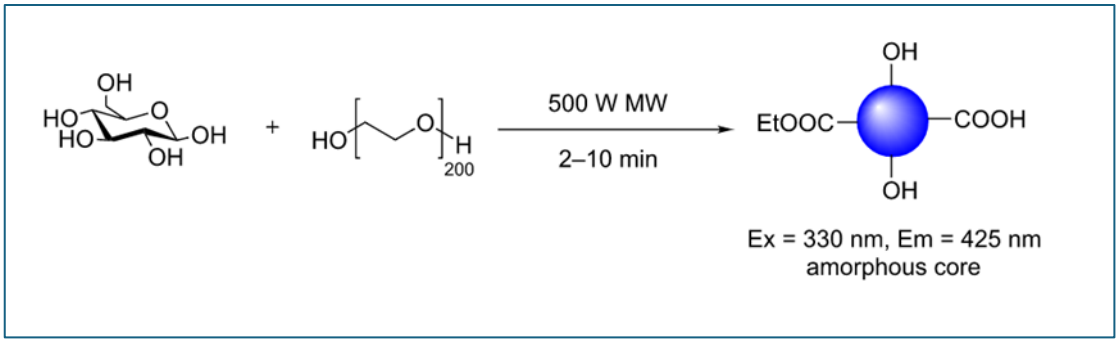

Yoshinaga and colleagues have endeavored to effectively manufacture consistent CNDs by employing a microwave heating mechanism that can sustain the reaction solution at an even temperature. By hydrothermally treating D-glucose at 200°C for five to sixty minutes, they were able to synthesize CNDs. According to transmission electron microscopy, the CNDs particle size increased with hydrothermal duration. Additionally, the CNDs aqueous dispersions (10 mg L−1) showed an increase in absorbance and maximum PL intensity as the hydrothermal time increased. The dispersion's maximum PL intensity declined for pH values less than 4 and higher than 10, whereas the absorbance at the excitation wavelength stayed constant. According to these findings, there were more emission and absorption sites as the particle size grew, and the emission sites were found closer to the surface of the produced CNDs. (146)

Furthermore, CNDs based on glucose were obtained by other researchers. In order to synthesize CNDs with remarkable PL, Travas-Sejdic et al. additionally reflux glucose substrates in an acidic solution (H_2SO_4). Utilizing PSA improves the QY and PL properties, as demonstrated by earlier investigations. Thus, Travas-Sejdic et al. improved the QY from 1% to 13% by obtaining the PSA under high temperature (120°C) in 4,7,10-trioxa-1,13-tridecanediamine (TTDDA) solution for 72 hr. Additionally, when TTDDA is used, the zeta potential (ZP) is increased from -37.3 mV (non-passivated CD) to 3.46 mV (TTDDA passivated CD). (104)

Wang and colleagues additionally developed a new protocol termed as the hydrothermal method, that may have the potential to replace the microwave approach. However, the alternate method included conjugating the glucose substrate with KH_2PO_4 in a Teflon-lined autoclave at a high temperature of 200 °C for 12 hours. Using this method, intrinsic

fluorescence emission is produced by simultaneously generating and surface passivating CNDs. Also, the CNDs show varied fluorescence emissions that can be produced by simply changing the KH_2PO_4 concentration. Wang and others concluded that a simple one-step approach for creating intrinsic fluorescence CNDs has been shown. Specifically, hydrothermally treating glucose with KH_2PO_4 results in the production of monodispersed and photostable fluorescent CNDs. The size of the CNDs that are so generated is mostly controlled by the KH_2PO_4. By altering the KH_2PO_4 concentration, the fluorescence emission of the resulting CNDs can be tuned. The luminous and hydrophilic CNDs showed promise for fluorescent cellular imaging through cellular uptake. (147)

Despite this, the majority of mammalian cells in this specific area are likewise autofluorescent. This means that QYs on most CNDs made with blue emission are unsuitable for bioimaging applications. A good substitute are CNDs with multicolor/excitation-dependent emission that can be red-shifted so as to circumvent the window of cellular autofluorescence. Regretfully, as the excitation is redshifted, the CNDs fluorescence usually becomes weaker. Either a high QY in the blue or sufficient green to red emission characterizes the perfect CNDs probe for bioimaging applications. The green-emitting glucose-based CNDs made by Wang et al. are perfect for the bioimaging applicationas as demonstrated by their use in HepG2 cellular internalization research. After exposure for 72 hours and concentrations up to 625 μg/mL, the green CNDs demonstrated biocompatibility with cells. Since cell internalization was shown by laser scanning confocal microscopy (LSCM), these materials are promising candidates for use as bioimaging agents. (141, 147, 148)

Hao and colleagues have also explored the incorporation of boron, an electron-accepting element, as an additive, alongside the introduction of electron-donating heteroatoms such as nitrogen (N) or sulfur (S) as dopant agents to enhance the photoluminescence (PL) properties of CNDs. Boric acid was added to glucose hydrothermally carbonized in a Teflon autoclave at 180 °C for 12 hours to create the CNDs. The resulting fluorescent nanoparticles were negatively charged, with ZP values of -40.7 mV, and had an average radius of 4 nm. The identification of B in the CNDs structure was verified by FTIR and XPS analyses. Compared to other published heteroatom-doping syntheses, the inclusion of boron did not dramatically alter the characteristic blue fluorescence profile. However, Fe3+ ions dynamically lowered the fluorescence of the CNDs. Mechanistic analyses

indicated that interactions between Fe^{3+} and the CNDs surface were likely responsible for the dynamic quenching model that predominated at low concentrations. This may indicate that the Fe3+ ion intercepts an excited CNDs state, triggering fluorescence quenching. The researchers demonstrated how the synthesized CNDs can detect Fe3+ in tap water samples with a limit of detection of 242 nM. (149)

Further, Xu and Collaeouse succeeded in synthesizing CNDs utilizing glugose and taurine in a hydrothermal technique. The mass ratio, reaction duration and temperature, pH, and solution's iron-ion sensitivity are among the elements that have been taken into account when determining the PL properties. The optical characteristics and chemical structures are assessed using X-ray photoelectron spectroscopy (XPS), photoluminescence (PL), UV-Vis absorption spectroscopy, Fourier transform infrared (FTIR) spectroscopy, and transmission electron microscopy (TEM). However, with 30 milliliters of pure water, the researcher reacted differently with taurine (2 mg) and glucose (2 mg). The solution was then heated for one to three hours at 150°C in a Teflon-lined thermal autoclave. Next, the cooled brownish-yellow mixture was centrifuged for 10 minutes at 12,000 rpm to remove the black precipitate. Subsequently, the yellowish supernatant was reserved for additional analysis. Therefore, Xu et al. present a straightforward and environmentally friendly technique for synthesizing CNDs from glucose and taurine using a hydrothermal process. (150)

However, due to their tiny size, nearly isotropic form, and abundance of hydrophilic functional groups on the surface, FCNDs with a diameter of less than 10 nm are highly appealing for biological imaging and biosensor uses. (116)

In recent years, several glucose-based CNDs have been described as drug-delivery vehicles. Yunus et al. created CNDs by ultrasonically sonicating glucose or sucrose in an atmosphere of oxidizing conditions provided by H_3PO_4/H_2SO_4 (151). Strong oxidizing conditions were used during the production of the resulting CNDs, which were blue-emissive and had surface carboxylic acids that could be functionalized. A steric blocking and enhanced permeation and retention (EPR) shell were obtained through surface conjugation with PEG-diamine, which also provided an amine functionality for additional surface conjugation. The anticancer medication methotrexate (MTX), which is extensively researched and used to treat lung cancer among other cancers, was then conjugated via amide coupling chemistry mediated by ethylenedicarbon (EDC).

Internalized MTX- CNDs were compared to cells exposed to non-functionalized amine-bearing C-Dots in H157 lung cancer cells. The MTX- CNDs were extremely toxic to H157 cell cultures, whereas the amine-CNDs exhibited negligible cellular toxicity. This finding emphasizes the potential utility of carbohydrate-derived CNDs as delivery systems for traditional cancer treatments. (152)

Li et al. synthesized carbon nanodots using glucose through a hydrothermal method at 180°C for 8 hours. The resulting CNDs exhibited a narrow size distribution (~3–5 nm), blue fluorescence with a quantum yield of 16.2%, and excellent water dispersibility. The study emphasized their potential in fluorescent imaging due to their strong photostability and minimal cytotoxicity. (153)

Moreover, Zhou et al. utilized fructose as a precursor to produce CNDs via microwave-assisted synthesis. Their nanodots showed high fluorescence intensity and uniform morphology. The authors highlighted the enhanced antioxidant properties of the fructose-derived dots compared to glucose-based counterparts. (154)

Further, Singh et al. used sucrose as a starting material for CNDs production. The synthesized nanodots had lower quantum yield but better functional group diversity. The study pointed out that the disaccharide nature of sucrose led to increased surface hydroxyl groups, enabling potential conjugation with biomolecules. (155)

As well, Liu et al. developed CNDs from starch using a pyrolytic technique. The carbon dots had a wider size distribution but showed promising biocompatibility. Despite lower fluorescence intensity, the starch-derived CNDs were effective in cellular imaging and drug delivery trials in vitro. (156)

Subsequently, Chen et al. extracted nanodots from cellulose and demonstrated that high carbonization temperature yielded CNDs with improved stability and surface passivation. These dots displayed moderate fluorescence but superior stability under various pH and temperature conditions. (157)

Whereas Wang et al. engineered lactose-based CNDs that showed specific targeting ability in gastrointestinal models. The dual sugar moieties enhanced receptor-mediated endocytosis, proving useful for targeted bioimaging applications.

Overall, the reviewed studies illustrate the critical role of sugar type and synthesis method in dictating the physicochemical and functional characteristics of CNDs. These findings support the ongoing exploration of carbohydrate-derived nanodots for use in cancer diagnosis, bioimaging, and targeted drug delivery.

1.9 Aim of the Thesis

In this study, we will use the hydrothermal process as a bottom-up strategy to manufacture carbon dots from different kinds of sugars, and we will test their anticancer activity on a range of cell lines in addition to possible mechanisms through the ROS production.

1.10 Objectives

1. Synthesis of carbon Nano dots from various types of sugars.
2. Optimizing the various conditions in the bottom-up synthetic approach
3. Characterization of the synthesized carbon dots.
4. Study the anticancer activity of the synthesized CNDs on various types of cancer cells lines with the possible mechanism.

Chapter Two

Materials and Methods

2.1 Materials and reagents

All materials used in the experiments were of analytical grade. Different type of sugars, Glucose (M.W: 108.16, Lot#: MFCD00063774), Galactose (M.W: 180.16, Lot#: PHR1206), Lactose (M.W: 342.30, Lot#: MFCD00166994), Fructose (M.W: 180, Lot#: MFCD00148910), Maltose (M.W:342.3 g/mol, Lot#: MFCD00149343) and Sucrose (M.W: 342 g/mol, Lot#: S0389) all purchased from Sigma Aldrich Company USA, and utilized without further modifications.

In the biological part, we used the following cell lines, Hep3B from ATCC (Manassas, VA, USA) (HB-8064), and LX-2 from Sigma-Aldrich (SCC064), We also used Dulbecco's free Ca+2 -phosphate-saline buffer (REF # 02-023-1A), Pen-Strep Solution (catalog #030311B), and L-glutamine solution (REF # 03-020-1B) which were purchased from Biological Industries, Jerusalem. Trizma base (Lot number SLBF2864V) purchased from Sigma Life Science.

2.2 Techniques and Instruments

A sterilizer was purchased from Memmert GmbH Company, Germany. Ultraviolet-visible (UV-Vis) spectra were recorded using a 7315 spectrophotometer, Jenway UK between 200 and 800nm, to determine the absorption spectra of the various synthesized CNDs, using 10mm quartz cuvettes. For the agitation of nanoparticles in a solution we used water bath sonicate (Elma sonic S70H, Elma, Germany) for 15 minutes. Accumax variable micropipette, UK, used for pipetting. Fluorescence spectroscopy [the PerkinElmer LS50B model] to determine the excitation and emission spectra of the synthesized CNDs in the emission range of 320 to 650 nm. Fluorescence spectra were collected at excitation wavelengths ranging from 320 to 460 nm, with a 20 nm increment. Fluorescence spectra also used to estimate quantum yield (Q.Y.). Fourier transformed infrared (FT-IR) spectroscopy to determine the essential functional groups found in the structure of the carbon dots. Here we used a Thermo Scientific Nicolet IS5 FTIR equipment fitted with an ATR sampling apparatus in the range of 4000−650 cm^{-1} with 64 scans at 8 cm^{-1} resolution. Atomic Force Microscopy (AFM), to determine the size and

morphology of the synthesized carbon dots. Nanosurf Core AFM microscope was utilized to collect (AFM) pictures and profiles, which were then processed using Gwyddion software. AFM samples were created by dropping a diluted CNDs solution onto mica surfaces and vacuum drying at 120 °C. All materials were measured for ζ-potential using the NanoBrook Omni equipment with phase analysis light scattering (PALS).

X-ray photoelectron spectroscopy (XPS) measurements were carried out with SPECS SAGE HR 100 system equipped with 100 mm mean radius PHOIBOS analyzer where MgKα X-ray source was used, for XPS samples, CDs solutions were drop casted on titanium-glass coated substrates and left dried under vacuum for 24 hrs

For biological purposes, we used the following: Cell culture CO_2 incubator (ESCO, serial#:2012-74317), Also, an Accumax Variable micropipette with normal and long narrow gel loading tips was used. Eppendorf Thermo mixer dry, Shaker, PH/ORP meter (by HANNA), Benchtop UV Transilluminator, Photodoc-it™ imaging system, XB-30 Flak Ice maker M.R.C LTD.

2.3 Synthesis of CNDs

Prior to establishing the final optimized protocol for synthesizing CNDs, a series of preliminary experiments were conducted to determine the most suitable synthesis conditions. These experiments involved variation of temperature, reaction time, and chemical-treatments.

Initially, hydrothermal synthesis was carried out at two different temperatures: 100 °C and 150 °C, with reaction durations of 3 hours, 6 hours, and 12 hours, respectively. The aim was to assess how temperature and time influenced the yield, fluorescence intensity, and particle size distribution of the resulting CNDs.

In parallel, alternative oxidation approaches were also explored. Attempts were made to chemically modify or enhance the fluorescence of the synthesized dots using hydrogen peroxide (H_2O_2) as an oxidizing agent. However, these trials led to inconsistent surface passivation and, in some cases, partial degradation of the nanostructures. Furthermore, experiments were performed using conventional heating methods instead of autoclaving, but these failed to produce homogenous or photoluminescent nanodots, likely due to insufficient pressure and thermal control.

Regarding the above observations, it was concluded that the optimal condition for high-quality CNDs required a hydrothermal reaction at higher temperature and pressure, which ultimately led to the selection of the final synthesis protocol described below.

Based on the optimization trials, the most effective procedure for synthesizing carbon nanodots was established as follows:

a defined quantity of (glucose, galactose, fructose, sucrose, lactose, and maltose) using the hydrothermal autoclave method technique, were dissolved at a specific concentration in deionized water (0.1 g/50 ml) for each one of them. Then, sugar solutions were stirred for 10 minutes under a magnetic stirrer rotation to attain homogenous solutions. After that, we inserted them in Teflon-lined stainless steel, and an autoclave process at 200 °C for 24 hours took place. Subsequently, the autoclave was cooled down to room temperature. Then, the resulting solution was filtered through a 0.2 μm Nylon membrane microfilter, and the yellowish product that was obtained was then sonicated for 15 minutes for further characterization and applications.

The optimization process required considerable time and effort, involving numerous iterations and critical evaluation of experimental parameters. Each step in the refinement process contributed to a deeper understanding of the synthesis behavior and its impact on the physicochemical properties of the CNDs. This meticulous trial-and-error approach was essential to achieve a stable, reproducible, and biocompatible nanomaterial suitable for biological applications.

2.4 Cell Culture and Cellular Viability

The Hep3B and LX-2 cell lines were acquired from the Central Research Lab storage at the Faculty of Medicine and Health Sciences, An-Najah National University. They were cultured in RPMI media (Gibco, USA) with 10% fetal bovine serum (FBS) (Gibco, USA) and supplemented with 100 units/mL penicillin (Gibco, USA) and 100 μg/mL streptomycin (Gibco, USA). The cells were maintained at 37 °C in a humidified atmosphere containing 5% CO2, following the provider's instructions.

For the viability assays, cells in the logarithmic growth phase were subculture after washing with Ca2+-free PBS. Trypsin (0.025%) was used to detach the cells for up to 5 minutes, and trypsin inactivation was achieved using CGM. After collecting, the viable

cell count was determined using trypan blue stain, following which the cell concentration was adjusted to 92000 cells for Hep3B and 59000 cells for LX-2. The cells were then seeded into 96-well culture plates at a density of 5000 cells per well. After 24 hours of incubation, the cells were treated with various concentrations of the synthesized CNDs for 48 hours in a final volume of 100 µL. The concentrations used were 150 µg/ml, 125 µg/ml, 100 µg/ml, 75 µg/ml, 50 µg/ml, and 25 µg/ml at pH 7.4. At the endpoint after 48 hours, 20 µL of MTS solution (Biotium, USA) was added to each well, and the cells were further incubated for 3-4 hours. The absorbance at a wavelength of 590 nm was then measured using an Elisa reader (BioTek, USA). The data were analyzed using GraphPad Prism V9.0 software to obtain IC50 (half-life) values with the [inhibitor] vs. normalized response (variable slope) model. The experiments were done in triplicate. (158)

To evaluate the selectivity and therapeutic window of the synthesized CNDs, the Selectivity Index (SI) was calculated. The SI provides a measure of the differential cytotoxicity of a compound between cancerous and normal cell lines. It was determined by dividing the IC_{50} value obtained for the normal hepatic LX2 cell line by the IC_{50} value obtained for the hepatocellular carcinoma Hep3B cell line.

A higher SI value indicates greater selectivity towards cancer cells with minimal toxicity to healthy cells, thus demonstrating better therapeutic potential. IC_{50} values for both cell lines were determined using nonlinear regression analysis with GraphPad Prism v9.0 software, employing the [inhibitor] vs. normalized response (variable slope) model. Each experiment was conducted in triplicate to ensure statistical reliability.

2.5 Glutathione Assay Procedure

The glutathione-deficient assay was employed to investigate the ability of synthesized CNDs to generate reactive oxygen species (ROS):

1. To initiate oxidation, 225 µl of GSH (0.8 mM in the 50 mM bicarbonate buffer) was added to CNDs dispersions (125 µl at 80 µg/mL) in 50 mM bicarbonate buffer (pH 8.6). The samples were processed in a quintuple format. As a negative control, a GSH solution devoid of nanomaterials was implemented. H2O2 (10 mM) was employed as a positive control for the oxidation of GSH (0.4 mM).

2. In order to prevent illumination, the mixtures were deposited in Eppendorf tubes and covered with alumina foil. Subsequently, they were subjected to a 150 rpm agitator at an ambient temperature for a duration of 2 hours.

3. Following incubation, the mixtures were treated with 785 µl of 0.05 M Tris-HCI and 15 µl of 100 mM DNTB (Ellman's reagent, 5,50-within-bis-(2-nitrobenzoic acid), Sigma-Aldrich) to produce a yellow product and/or dispersion. Dissolve 39.6 mg of 5,5-dithio-bis(2-nitrobenzene- acid) (DTNB) in 10 ml. A buffer containing phosphate (0.1M) at a pH of 7.0 is required.

4. A spectrophotometer was employed to measure their absorbance at 405 nm. The oxidation of GSH was quantified in the following manner: GSH loss percentage = (abs. of negative control - abs. of sample) /abs. of negative control × 100. (159)

Chapter Three

Results and Discussion

3.1 Synthesis and characterization of Carbon nanodots

3.1.1 CNDs synthesis

The synthesis of CNDs from various types of sugars (Glucose, Galactose, Fructose, Lactose, Maltose, and Sucrose), was achieved by a bottom-up approach, which included a 24-hour hydrothermal carbonization process at 200 °C. Sugars are a biocompatible, low-cost material that can make carbon dots with many carboxylic groups. Therefore, the goal of using sugar is to create biocompatible CNDs that are suitable for medical applications and prevent the formation of harmful chemical compounds.

After synthesizing the CNDs, we used a range of purification processes to remove any intermediate or precursor components. We employed filtration and centrifugation in this operation. The synthesized CNDs had a product yield of 15%. Scheme 3.1. illustrates the synthesis process.

Scheme 3.1

Synthetic steps to produce CNDs from sugars

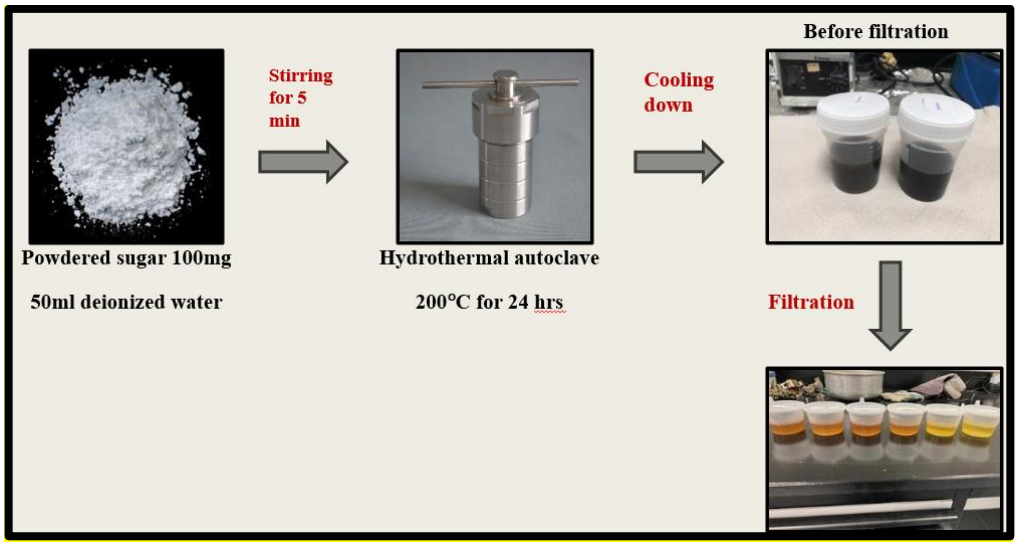

3.1.2 Size and Chemical Surface Composition

The morphology and size of produced CNDs were studied using AFM. The AFM findings in Fig.3.1 (A1-F1) demonstrate that the CND heights for glucose, fructose, galactose, lactose, maltose, and sucrose. having an average particle size range of 2.7-4.5 nm.

Figure 3.1

AFM Images of Synthesized CNDs

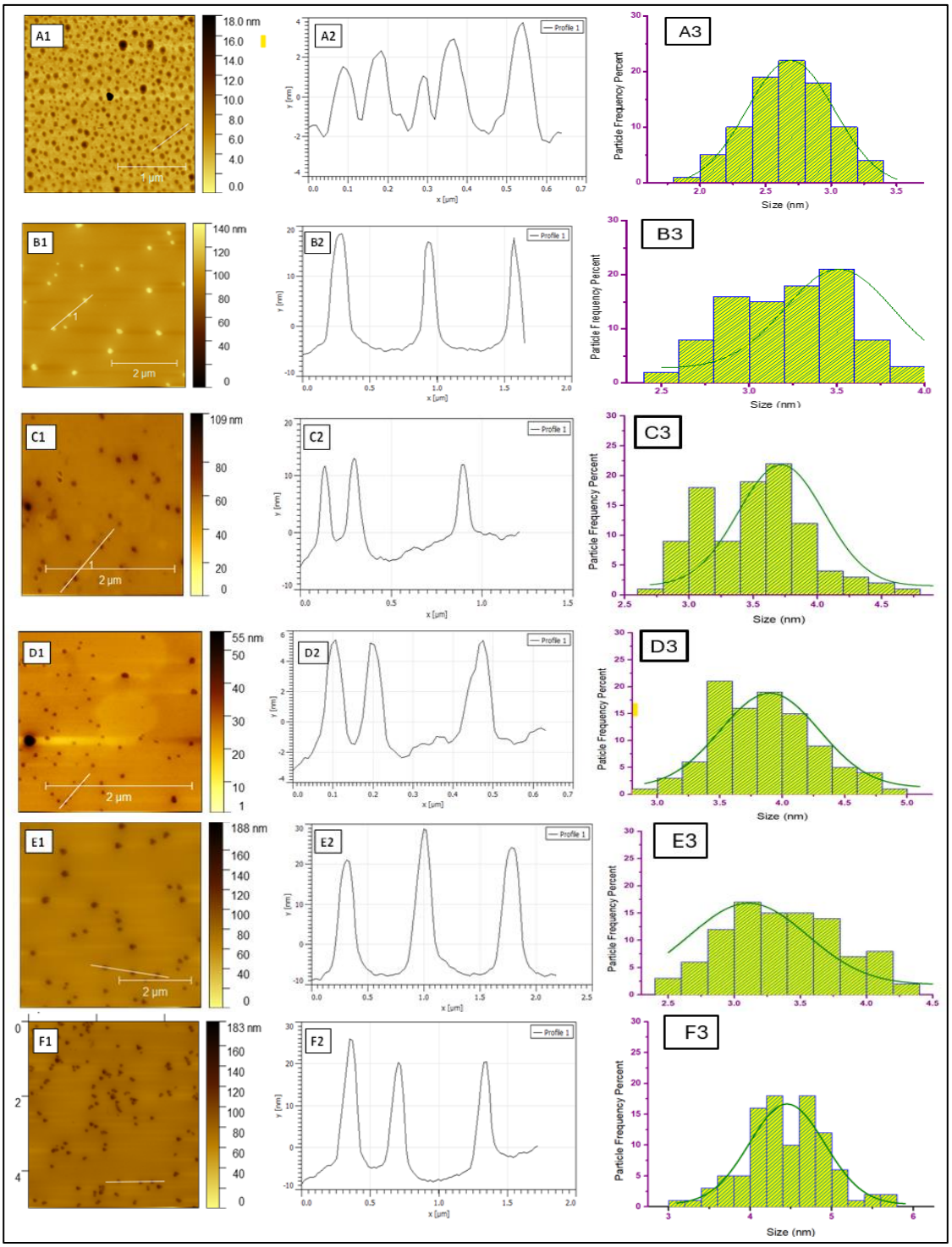

Note: A1: AFM image of Glucose CNDs. A2: The height profile of Glucose CNDs.A3: size distribution histogram extracted from AFM images of the prepared Glucose CNDs sample. B1: AFM image of Fructose CNDs. B2: The height profile of Fructose CNDs.B3: size distribution histogram extracted from AFM images of the prepared Fructose CNDs sample. C1: AFM image of Galactose CNDs. C2: The height profile of Galactose CNDs. C3: size distribution histogram extracted from AFM images of the prepared Galactose CNDs sample. D1: AFM image of Lactose CNDs. D2: The height profile of Lactose CNDs. D3: size distribution histogram extracted from AFM images of the prepared Lactose CNDs sample E1: AFM image of Maltose CNDs. E2: The height profile of Maltose CNDs. E3: size distribution histogram extracted from AFM images of the prepared Maltose CNDs sample F1: AFM image of Sucrose CNDs. F2: The height profile of Sucrose CNDs. F3: size distribution histogram extracted from AFM images of the prepared Sucrose CNDs sample.

The chemical composition and surface functional groups were determined using FTIR and XPS, as illustrated in Figures 3.2-3.5. As shown in Figure 3.2, the FTIR spectrum peaks at 3390, 2920, 2860, 1600, 1259, and 1084 cm^{-1} . These may be the O-H (hydroxyl), C-H, C=C/C=O (carbonyl), COO- (carboxylates), and C-O-C (epoxides) bands, respectively. (160)

To ensure comparability between samples, FTIR spectra were normalized based on the intensity of the most prominent absorption peak (e.g., O–H stretching at ~3400 cm^{-1}). All spectra were adjusted so that the reference peak intensity was set to 1.0, and the relative intensities of other peaks were recalculated accordingly. This normalization allowed a more accurate assessment of changes in surface functional groups among different synthesis conditions.

All spectra exhibit characteristic bands commonly associated with CNDs, including broad O–H stretching vibrations around ~3400 cm^{-1}, C–H stretching near ~2900 cm^{-1}, and strong bands between 1600–1000 cm^{-1} corresponding to C=O, C=C, COO^{-}, and C–O–C functional groups.

Normalization enabled qualitative comparison of functional group intensity and distribution across different sugar-derived CNDs, regardless of variations in concentration or sample preparation. This approach highlights differences in chemical structure that may influence solubility, fluorescence, and biocompatibility in subsequent biological applications.

Figure 3.2

Normalized FT-IR spectrum of all synthesized CNDs from various sugars

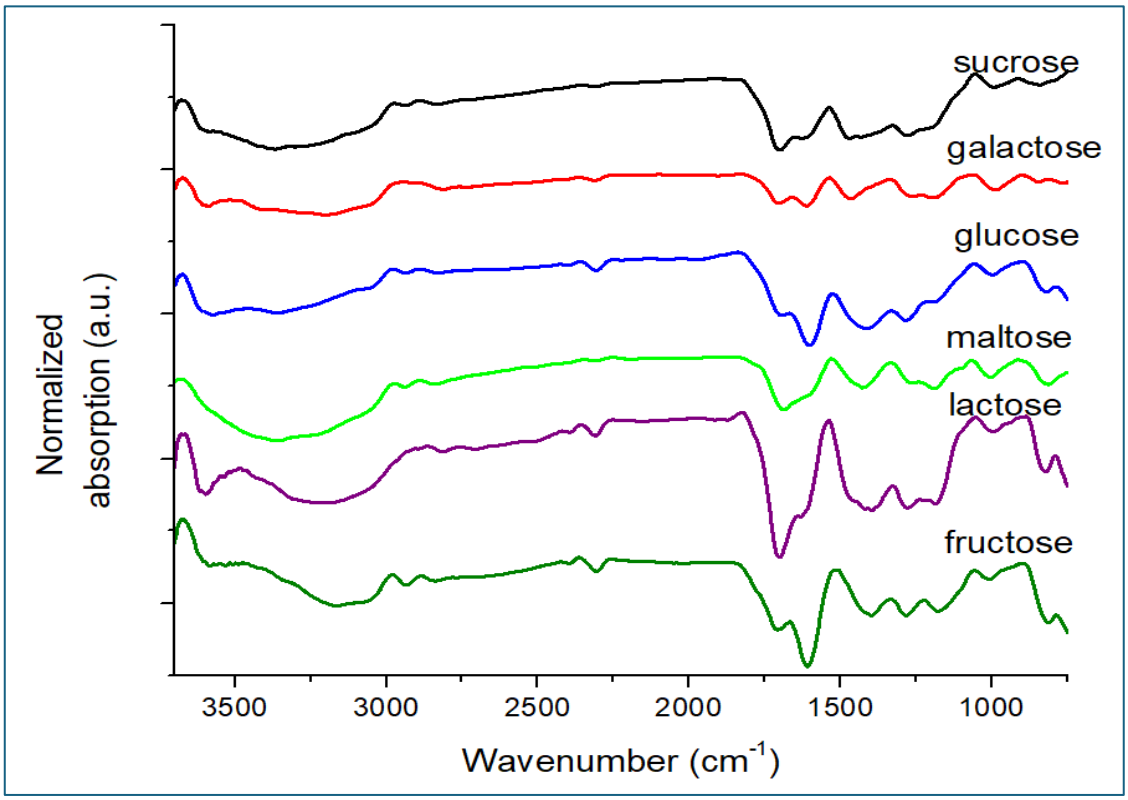

The XPS measurement indicates that the elements carbon and oxygen make up the synthetic CNDs with respective atomic percentages of 65.22 and 33.47 %for Fructose, 74.1 and 25.9% for Sucrose, 72.79 and 27.03% for Glucose, 69.72 and 30.28% for galactose, 74.82 and 25.18 % for maltose and 71.08 and 28.82% for lactose, respectively as shown in Figure 3.3 that illustrates the two peaks at 285 and 532 eV in the XPS survey spectrum. The deconvolution of the high-resolution C 1s core Fig. (3.4 A-F) revealed three peaks at 284.8, 286.3, and 288.3 eV, which may correspond to the C–C/C=C, C–O, and C=O functional groups, respectively. Moreover, Fig. (3.5 A-F) shows the deconvolution of the O 1s into two peaks, O=C at 532.4 eV and O-C at 533.2 eV. (161)

The XPS results are very similar to the FT-IR results. They show that the produced CNDs have different oxygen groups on their surface, including hydroxyl, carbonyl, and carboxylic acid. On the surfaces of the CNDs, the identified functional groups work as a passivation layer. This layer improves photoluminescence and makes CNDs easier to dissolve in water. A high number of remaining hydroxyl groups enhances CND stability and hydrophilicity in polar liquids. These hydrophilic groups not only help to explain the

luminescence mechanisms, but also increase the product's safety for use in biochemical research. (52)

PALS ζ potential studies verified the presence of oxygenated groups on the CNDs surface, showing a strong negative charge of −29.32, 18.03, -24.14, -27.88, -23.96, and -21.15 ±1.5 mV related to glucose, galactose, fructose, lactose, maltose and sucrose CNDs respectively in phosphate buffer solution (PBS @ PH = 7.4), thereby explaining the CNDs excellent dispersibility in water.

Figure 3.3

XPS Survey

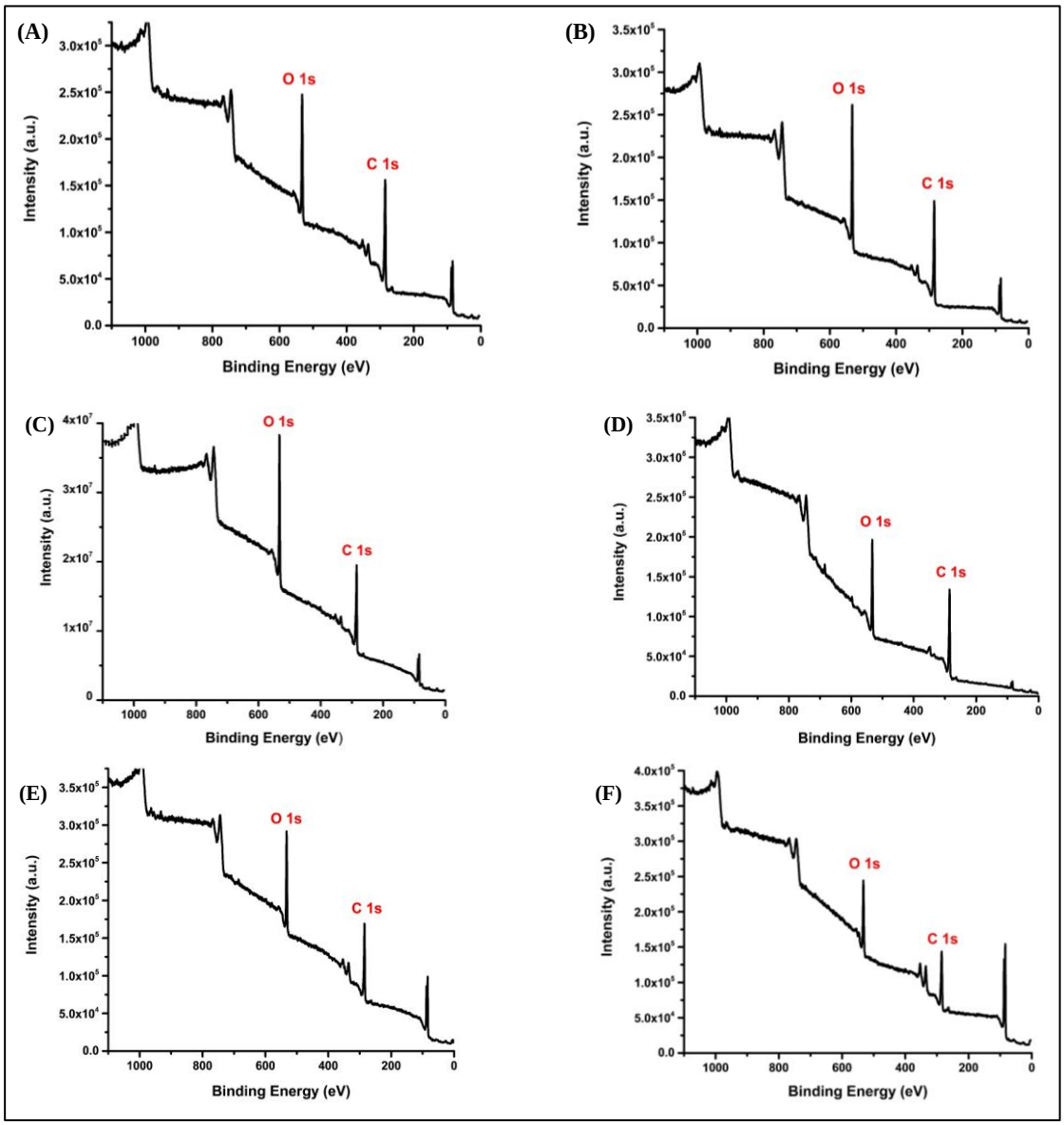

Note: (A) Glucose, (B) Galactose, (C) Fructose, (D) Maltose, (E) Lactose and (F) Sucrose.

Figure 3.4

High-resolution C1s XPS spectra

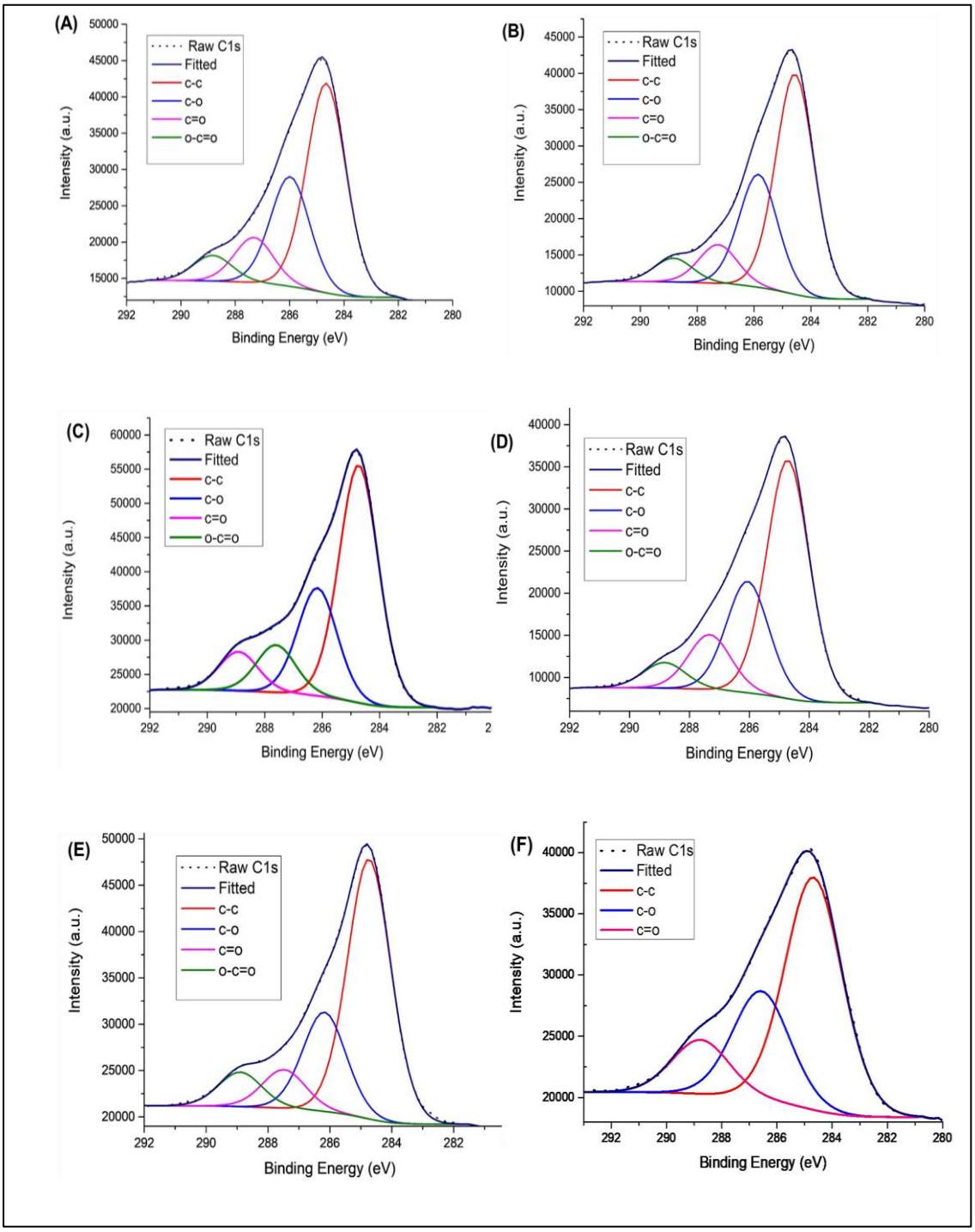

Note: (A) Glucose, (B) Galactose, (C) Fructose, (D) Maltose, (E)Lactose and (F) Sucrose.

Figure 3.5

High-resolution O1s XPS spectra

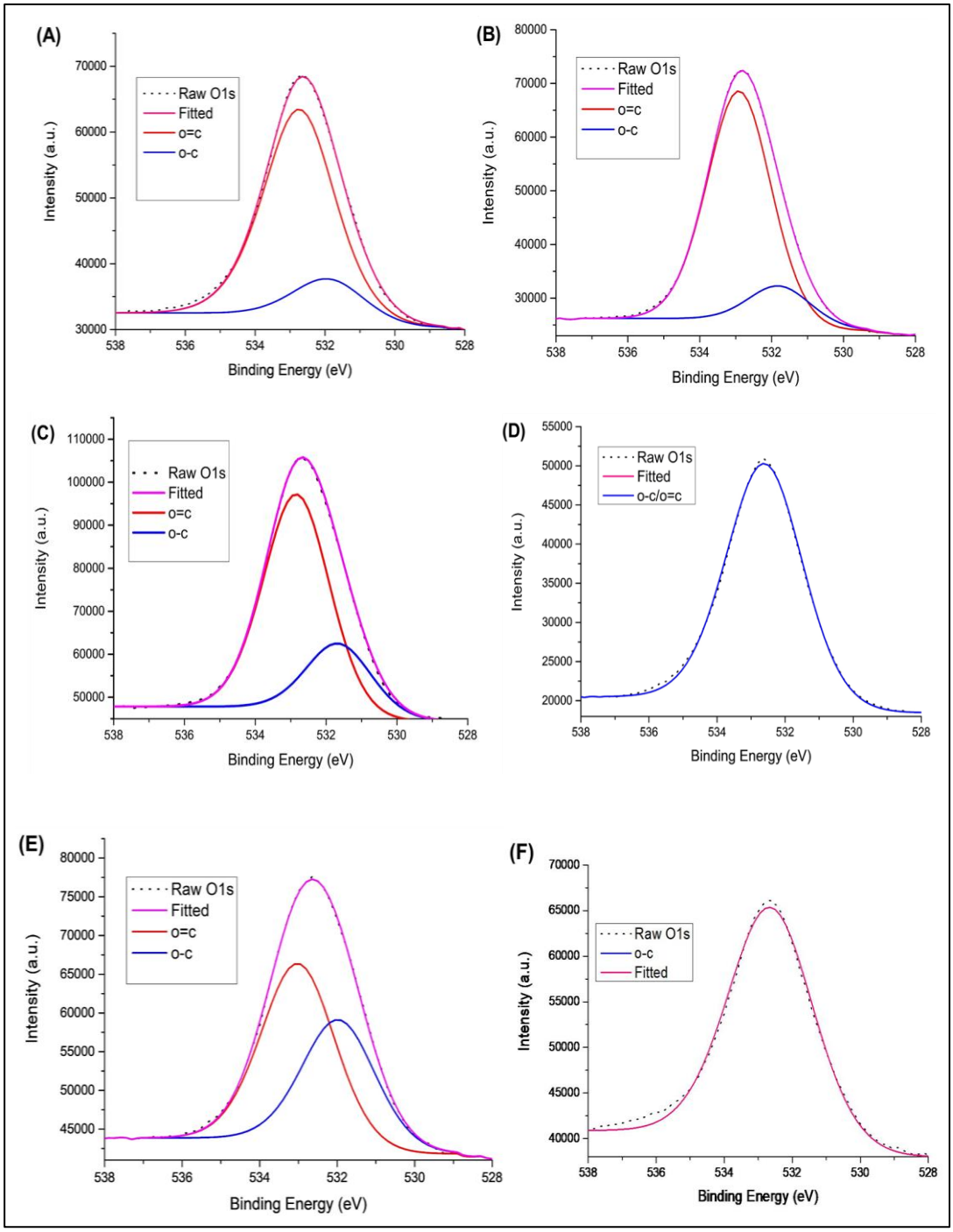

Note: (A) Glucose, (B) Galactose, (C) Fructose, (D) Maltose, (E) Lactose and (F) Sucrose

3.1.3 Optical Properties

UV-Vis and photoluminescence spectra was utilized to analyze the optical properties of the produced CNDs. The synthesized CNDs appear light yellow and transparent in the daytime but change to blue under UV light. As illustrated in Fig (3.6 A-F) The UV-Vis spectrum exhibits significant absorption in the UV range, combined eith a tail extending to the visible region.The spectra display an absorption peak at 203 nm (shoulder) attributable to π-π* of the aromatic sp2 hybridized carbon core, as well as two peaks at 280 nm and 360 nm assigned to n-π*, indicating the presence of the C=O band. (162)

Figure 3.6

The UV-Vis absorption spectrum of produced CNDs

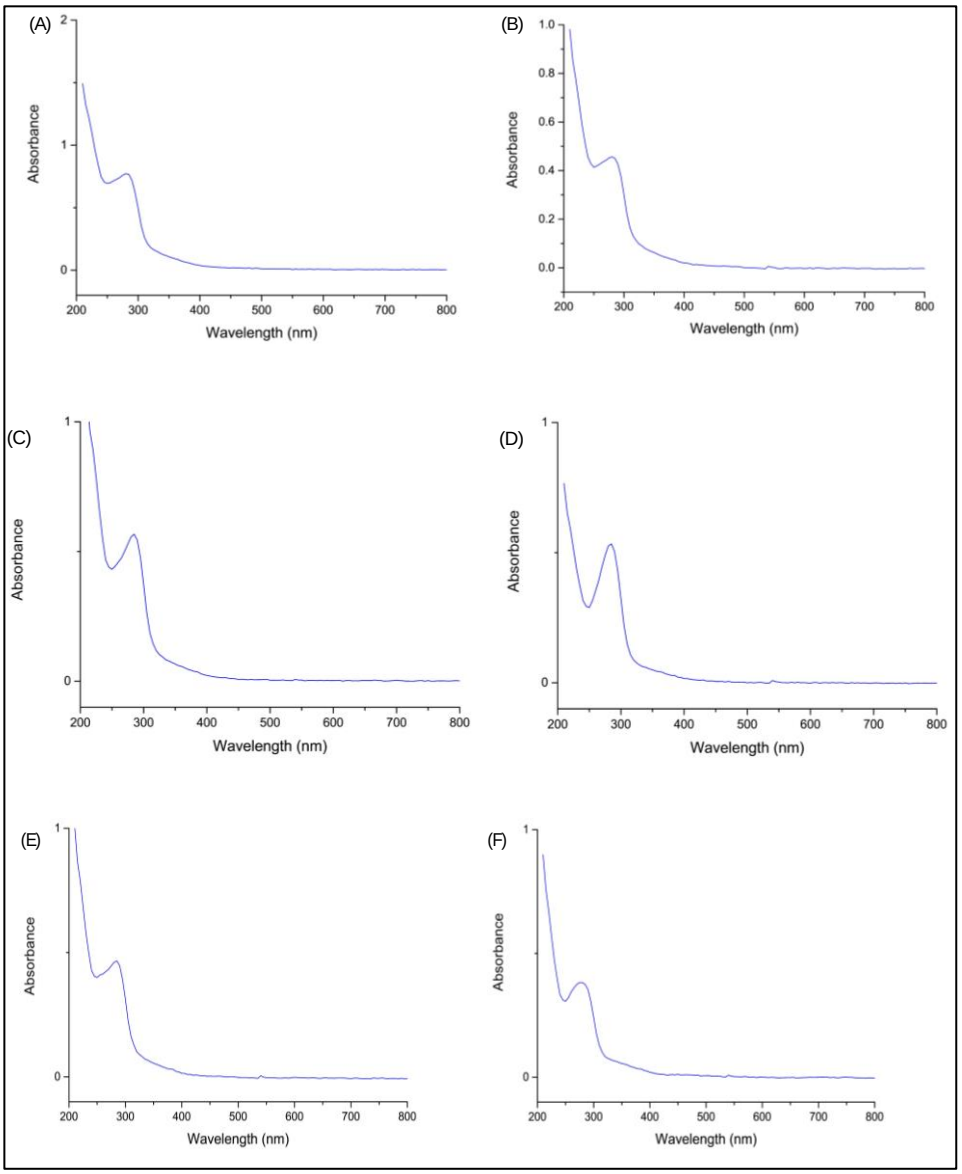

Note: (A) Glucose, (B) Galactose, (C) Fructose, (D) Maltose, (E) Lactose, and (F) Sucrose.

Equation 1 was used to estimate the quantum yield of CNDs at 360 nm using quinine sulfate (QY = 55%) as a reference.

$$QY = Q_R \times \frac{\mathrm{I}}{I_R} \times \frac{\mathrm{A}_R}{A} \times \frac{\mathrm{I}}{n_R^2} \quad (1)$$

A is the sample's absorption, n is the refractive index, I is the predicted integrated emission intensity, and QY is the quantum yield. The reference fluorophore, quinine sulfate dissolved in 0.1 M H_2SO_4, is denoted by R. Its quantum yield is known. For water, n is equal to 1.33(163). Table 3.1. displays the quantum yield average of the sugars.

Table 3.1

Quantum yield of sugars

	QY%
Fructose	2.09
Lactose	2.76
Galactose	2.44
Maltose	2.14
Glucose	2.19
Sucrose	2.59

As illustrated in Figure (3.7 A-F), the fluorescence of synthesized CNDs was assessed at various excitation wavelengths ranging from 300 to 440 nm. When the excited λex was 360 nm, the CNDs emitted a maximum of 443 nm. When the excitation increased above 360 nm, the CNDs displayed a red shift and an erosion of the fluorescence. Surface emission traps, surface defects, and surface functional groups may explain the photoluminescence of CNDs, a well-known phenomenon in CND fluorescence. (55, 164)

Figure 3.7

The PL spectra of the produced CNDs at various excitation wavelengths

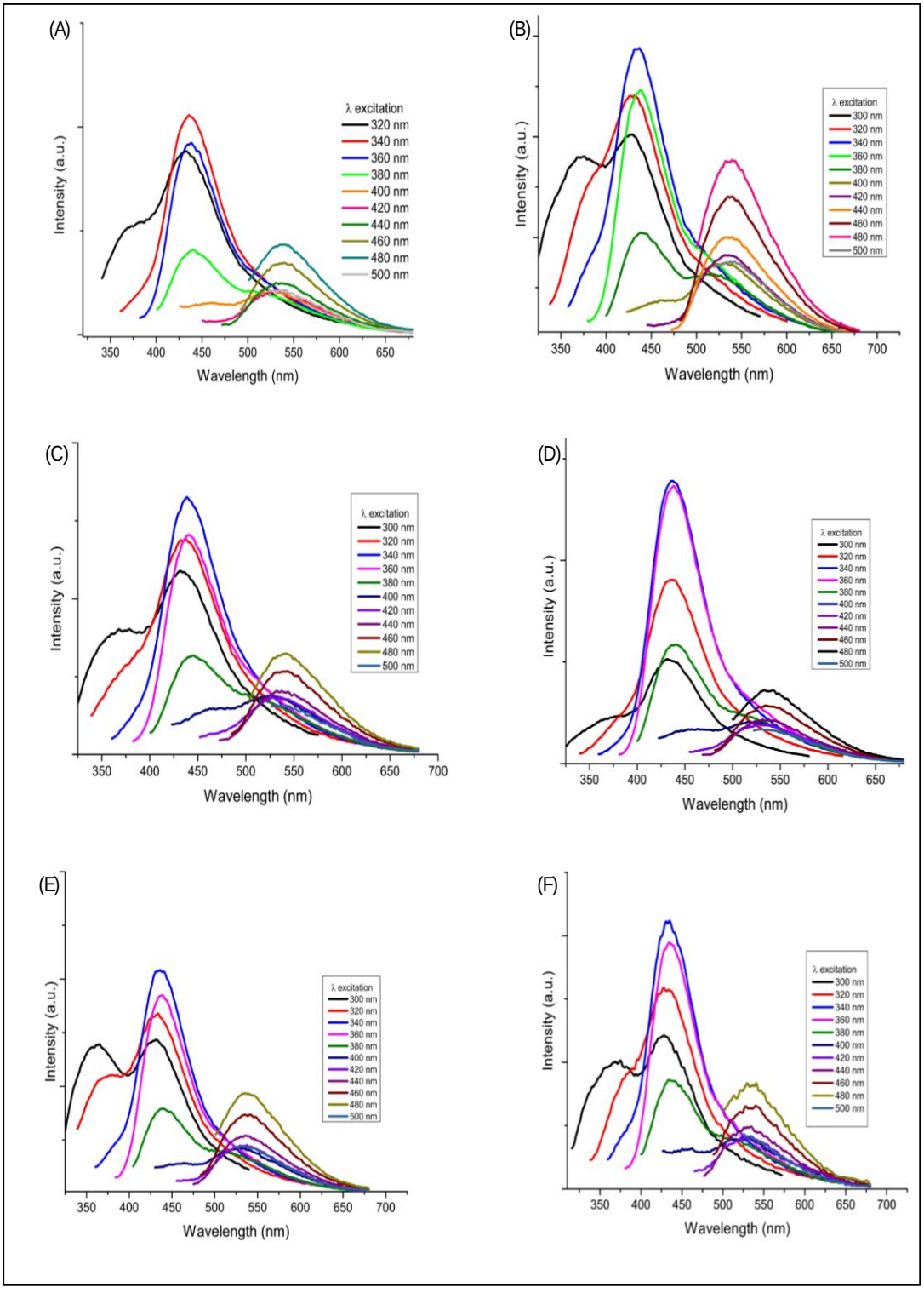

Note: (A) Glucose, (B) Galactose, (C) Fructose, (D) Maltose, (E) Lactose and (F) Sucrose

3.2 Anticancer Activity Results

3.2.1 Cell Viability Assay

3.2.1.1 Cytotoxicity Assay on the Hep3B Cell Line

We investigated the anti-cancer activity and selectivity of the synthesized sugar-based carbon nanodots using a proliferation assay on Hep3B cancer cells and normal LX-2 cells, following the protocol mentioned in the methodology.

Figure 3.8

The cytotoxicity assay of (150, 125, 100, 75, and 50) µg/ml

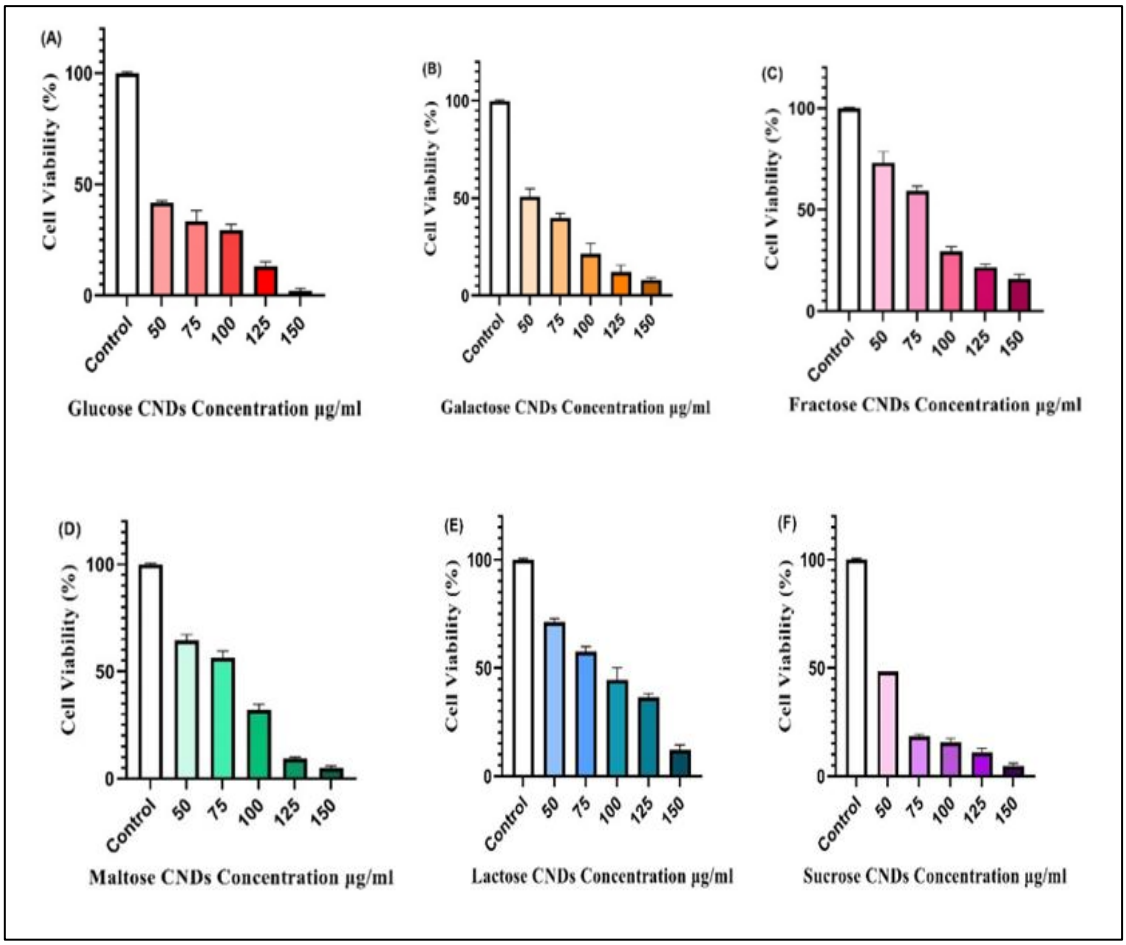

Note: (A) Glucose CNDs, (B) Galactose CNDs, (C) Fructose CNDs, (D) Maltose CNDs, (E) Lactose CNDs, (F) Sucrose CNDs against Hep3B cancer cell line compared to the negative control. Pv<0.05 compared to the negative control. The data was analyzed using a one-way ANOVA test.

3.2.1.2 Cell Viability Assay on the LX-2 Cell Line

Figure 3.9

The viability assay of (150, 125, 100, 75, and 50) µg/ml

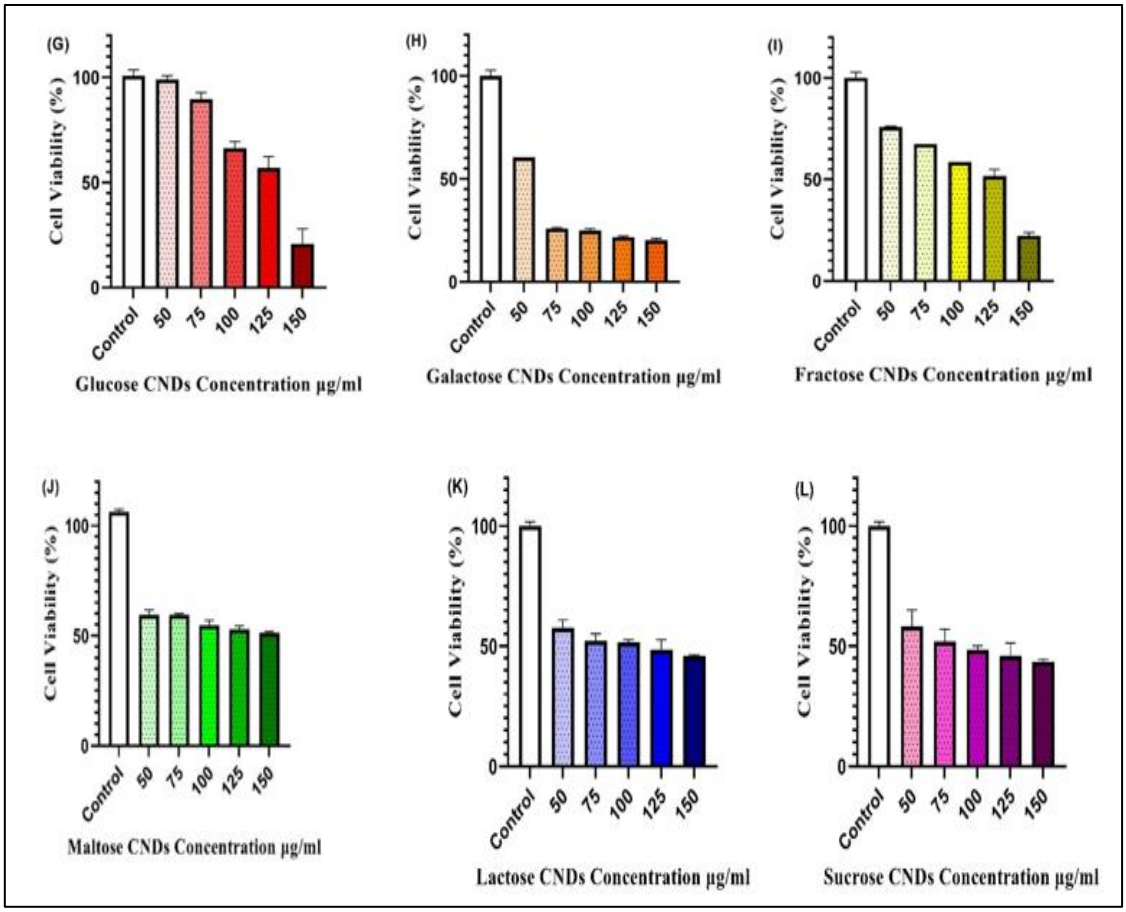

Note: *(G) Glucose CNDs, (H) Galactose CNDs, (I) Fructose CNDs, (J) Maltose CNDs, (K) Lactose CNDs, (L) Sucrose CNDs against LX-2 cancer cell line compared to the negative control. Pv<0.05 . The data was analyzed using a one-way ANOVA test.*

Using two distinct cell lines, the synthesized CNDs were tested for cytotoxicity effect on the liver cancer cell line Hep3B and the normal liver cell line LX-2, as described in the methodology section. As part of the viability test, the synthesized CNDs were assessed for their cytotoxicity and efficacy, in addition to their capability to selectively target cancer cells. The synthesized CNDs showed excellent anti-cancer activity against the Hep3B cell line in all concentrations tested (50 - 150) µg/ml within different percentages. However, with more than 52% of cell viability, most of the synthesized CNDs showed minimal effect on the normal liver cell line LX-2, indicating selective behavior against liver cancer cells with slight differences. For more details and as shown in Figures 3.8 and **3.9**, The percentage viability of the liver cancer cells Hep3B decreases as the concentration increases to reach 150 µg/ml. For instance, at a concentration of 75 µg/ml,

the synthesized CNDs demonstrated excellent antiproliferative activity with some variability in their efficacy against the liver cancer cells Hep3B. Additionally, they displayed a good selective profile, showing acceptable efficacy against the normal LX-2, as shown in Figures 3.8 and 3.9. Furthermore, as illustrated in Tables 2 and 3, at 75 µg/ml of sugar-based CNDs, the glucose CNDs demonstrated the highest anticancer activity. Simultaneously, they exhibited good selectivity against normal cells, reducing their viability by half compared to the control. Glucose and galactose CNDs had significant anticancer activity against Hep3B, but their efficacy was slightly lower than sucrose CNDs. However, the glucose CNDs recorded the highest selectivity with minimal activity against normal cells LX-2. Galactose CNDs, on the other hand, have the highest activity against normal cells, approximating they have a quarter of the glucose selectivity. At the same concentration, fructose, maltose, and lactose CNDs were almost equally effective against liver cancer cells. Furthermore, those compounds showed favorable activity against normal cells. As for the selective behavior of CNDs, fructose CNDs were the most selective, followed by maltose and lactose CNDs.

Table 3.2

IC50% percentages and cell viability assay summary of galactose, sucrose, glucose, maltose, fructose, and lactose CNDs at concentrations of 50 µg/ml, 75 µg/ml, 100 µg/ml, 125 µg/ml, and 150 µg/ml on Hep3B cell line

	Cell Viability Percentage %, (Hep3B)					
Conc. µg/ml	50	75	100	125	150	IC50 µg/ml
Glucose CNDs	41.79	33.47	29.47	13.14	2.07	45.19
Galactose CNDs	50.77	39.87	21.46	12.00	8.07	54.10
Fructose CNDs	73.14	59.28	29.5	21.70	15.90	76.69
Maltose CNDs	64.52	56.22	32.03	9.45	4.96	71.24
Lactose CNDs	71.03	57.61	44.53	36.46	12.27	84.17
Sucrose CNDs	48.58	18.42	15.71	11.08	4.82	51.69

Table 3.3

Cell viability assay as well as the cell viability at IC50% concentration summary of galactose, sucrose, glucose, maltose, fructose, and lactose CNDs at concentrations of 50 μg/ml, 75 μg/ml, 100 μg/ml, 125 μg/ml, and 150 μg/ml on LX2 cell line

	Cell Viability Percentage %, (LX-2)					
Conc. μg/ml	50	75	100	125	150	IC50 μg/ml
Glucose CNDs	99.06	89.69	66.37	56.92	20.85	121.9
Galactose CNDs	60.58	25.90	27.98	21.77	20.33	46.92
Fructose CNDs	75.78	67.45	58.56	51.64	22.37	103
Maltose CNDs	59.47	59.43	54.69	52.97	51.39	181.9
Lactose CNDs	57.65	52.10	51.61	48.34	45.97	105.2
Sucrose CNDs	58.22	51.88	48.58	45.87	43.51	90.55

Considering the high anti-proliferative effect of sugar-synthesized CNDs on Hep3B than the LX2 cells line it was postulated that there were three possibilities to explain this. The first approach is that the cancer cell is able to express different types and number of cell surface receptors which can mediate the CNDs delivery or activate single or multiple downstream signaling pathways which can activate the program cell death mechanism inside the tumor cells. As we stated before, when the concentration of CNDs increased the cytotoxicity increased as well, this suggests that the anti-cancer activity of the prepared CNDs on the Hep3B cell line is concentration dependent. Furthermore, the cell viability assay showed that the sugars-based CNDs have a different pharmacological effect within the Hep3B cell line as well as within the LX2 cell line. Therefore, we hypothesized that the pharmacological activity of the CNDs-sourced sugars and the loaded CNDs into a cancer cell is mediated through cell surface receptor endocytosis by two types of transport mechanisms known as clathrin-mediated endocytosis and caveolae-mediated endocytosis which is a type of energy dependent transportation, with an excellent tumor inhibition effect as mentioned by Li et al and Zhou et al(165, 166). At the same time, since prepared CNDs were nutritional substances, they showed acceptable cell viability percentages compared with the cancer cell line which can explain the different effect on the two cell types.

The second approach is based on the biological structure of the cancer cell as proven scientifically, cancer cells have lost membrane structure compared to normal cells which can facilitate the entrance of large amounts of CNDs by passive diffusion transport compared to normal cells (167, 168). The third approach is the genome level effect, which means the formation of the cancer cell resulting from multiple gene mutation in single or multiple genes promotes cancer cell formation and survival. Moreover, sugar-based CNDs may cause Hep3B gen manipulation which can inhibit the cancer cell viability via formation of Reactive Oxygen species (ROS) (169).

The Selectivity Index (SI) was calculated for each type of sugar-derived CNDs by dividing the IC_{50} value in LX-2 (normal liver cells) by the IC_{50} in Hep3B (hepatocarcinoma cells), to evaluate their preferential cytotoxicity toward hepatocellular carcinoma cells (Hep3B) over non-cancerous hepatic stellate cells (LX2). The SI values obtained were as follows: glucose (2.69), galactose (0.86), fructose (1.34), maltose (2.55), lactose (1.24), and sucrose (1.75), as shown in Table 3.4. A SI value greater than 2 is generally considered indicative of selective cytotoxicity toward cancer cells with reduced toxicity to normal cells. Based on this criterion, CNDs synthesized from glucose and maltose demonstrated the highest selectivity and are therefore the most promising candidates for further development as anticancer agents. In contrast, galactose-derived CNDs, with an SI of 0.86, exhibited higher toxicity to normal cells than to cancer cells, indicating poor selectivity. These findings emphasize the importance of precursor selection in CND synthesis and suggest that structurally optimized glucose- and maltose-derived CNDs may offer safer and more effective options for targeted liver cancer therapy.

Table 3.4

Selective Index for all sugar-derived CNDs

	Fructose	Lactose	Galactose	Maltose	Glucose	Sucrose
SI	1.34	1.24	0.86	2.55	2.69	1.75

3.2.2 Glutathione deficiency test and CNDs mechanism of action

Figure 3.10

Glutathione deficiency test Glutathione oxidation percentage of 125 µg/ml Galactose CNDs, Sucrose CNDs, Glucose CNDs, Maltose CNDs, Fructose CNDs, and Lactose CNDs compared with H2O2 as positive control

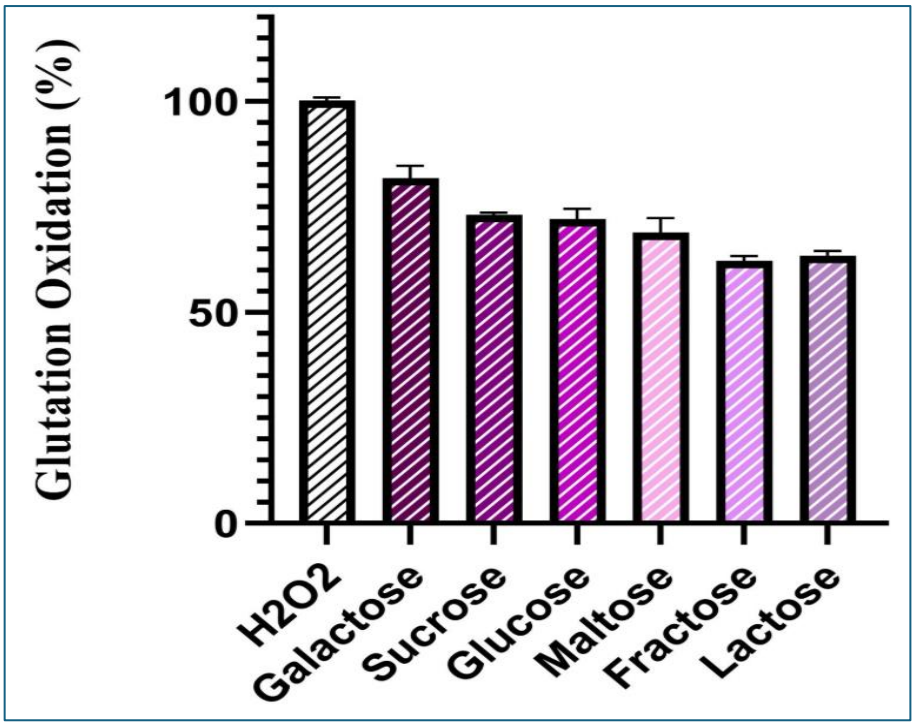

To determine the molecular pharmacological anti-cancer mechanism for the synthesized CNDs from mono- and disaccharides we did a glutathione oxidation test to investigate the CNDs ability to consume the intracellular level of the antioxidant glutathione by the creation of ROS comparing to the H_2O_2 as positive control, Figure 3.10. To dive into the deep details of the molecular-biochemical nature of (ROS), ROS is a normal byproduct of many cellular, chemical, and biological processes. Generally, ROS are tiny active molecules with half-lives ranging from nanoseconds to hours (170-172). Furthermore, the ROS abbreviation is a cooperative term representing the non-stable, hyper-reactive, and reduced oxygen molecules, for instance, hydrogen peroxide (H2O2), superoxide anion (O2−), hypochlorous acid (HOCl), singlet oxygen (1O2), and hydroxyl radical (•OH), etc.. (173)

The reactive oxygen species have a balanced dualism effect on cancer cells depending on their concentration. For instance, at low concentrations, they appeared to be a complementary country effect which can make the cancer cells alive and in a proliferation state through their work as secondary signaling transducer molecules while at high concentrations, they have a complementary opposite effect, consequently promoting program cell death (apoptosis) by different mechanisms of action. Peroxide membrane lipids, scission DNA double-strands, or oxidize purine, pyrimidine, thiol, and amine bases directly, as examples. (174)

Furthermore, excessive levels of ROS can Reduces the expression of epidermal growth factor (EGF) and its receptor (EGFR), thereby inhibiting the downstream proliferation signaling molecules such as ERK and PI3K/Akt. Therefore, tumor cells are prevented from proliferating, migrating, and growing. (175)

Compared to normal cells the production rate of the ROS is much higher in cancer cells, and this phenomenon appears more aggressively in cancer cells due to the high metabolic rate, different types of gene mutations, and the acidic environment of these cells. Also, cancer cells have a good ability to adapt to the high levels of ROS and remove them by cellular clearance, in other words, cancer cells have their own self-antioxidant mechanism to control the ROS. On the other hand, the natural occurrence of ROS inside cancer with this amount makes them susceptible to be sensitive to the chemotherapeutics agents that boost the creation and the accumulation of ROS to reach the level over the cytotoxic threshold of which can kill cancer cell selectively or with minimal effect on normal cells. (176)

Concerning the sources of ROS, the reactive oxygen species can produce many origins. For instance, large amounts of the ROS formed by the mitochondria during the oxidation-phosphorylation pathway to produce ATP from sugar, some products such as NADH during the electron transport chain, or by some transition metallic ions such as iron which can make the ROS through the Fenton reaction. In addition to the intracellular factors, many extracellular factors that can be involved in ROS formation such as radiation and drugs. (177-179)

Our results showed that sugar-synthesized CNDs able to produce ROS in different amounts compared to the positive control. The glutathione oxidation percentage for

galactose, sucrose, glucose, maltose, fructose, and lactose was 81.88, 73.15, 73.136, 67.682, 65.048, and 63.4917, consecutively.

According to these results, we can state that our CNDs were able to destroy the Hep3B cell significantly compared to the negative control through the formation of several types of ROS for example hydrogen peroxide (H2O2), superoxide anion (O2 −), hypochlorous acid (HOCl), singlet oxygen (O2), and hydroxyl radical (OH).

Turning back to cancer cell nature and specifically the well-known feature of cancer which is defined as the Warburg Effect. The cancer Warburg Effect means an increase in the glucose metabolism by aerobic glycolysis in the cancer cells' cytoplasm even in complete mitochondria health and function (180). So, depending on this proven fact, the reactive oxygen species source will be diminished from the mitochondria during oxidative phosphorylation of the glucose. However, in this case, transition metallic ions, NADPH oxidase, NADH, and glutaminolysis will be the key sources of ROS production. Interestingly, killing the cell by the creation of ROS through metabolic disturbances was reported as a new mechanism for cell death known as ferroptosis (181). Ferroptosis is a new type of cell death characterized by the oxidation of lipids' cell membrane due to the creation of ROS due to metabolic dysfunction (182). Specifically, glutathione (GSH) is the main regulator of ferroptosis mechanically (183, 184). By consuming or oxidizing GSH, glutathione peroxidase 4 (GPX4) is deactivated, leading to ROS accumulation and ultimately lipid peroxidation that leads to cell death by ferroptosis (185, 186). Uniquely, some published reports state that the process occurrence of ferroptosis inside cancer cells has an immunogenic effect, which means the cancer cells able to release some antigens and alarmins to start an immune response as a result of the cellular damage (187, 188). Recent research by Lu Yao and his co-workers has focused on synthesizing quantum carbon dots from caffeine. The results showed that these quantum carbon doses have a potent GSH-oxidase effect as well as anti-tumor activity against hepatocellular carcinoma resulting from ferroptosis and consequently causing an anticancer immune response (189). Herein, we hypothesized that the mono- and disaccharide-based carbon dots can cause cancer cell death by ferroptosis. Further experimental investigation is needed to prove this concept on our compounds.

Exceptionally, our work demonstrated that our synthesized CNDs from sugars were able to limit the proliferation and growth of the liver cell carcinoma (Hep3B) cell line with an acceptable selective profile toward the Liver normal cell line (LX2), So far as we know,

this is the primary instance in which CNDs synthesized from mono- and disaccharides and used as anticancer agents with high efficacy and acceptable selectivity profile.

3.3 Conclusion

In this thesis, we successfully synthesized carbon nanodots (CNDs) from various sugars applying a hydrothermal bottom-up approach. The reaction was carried out in an autoclave at 200˚C for 24 hours, with no additional chemicals or passivating agents. The final product was stable, photoluminescent, and extremely water-soluble CNDs with an average quantum yield of 2.35% and an average particle size range from 2.7-4.5 nm. These CNDs exhibited promising cytotoxicity properties, demonstrating significant anticancer activity against hepatocellular carcinoma cells (Hep3B) at various concentrations, with minimal impact on normal LX2 cells, suggesting a selective cancer-targeting effect. The anticancer mechanism appears to be mediated through the production of reactive oxygen species (ROS). These results highlight the promise of sugar-based CNDs as a novel and effective cancer treatment approach, especially for liver cancer. This study, being the first in this area, provides opportunities for further research to enhance synthesis methods and explore additional applications of sugar-derived CNDs in biomedicine.

List of Abbreviations

Abbreviation	Meaning
CNDs	Carbon nano dots
AFM	Atomic force microscopy
FT-IR	Fourier-transform infrared spectroscopy
XPS	X-ray photoelectron microscopy
UV-VIS	Ultraviolet visible spectroscopy
QY	Quantum yield
WHO	World health organization
EPR	Enhanced permeability and retention
GI	Gastrointestinal
EPA	Environmental protection agency
NNI	National nanotechnology initiative
STM	Scanning tunneling microscope
NMs	Nanomaterials
0D	Zero-dimensional
1D	One-dimensional
2D	Two-dimensional
3D	Three-dimensional
RI	Refractive index
GQD	Graphene quantum dots
TRG	Thermally reduced graphene oxide
rGO	reduced graphene oxide
GO	Graphene oxide
CNTs	Carbon nano tubes
MWCNTs	Multi walled carbon nanotubes
SWCNTs	Single walled carbon nanotubes
SWCNHs	Single walled carbon nano-horns
OLCs	Onion like carbons
GQDs	Graphene quantum dots
NDs	Nano diamonds

CNPs	Carbon quantum dots
PL	Photoluminescence
DMF	Dimethyl formamide
AcD	Arc discharge
LA	Laser ablation
PEG	Polyethylene glycol
HNO3	Nitric acid
H2SO4	Sulfuric acid
H2O2	Hydrogen peroxide
PEI	Polyethyleneimine
BBB	Blood brain barrier
CCL4	Carbon tetrachloride
TEM	Transmission electron microscopy
EDA	Ethylenediamine
SEM	Scanning electron microscope
XRD	X-ray diffraction
QCE	Quantum confinement effect
UCPL	Up conversion photoluminescence
NIR	Near infrared
PET	Photo-induced electron transfer
ROS	Reactive oxygen species
NSC	Neural stem cells
DOX	Doxorubicin
MCF7	Human breast cancer cell line
HT-29	Human colorectal carcinoma
MRI	Magnetic resonance imaging
OLEDs	Organic light-emitting diodes
PDT	Photodynamic therapy
DPP	Diketopyrrolopyrrole
PTT	Photothermal therapy
SPA	Surface passivation agent
TTDDA	4,7,10-trioxa-1,13-tridecanediamine
ZP	Zeta potential

LSCM	Laser scanning confocal microscopy
EDC	Ethylene dicarbon
MTX	Methotrexate
LX2	Normal liver cell line
Hep3B	Liver cancer cell line
EGF	Epidermal growth factor
GSH	Glutathione
λ_{max}	Lambda max
HCC	Hepatocellular carcinoma
SI	Selectivity index

References

1. Nocito G, Calabrese G, Forte S, Petralia S, Puglisi C, Campolo M, et al. Carbon Dots as Promising Tools for Cancer Diagnosis and Therapy. Cancers. 2021;13.(9)
2. Chen S, Cao Z, Prettner K, Kuhn M, Yang J, Jiao L, et al. Estimates and Projections of the Global Economic Cost of 29 Cancers in 204 Countries and Territories From 2020 to 2050. JAMA Oncology. 2023;9.(4)
3. Lugano R, Ramachandran M, Dimberg A. Tumor angiogenesis: causes, consequences, challenges and opportunities. Cellular and Molecular Life Sciences. 2019;77(9):1745-70.
4. Pekarek L, Torres-Carranza D, Fraile-Martinez O, García-Montero C, Pekarek T, Saez MA, et al. An Overview of the Role of MicroRNAs on Carcinogenesis: A Focus on Cell Cycle, Angiogenesis and Metastasis. International Journal of Molecular Sciences. 2023;24.(8)
5. Wu J. The Enhanced Permeability and Retention (EPR) Effect: The Significance of the Concept and Methods to Enhance Its Application. Journal of Personalized Medicine. 2021;11.(8)
6. Xie X, Zhang Y, Li F, Lv T, Li Z, Chen H, et al. Challenges and Opportunities from Basic Cancer Biology for Nanomedicine for Targeted Drug Delivery. Current Cancer Drug Targets. 2019;19(4):257-76.
7. Safdie FM, Dorff T, Quinn D, Fontana L, Wei M, Lee C, et al. Fasting and cancer treatment in humans: A case series report. Aging. 2009;1(12):988-1007.
8. Heo HJ, Park Y, Lee JH, Kim Y, Kim EK, Kim GH, et al. Clinical big-data-based design of GLUT2-targeted carbon nanodots for accurate diagnosis of hepatocellular carcinoma. Nanoscale. 2022;14(4.17053-64:(5
9. Nasrollahzadeh M, Sajadi SM, Sajjadi M, Issaabadi Z. An Introduction to Nanotechnology. An Introduction to Green Nanotechnology. Interface Science and Technology2019. p. 1-27.
10. Baig N, Kammakakam I, Falath W. Nanomaterials: a review of synthesis methods, properties, recent progress, and challenges. Materials Advances. 2021;2(6):1821-71.

11. Mekuye B, Abera B. Nanomaterials: An overview of synthesis, classification, characterization, and applications. Nano Select. 2023;4(8):486-501.
12. Wolkenstein AFX. What is Nanotechnology and Why does It Matter: From Science to Ethics - By F. Allhoff, P. Lin & D. Moore. Journal of Applied Philosophy. 2011;28(3):321-3.
13. El-Diasty AI, Ragab AM. Applications of Nanotechnology in the Oil & Gas Industry: Latest Trends Worldwide & Future Challenges in Egypt. All Days2013.
14. Feynman RP. There's plenty of room at the bottom. Resonance. 2011;16(9):890-905.
15. Rafique M, Tahir MB, Rafique MS, Hamza M. History and fundamentals of nanoscience and nanotechnology. Nanotechnology and Photocatalysis for Environmental Applications2020. p. 1-25.
16. Drexler E. Engines of creation: The coming era of nanotechnology: Anchor; 1987.
17. Binnig G, Rohrer H. Scanning tunneling microscopy. IBM Journal of research and development. 2000;44(1/2):279.
18. Bratovcic A. Different Applications of Nanomaterials and Their Impact on the Environment. International Journal of Material Science and Engineering. 2019;5(1):1-7.
19. El-Kady MM, Ansari I, Arora C, Rai N, Soni S, Verma DK, et al. Nanomaterials: A comprehensive review of applications, toxicity, impact, and fate to environment. Journal of Molecular Liquids. 2023;370.
20. Saleh TA. Nanomaterials: Classification, properties, and environmental toxicities. Environmental Technology & Innovation. 2020;20.
21. Wood BJ. Carbon in the core. Earth and Planetary Science Letters. 1993;117(3-4):593-607.
22. Jampilek J, Kralova K. Advances in Drug Delivery Nanosystems Using Graphene-Based Materials and Carbon Nanotubes. Materials (Basel). 2021;14(5.(
23. Chabot NL, Agee CB. Core formation in the Earth and Moon: new experimental constraints from V, Cr, and Mn. Geochimica et Cosmochimica Acta. 2003;67(11):2077-91.
24. Karthik PS, Himaja AL, Singh SP. Carbon-allotropes: synthesis methods, applications and future perspectives. Carbon letters. 2014;15(4):219-37.
25. Georgakilas V, Perman JA, Tucek J, Zboril R. Broad Family of Carbon Nanoallotropes: Classification, Chemistry, and Applications of Fullerenes, Carbon

Dots, Nanotubes, Graphene, Nanodiamonds, and Combined Superstructures. Chemical Reviews. 2015;115(11):4744-822.

26. Verdanova M, Rezek B, Broz A, Ukraintsev E, Babchenko O, Artemenko A, et al. Nanocarbon Allotropes-Graphene and Nanocrystalline Diamond-Promote Cell Proliferation. Small. 2016;12(18):2499-509.
27. Park S, Abate II, Liu J, Wang C, Dahl JEP, Carlson RMK, et al. Facile diamond synthesis from lower diamondoids. Science Advances. 2020;6.(8)
28. Murugan P, Nagarajan RD, Shetty BH, Govindasamy M, Sundramoorthy AK. Recent trends in the applications of thermally expanded graphite for energy storage and sensors – a review. Nanoscale Advances. 2021;3(22):6294-309.
29. Chung S, Revia RA, Zhang M. Graphene Quantum Dots and Their Applications in Bioimaging, Biosensing, and Therapy. Advanced Materials. 2019;33.(22)
30. Rode A, Sharma S, Mishra DK. Carbon Nanotubes: Classification, Method of Preparation and Pharmaceutical Application. Current Drug Delivery. 2018;15(5):620-9.
31. Negri V, Pacheco-Torres J, Calle D, López-Larrubia P. Carbon Nanotubes in Biomedicine. Topics in Current Chemistry. 2020;378.(1)
32. Simon J, Flahaut E, Golzio M. Overview of Carbon Nanotubes for Biomedical Applications. Materials. 2019;12.(4)
33. Gomez-Gualdrón DA, Burgos JC, Yu J, Balbuena PB. Carbon Nanotubes. Nanoparticles in Translational Science and Medicine. Progress in Molecular Biology and Translational Science2011. p. 175-245.
34. Moreno-Lanceta A, Medrano-Bosch M, Melgar-Lesmes P. Single-Walled Carbon Nanohorns as Promising Nanotube-Derived Delivery Systems to Treat Cancer. Pharmaceutics. 2020;12.(9)
35. Kausar A. Fullerene Reinforced Polymeric Nanocomposites for Energy Storage—Status and Prognoses. Frontiers in Materials. 2022;9.
36. Yao S, Yuan X, Jiang L, Xiong T, Zhang J. Recent Progress on Fullerene-Based Materials: Synthesis, Properties, Modifications, and Photocatalytic Applications. Materials. 2020;13.(13)
37. Bobrowska DM, Olejnik P, Echegoyen L, Plonska-Brzezinska ME. Onion-Like Carbon Nanostructures: An Overview of Bio-Applications. Current Medicinal Chemistry. 2019;26(38):6896-914.

38. Speranza G. Carbon Nanomaterials: Synthesis, Functionalization and Sensing Applications. Nanomaterials. 2021;11.(4)
39. Sagbas S, Sahiner N. Carbon dots: preparation, properties, and application. Nanocarbon and its Composites2019. p. 651-76.
40. Liu J, Li R, Yang B. Carbon Dots: A New Type of Carbon-Based Nanomaterial with Wide Applications. ACS Central Science. 2020;6(12):2179-95.
41. Mansuriya B, Altintas Z. Applications of Graphene Quantum Dots in Biomedical Sensors. Sensors. 2020;20.(4)
42. Dar MS, Tabish TA, Thorat ND, Swati G, Sahu NK. Photothermal therapy using graphene quantum dots. APL Bioengineering. 2023;7.(3)
43. Chung PH, Perevedentseva E, Cheng CL. The particle size-dependent photoluminescence of nanodiamonds. Surface Science. 2007;601(18):3866-70.
44. Xu J, Chow EK-H. Biomedical applications of nanodiamonds: From drug-delivery to diagnostics. SLAS Technology. 2023;28(4):214-22.
45. Das S, Ngashangva L, Goswami P. Carbon Dots: An Emerging Smart Material for Analytical Applications. Micromachines. 2021;12.(1)
46. Mintz KJ, Bartoli M, Rovere M, Zhou Y, Hettiarachchi SD, Paudyal S, et al. A deep investigation into the structure of carbon dots. Carbon. 2021;173:433-47.
47. Azam N, Najabat Ali M, Javaid Khan T. Carbon Quantum Dots for Biomedical Applications: Review and Analysis. Frontiers in Materials. 2021;8.
48. Sun Y-P, Zhou B, Lin Y, Wang W, Fernando KAS, Pathak P, et al. Quantum-Sized Carbon Dots for Bright and Colorful Photoluminescence. Journal of the American Chemical Society. 2006;128(24):7756-7.
49. Xu J, Ning J, Wang Y, Xu M, Yi C, Yan F. Carbon dots as a promising therapeutic approach for combating cancer. Bioorganic & Medicinal Chemistry. 2022;72.
50. Kang Z, Lee S-T. Carbon dots: advances in nanocarbon applications. Nanoscale. 2019;11(41):19214-24.
51. Tuerhong M, Xu Y, Yin X-B. Review on Carbon Dots and Their Applications. Chinese Journal of Analytical Chemistry. 2017;45(1):139-50.
52. Egorova MN, Tomskaya AE, Kapitonov AN, Alekseev AA, Smagulova SA. Hydrothermal Synthesis of Luminescent Carbon Dots from Glucose and Birch Bark Soot. Journal of Structural Chemistry. 2018;59(4):780-5.

53. Zhu S, Meng Q, Wang L, Zhang J, Song Y, Jin H, et al. Highly Photoluminescent Carbon Dots for Multicolor Patterning, Sensors, and Bioimaging. Angewandte Chemie International Edition. 2013;52(14):3953-7.
54. Pan L, Sun S, Zhang A, Jiang K, Zhang L, Dong C, et al. Truly Fluorescent Excitation-Dependent Carbon Dots and Their Applications in Multicolor Cellular Imaging and Multidimensional Sensing. Advanced Materials. 2015;27(47):7782-7.
55. Sharma A, Gadly T, Gupta A, Ballal A, Ghosh SK, Kumbhakar M. Origin of Excitation Dependent Fluorescence in Carbon Nanodots. The Journal of Physical Chemistry Letters. 2016;7(18):3695-702.
56. Liu W, Li C, Ren Y, Sun X, Pan W, Li Y, et al. Carbon dots: surface engineering and applications. Journal of Materials Chemistry B. 2016;4(35):5772-88.
57. Choi Y, Choi Y, Kwon OH, Kim BS. Carbon Dots: Bottom-Up Syntheses, Properties, and Light-Harvesting Applications. Chemistry – An Asian Journal. 2018;13(6):586-98.
58. Das SK, Liu Y, Yeom S, Kim DY, Richards CI. Single-Particle Fluorescence Intensity Fluctuations of Carbon Nanodots. Nano Letters. 2014;14(2):620-5.
59. Choi Y, Kang B, Lee J, Kim S, Kim GT, Kang H, et al. Integrative Approach toward Uncovering the Origin of Photoluminescence in Dual Heteroatom-Doped Carbon Nanodots. Chemistry of Materials. 2016;28(19):6840-7.
60. Jiang K, Sun S, Zhang L, Lu Y, Wu A, Cai C, et al. Red, Green, and Blue Luminescence by Carbon Dots: Full-Color Emission Tuning and Multicolor Cellular Imaging. Angewandte Chemie International Edition. 2015;54(18):5360-3.
61. Yuan F, Wang Z, Li X, Li Y, Tan Za, Fan L, et al. Bright Multicolor Bandgap Fluorescent Carbon Quantum Dots for Electroluminescent Light-Emitting Diodes. Advanced Materials. 2016;29.(3)
62. Zhu H, Wang X, Li Y, Wang Z, Yang F, Yang X. Microwave synthesis of fluorescent carbon nanoparticles with electrochemiluminescence properties. Chemical Communications. 2009(34):5118.
63. Qu S, Zhou D, Li D, Ji W, Jing P, Han D, et al. Toward Efficient Orange Emissive Carbon Nanodots through Conjugated sp2-Domain Controlling and Surface Charges Engineering. Advanced Materials. 2016;28(18):3.516-21
64. Wang Z, Yuan F, Li X, Li Y, Zhong H, Fan L, et al. 53% Efficient Red Emissive Carbon Quantum Dots for High Color Rendering and Stable Warm White-Light-Emitting Diodes. Advanced Materials. 2017;29.(37)

65. Cailotto S, Amadio E, Facchin M, Selva M, Pontoglio E, Rizzolio F, et al. Carbon Dots from Sugars and Ascorbic Acid: Role of the Precursors on Morphology, Properties, Toxicity, and Drug Uptake. ACS Medicinal Chemistry Letters. 2018;9(8):832-7.
66. sharma; N, Yashika;, bhullar; Gk, saini; A, Nandiny;, Sheetal;, et al. "A Review based on the Synthesis of Carbon Quantum Dots: Top-Down, Bottom-up Approaches and their Properties.". International Journal of Innovative Science and Research Technology (IJISRT),. 2023;8(6):670-81.
67. Qu D, Sun Z. The formation mechanism and fluorophores of carbon dots synthesized via a bottom-up route. Materials Chemistry Frontiers. 2020;4(2):400-20.
68. Hutton GAM, Martindale BCM, Reisner E. Carbon dots as photosensitisers for solar-driven catalysis. Chemical Society Reviews. 2017;46(20):6111-23.
69. Hu S-L, Niu K-Y, Sun J, Yang J, Zhao N-Q, Du X-W. One-step synthesis of fluorescent carbon nanoparticles by laser irradiation. J Mater Chem. 2009;19(4):484-8.
70. Xu Q, Liu Y, Gao C, Wei J, Zhou H, Chen Y, et al. Synthesis, mechanistic investigation, and application of photoluminescent sulfur and nitrogen co-doped carbon dots. Journal of Materials Chemistry C. 2015;3(38):9885-93.
71. Khayal A, Dawane V, Amin MA, Tirth V, Yadav VK, Algahtani A, et al. Advances in the Methods for the Synthesis of Carbon Dots and Their Emerging Applications. Polymers. 2021;13.(18)
72. Mishra V, Patil A, Thakur S, Kesharwani P. Carbon dots: emerging theranostic nanoarchitectures. Drug Discovery Today. 2018;23(6):1219-32.
73. Xu X, Ray R, Gu Y, Ploehn HJ, Gearheart L, Raker K, et al. Electrophoretic Analysis and Purification of Fluorescent Single-Walled Carbon Nanotube Fragments. Journal of the American Chemical Society. 2004;126(40):12736-7.
74. Li H, He X, Liu Y, Huang H, Lian S, Lee S-T, et al. One-step ultrasonic synthesis of water-soluble carbon nanoparticles with excellent photoluminescent properties. Carbon. 2011;49(2):605-9.
75. Huang H, Cui Y, Liu M, Chen J, Wan Q, Wen Y, et al. A one-step ultrasonic irradiation assisted strategy for the preparation of polymer-functionalized carbon quantum dots and their biological imaging. Journal of Colloid and Interface Science. 2018;532:767-73.

76. Mansuriya BD, Altintas Z. Carbon Dots: Classification, Properties, Synthesis, Characterization, and Applications in Health Care—An Updated Review (2018–2021). Nanomaterials. 2021;11.(10)
77. Pan M, Xie X, Liu K, Yang J, Hong L, Wang S. Fluorescent Carbon Quantum Dots—Synthesis, Functionalization and Sensing Application in Food Analysis. Nanomaterials.(5)10;2020 .
78. Liu M, Xu Y, Niu F, Gooding JJ, Liu J. Carbon quantum dots directly generated from electrochemical oxidation of graphite electrodes in alkaline alcohols and the applications for specific ferric ion detection and cell imaging. The Analyst . .2657-64:(9)141;2016
79. Shi X, Wei W, Fu Z, Gao W, Zhang C, Zhao Q, et al. Review on carbon dots in food safety applications. Talanta. 2019;194:809-21.
80. Zhuo Y, Miao H, Zhong D, Zhu S, Yang X. One-step synthesis of high quantum-yield and excitation-independent emission carbon dots for cell imaging. Materials Letters. 2015;139:197-200.
81. Zeng Y-W, Ma D-K, Wang W, Chen J-J, Zhou L, Zheng Y-Z, et al. N, S co-doped carbon dots with orange luminescence synthesized through polymerization and carbonization reaction of amino acids. Applied Surface Science. 2015;342:136-43.
82. Lu S, Guo S, Xu P, Li X, Zhao Y, Gu W, et al. Hydrothermal synthesis of nitrogen-doped carbon dots with real-time live-cell imaging and blood–brain barrier penetration capabilities. International Journal of Nanomedicine. 2016;Volume 11:6325-36.
83. Wu H, Mi C, Huang H, Han B, Li J, Xu S. Solvothermal synthesis of green-fluorescent carbon nanoparticles and their application. Journal of Luminescence. 2012;132(6):1603-7.
84. Dong Y, Pang H, Yang HB, Guo C, Shao J, Chi Y, et al. Carbon-Based Dots Co-doped with Nitrogen and Sulfur for High Quantum Yield and Excitation-Independent Emission. Angewandte Chemie International Edition. 2013;52(30):7800-4.
85. Qian Z, Shan X, Chai L, Ma J, Chen J, Feng H. Si-Doped Carbon Quantum Dots: A Facile and General Preparation Strategy, Bioimaging Application, and Multifunctional Sensor. ACS Applied Materials & Interfaces. 2014;6(9):6797-805.

86. Ng HKM, Lim GK, Leo CP. Comparison between hydrothermal and microwave-assisted synthesis of carbon dots from biowaste and chemical for heavy metal detection: A review. Microchemical Journal. 2021;165.
87. Stefanakis D, Philippidis A, Sygellou L, Filippidis G, Ghanotakis D, Anglos D. Synthesis of fluorescent carbon dots by a microwave heating process: structural characterization and cell imaging applications. Journal of Nanoparticle Research. 2014;16.(10)
88. Song Y, Zhu S, Zhang S, Fu Y, Wang L, Zhao X, et al. Investigation from chemical structure to photoluminescent mechanism: a type of carbon dots from the pyrolysis of citric acid and an amine. Journal of Materials Chemistry C. 2015;3(23):5976-84.
89. Ludmerczki R, Mura S, Carbonaro CM, Mandity IM, Carraro M, Senes N, et al. Carbon Dots from Citric Acid and its Intermediates Formed by Thermal Decomposition. Chemistry – A European Journal. 2019;25(51):11963-74.
90. Wang H, Ning G, He X, Ma X, Yang F, Xu Z, et al. Carbon quantum dots derived by direct carbonization of carbonaceous microcrystals in mesophase pitch. Nanoscale. 2018;10(45):21492-8.
91. Ma Ca, Yin C, Fan Y, Yang X, Zhou X. Highly efficient synthesis of N-doped carbon dots with excellent stability through pyrolysis method. Journal of Materials Science. 2019;54(13):9372-84.
92. Feng T, Ai X, An G, Yang P, Zhao Y. Charge-Convertible Carbon Dots for Imaging-Guided Drug Delivery with Enhanced in Vivo Cancer Therapeutic Efficiency. ACS Nano. 2016;10(4):4410-20.
93. Ge G, Li L, Wang D, Chen M, Zeng Z, Xiong W, et al. Carbon dots: synthesis, properties and biomedical applications. Journal of Materials Chemistry B. 2021;9(33):6553-75.
94. Wei Z, Wang B, Liu Y, Liu Z, Zhang H, Zhang S, et al. Green synthesis of nitrogen and sulfur co-doped carbon dots from Allium fistulosum for cell imaging. New Journal of Chemistry. 2019;43(2):718-23.
95. Yan F, Jiang Y, Sun X, Bai Z, Zhang Y, Zhou X. Surface modification and chemical functionalization of carbon dots: a review. Microchimica Acta. 2018;185.(9)
96. Dong W, Zhou S, Dong Y, Wang J, Ge X, Sui L. The preparation of ethylenediamine-modified fluorescent carbon dots and their use in imaging of cells. Luminescence. 2015;30(6):867-71.

97. Lim SY, Shen W, Gao Z. Carbon quantum dots and their applications. Chemical Society Reviews. 2015;44(1):362-81.
98. Sekar R, Basavegowda N, Jena S, Jayakodi S, Elumalai P, Chaitanyakumar A, et al. Recent Developments in Heteroatom/Metal-Doped Carbon Dot-Based Image-Guided Photodynamic Therapy for Cancer. Pharmaceutics. 2022;14.(9)
99. Kumar VB, Porat Ze, Gedanken A. Synthesis of Doped/Hybrid Carbon Dots and Their Biomedical Application. Nanomaterials. 2022;12.(6)
100. Tajik S, Dourandish Z, Zhang K, Beitollahi H, Le QV, Jang HW, et al. Carbon and graphene quantum dots: a review on syntheses, characterization, biological and sensing applications for neurotransmitter determination. RSC Advances. 2020;10(26):15406-29.
101. Sun X, Liu Y, Niu N, Chen L. Synthesis of molecularly imprinted fluorescent probe based on biomass-derived carbon quantum dots for detection of mesotrione. Analytical and Bioanalytical Chemistry. 2019;411(21):5519-30.
102. Zhao P, Zhu L. Dispersibility of carbon dots in aqueous and/or organic solvents. Chemical Communications. 2018;54(43):5401-6.
103. Kang Z, Lee ST. Carbon dots: advances in nanocarbon applications. Nanoscale. 2019;11(41):19214-24.
104. Peng H, Travas-Sejdic J. Simple Aqueous Solution Route to Luminescent Carbogenic Dots from Carbohydrates. Chemistry of Materials. 2009;21(23):5563-5.
105. Verhagen A, Kelarakis A. Carbon Dots for Forensic Applications: A Critical Review. Nanomaterials. 2020;10(8):1535.
106. Nurunnabi M, Khatun Z, Huh KM, Park SY, Lee DY, Cho KJ, et al. In Vivo Biodistribution and Toxicology of Carboxylated Graphene Quantum Dots. ACS Nano. 2013;7(8):6858-67.
107. Chen W, Shen J, Wang Z, Liu X, Xu Y, Zhao H, et al. Turning waste into wealth: facile and green synthesis of carbon nanodots from pollutants and applications to bioimaging. Chemical Science. 2021;12(35):11722-9.
108. Zhang J, Li X, Huang L. Anticancer activities of phytoconstituents and their liposomal targeting strategies against tumor cells and the microenvironment. Advanced Drug Delivery Reviews. 2020;154-155:245-73.

109. Milenković M, Mišović A, Jovanović D, Popović Bijelić A, Ciasca G, Romanò S, et al. Facile Synthesis of L-Cysteine Functionalized Graphene Quantum Dots as a Bioimaging and Photosensitive Agent. Nanomaterials. 2021;11(8):1879.
110. Liu R, Wu D, Liu S, Koynov K, Knoll W, Li Q. An Aqueous Route to Multicolor Photoluminescent Carbon Dots Using Silica Spheres as Carriers. Angewandte Chemie. 2009;121(25):4668-71.
111. Zhu S, Zhang J, Qiao C, Tang S, Li Y, Yuan W, et al. Strongly green-photoluminescent graphene quantum dots for bioimaging applications. Chemical Communications. 2011;47(24):6858.
112. Tang J, Kong B, Wu H, Xu M, Wang Y, Wang Y, et al. Carbon Nanodots Featuring Efficient FRET for Real-Time Monitoring of Drug Delivery and Two-Photon Imaging. Advanced Materials. 2013;25(45):6569-74.
113. Bhunia SK, Saha A, Maity AR, Ray SC, Jana NR. Carbon Nanoparticle-based Fluorescent Bioimaging Probes. Scientific Reports. 2013;3.(1)
114. Choi Y, Kim S, Choi MH, Ryoo SR, Park J, Min DH, et al. Highly Biocompatible Carbon Nanodots for Simultaneous Bioimaging and Targeted Photodynamic Therapy In Vitro and In Vivo. Advanced Functional Materials. 2014;24(37):5781-9.
115. Kang Y-F, Fang Y-W, Li Y-H, Li W, Yin X-B. Nucleus-staining with biomolecule-mimicking nitrogen-doped carbon dots prepared by a fast neutralization heat strategy. Chemical Communications. 2015;51.16956-9:(95)
116. Baker SN, Baker GA. Luminescent Carbon Nanodots: Emergent Nanolights. Angewandte Chemie International Edition. 2010;49(38):6726-44.
117. Song Y, Shi W, Chen W, Li X, Ma H. Fluorescent carbon nanodots conjugated with folic acid for distinguishing folate-receptor-positive cancer cells from normal cells. Journal of Materials Chemistry. 2012;22(25):12568.
118. Lai C-W, Hsiao Y-H, Peng Y-K, Chou P-T. Facile synthesis of highly emissive carbon dots from pyrolysis of glycerol; gram scale production of carbon dots/mSiO2 for cell imaging and drug release. Journal of Materials Chemistry. 2012;22(29):14403.
119. Liu C, Zhang P, Zhai X, Tian F, Li W, Yang J, et al. Nano-carrier for gene delivery and bioimaging based on carbon dots with PEI-passivation enhanced fluorescence. Biomaterials. 2012;33(13):3604-13.

120. Li J, Cai C, Li J, Li J, Li J, Sun T, et al. Chitosan-Based Nanomaterials for Drug Delivery. Molecules. 2018;23(10):2661.
121. Wang H, Di J, Sun Y, Fu J, Wei Z, Matsui H, et al. Biocompatible PEG-Chitosan@Carbon Dots Hybrid Nanogels for Two-Photon Fluorescence Imaging, Near-Infrared Light/pH Dual-Responsive Drug Carrier, and Synergistic Therapy. Advanced Functional Materials. 2015;25(34):5537-47.
122. Ray SC, Saha A, Jana NR, Sarkar R. Fluorescent Carbon Nanoparticles: Synthesis, Characterization, and Bioimaging Application. The Journal of Physical Chemistry C. 2009;113(43):18546-51.
123. Yang S-T, Cao L, Luo PG, Lu F, Wang X, Wang H, et al. Carbon Dots for Optical Imaging in Vivo. Journal of the American Chemical Society. 2009;131(32):11308-9.
124. Yang S-T, Wang X, Wang H, Lu F, Luo PG, Cao L, et al. Carbon Dots as Nontoxic and High-Performance Fluorescence Imaging Agents. The Journal of Physical Chemistry C. 2009;113(42):18110-4.
125. Zhao Q-L, Zhang Z-L, Huang B-H, Peng J, Zhang M, Pang D-W. Facile preparation of low cytotoxicity fluorescent carbon nanocrystals by electrooxidation of graphite. Chemical Communications. 2008(41):5116.
126. Zheng M, Ruan S, Liu S, Sun T, Qu D, Zhao H, et al. Self-Targeting Fluorescent Carbon Dots for Diagnosis of Brain Cancer Cells. ACS Nano. 2015;9(11):11455-61.
127. Tong X, Ma Y, Li Y. Biomass into chemicals: Conversion of sugars to furan derivatives by catalytic processes. Applied Catalysis A: General. 2011-:(1-2)385;0 .13
128. Su Y, Wang T, Su Y, Li M, Zhou J, Zhang W, et al. A neutrophil membrane-functionalized black phosphorus riding inflammatory signal for positive feedback and multimode cancer therapy. Materials Horizons. 2020;7(2):574-85.
129. Tang L, Li J, Pan T, Yin Y, Mei Y, Xiao Q, et al. Versatile carbon nanoplatforms for cancer treatment and diagnosis: strategies, applications and future perspectives. Theranostics. 2022;12(5):2290-321.
130. Wang L, Gu D, Su Y, Ji D, Yang Y, Chen K, et al. Easy Synthesis and Characterization of Novel Carbon Dots Using the One-Pot Green Method for Cancer Therapy. Pharmaceutics. 2022;14.(11)

131. Havrdová M, Urbančič I, Tománková KB, Malina L, Poláková K, Štrancar J, et al. Intracellular Trafficking of Cationic Carbon Dots in Cancer Cell Lines MCF-7 and HeLa—Time Lapse Microscopy, Concentration-Dependent Uptake, Viability, DNA Damage, and Cell Cycle Profile. International Journal of Molecular Sciences. 2022;23.(3)
132. Bayda S, Amadio E, Cailotto S, Frión-Herrera Y, Perosa A, Rizzolio F. Carbon dots for cancer nanomedicine: a bright future. Nanoscale Advances. 2021;3(18):5183-221.
133. He H, Zheng X, Liu S, Zheng M, Xie Z, Wang Y, et al. Diketopyrrolopyrrole-based carbon dots for photodynamic therapy. Nanoscale. 20.10991-8:(23)10;18
134. Li Y, Zheng X, Zhang X, Liu S, Pei Q, Zheng M, et al. Porphyrin-Based Carbon Dots for Photodynamic Therapy of Hepatoma. Advanced Healthcare Materials. 2016;6.(1)
135. Li C-L, Ou C-M, Huang C-C, Wu W-C, Chen Y-P, Lin T-E, et al. Carbon dots prepared from ginger exhibiting efficient inhibition of human hepatocellular carcinoma cells. Journal of Materials Chemistry B. 2014;2(28):4564.
136. Zheng M, Li Y, Liu S, Wang W, Xie Z, Jing X. One-Pot To Synthesize Multifunctional Carbon Dots for Near Infrared Fluorescence Imaging and Photothermal Cancer Therapy. ACS Applied Materials & Interfaces. 2016;8(36):23533-41.
137. Nurunnabi M, Khatun Z, Reeck GR, Lee DY, Lee Y-k. Photoluminescent Graphene Nanoparticles for Cancer Phototherapy and Imaging. ACS Applied Materials & Interfaces. 2014;6(15):12413-21.
138. Bao X, Yuan Y, Chen J, Zhang B, Li D, Zhou D, et al. In vivo theranostics with near-infrared-emitting carbon dots—highly efficient photothermal therapy based on passive targeting after intravenous administration. Light: Science & Applications. 2018;7.(1)
139. Papaioannou N, Marinovic A, Yoshizawa N, Goode AE, Fay M, Khlobystov A, et al. Structure and solvents effects on the optical properties of sugar-derived carbon nanodots. Scientific Reports. 2018;8.(1)
140. Piasek A, Pulit-Prociak J, Zielina M, Banach M. Fluorescence of D-Glucose-Derived Carbon Dots: Effect of Process Parameters. Journal of Fluorescence. 2023.

141. Hill S, Galan MC. Fluorescent carbon dots from mono- and polysaccharides: synthesis, properties and applications. Beilstein Journal of Organic Chemistry. 2017;13:675-93.
142. Qu D, Zheng M, Zhang L, Zhao H, Xie Z, Jing X, et al. Formation mechanism and optimization of highly luminescent N-doped graphene quantum dots. Scientific Reports. 2014;4.(1)
143. Moon BJ, Oh Y, Shin DH, Kim SJ, Lee SH, Kim T-W, et al. Facile and Purification-Free Synthesis of Nitrogenated Amphiphilic Graphitic Carbon Dots. Chemistry of Materials. 2016;28(5):1481-8.
144. Tang L, Ji R, Cao X, Lin J, Jiang H, Li X, et al. Deep Ultraviolet Photoluminescence of Water-Soluble Self-Passivated Graphene Quantum Dots. ACS Nano. 2012;6(6):5102-10.
145. Fois L, Stagi L, Carboni D, Alboushi M, Khaleel A, Anedda R, et al. The Formation of Carbon Dots from D-Glucose Studied by Infrared Spectroscopy. Chemistry – A European Journal. 2024.
146. Yoshinaga T, Iso Y, Isobe T. Particulate, Structural, and Optical Properties of D-Glucose-Derived Carbon Dots Synthesized by Microwave-Assisted Hydrothermal Treatment. ECS Journal of Solid State Science and Technology. 2017;7(1):R3034-R9.
147. Yang Z-C, Wang M, Yong AM, Wong SY, Zhang X-H, Tan H, et al. Intrinsically fluorescent carbon dots with tunable emission derived from hydrothermal treatment of glucose in the presence of monopotassium phosphate. Chemical Communications. 2011;47(42):11615.
148. Berezin MY, Achilefu S. Fluorescence Lifetime Measurements and Biological Imaging. Chemical Reviews. 2010;110(5):2641-84.
149. Wang F, Hao Q, Zhang Y, Xu Y, Lei W. Fluorescence quenchometric method for determination of ferric ion using boron-doped carbon dots. Microchimica Acta. 2015;183(1):273-9.
150. Xu Y, Yan L, Yue M, Yu Y. Green Hydrothermal Synthesis of Fluorescent Carbon Dots from Glucose and Taurine for Fe3+ and pH Sensing. Nano. 2019;14(01):1950014.
151. Ajmal M, Yunus U, Matin A, Haq NU. Synthesis, characterization and in vitro evaluation of methotrexate conjugated fluorescent carbon nanoparticles as drug

delivery system for human lung cancer targeting. Journal of Photochemistry and Photobiology B: Biology. 2015;153:111-20.

152. Gottesman MM, Fojo T, Bates SE. Multidrug resistance in cancer: role of ATP–dependent transporters. Nature Reviews Cancer. 2002;2(1):48-58.
153. Kapitonov AN, Egorova MN, Tomskaya AE, Smagulova SA, Alekseev AA. Hydrothermal synthesis of carbon dots and their luminescence. 2018.
154. Weinberger C, Haffer S, Wagner T, Tiemann M. Fructose as a Precursor for Mesoporous Carbon: Straightforward Solvent-Free Synthesis by Nanocasting. The Science and Function of Nanomaterials: From Synthesis to Application. ACS Symposium Series2014. p. 3-12.
155. Gvozdev DA, Nesterova VV, Lukashev EP, Tsoraev GV, Maksimov EG. Hydrothermal synthesis of carbon nanodots from sucrose and sodium citrate: repeatability of structural and spectral properties. Journal of Nanoparticle Research. 2025;27.(5)
156. Zheng J-x, Liu X-h, Yang Y-z, Liu X-g, Xu B-s. Rapid and green synthesis of fluorescent carbon dots from starch for white light-emitting diodes. New Carbon Materials. 2018;33.276-88:(3)
157. Marpongahtun, Gea S, Muis Y, Andriayani, Novita T, Piliang AF. Synthesis of Carbon Nanodots from Cellulose Nanocrystals Oil Palm Empty Fruit by Pyrolysis Method. Journal of Physics: Conference Series. 2018;1120.
158. Riss TL, Moravec RA, Niles AL, Duellman S, Benink HA, Worzella TJ, et al. Cell Viability Assays. In: Markossian S, Grossman A, Baskir H, Arkin M, Auld D, Austin C, et al., editors. Assay Guidance Manual. Bethesda (MD)2004.
159. Ray PC, Yu H, Fu PP. Toxicity and Environmental Risks of Nanomaterials: Challenges and Future Needs. Journal of Environmental Science and Health, Part C. 2009;27(1):1-35.
160. Sawalha S, Abdallah S, Barham A, Badawi H, Barham Z, Ghareeb A, et al. Green synthesis of fluorescent carbon nanodots from sage leaves for selective anticancer activity on 2D liver cancer cells and 3D multicellular tumor spheroids. Nanoscale Advances. 2023;5(21):5974-82.
161. Zhu C, Zhai J, Dong S. Bifunctional fluorescent carbon nanodots: green synthesis via soy milk and application as metal-free electrocatalysts for oxygen reduction. Chemical Communications. 2012;48.(75)

162. Chatzimitakos TG, Kasouni AI, Troganis AN, Stalikas CD. Carbonization of Human Fingernails: Toward the Sustainable Production of Multifunctional Nitrogen and Sulfur Codoped Carbon Nanodots with Highly Luminescent Probing and Cell Proliferative/Migration Properties. ACS Applied Materials & Interfaces. 2018;10(18):16024-32.
163. Fan R-J, Sun Q, Zhang L, Zhang Y, Lu A-H. Photoluminescent carbon dots directly derived from polyethylene glycol and their application for cellular imaging. Carbon. 2014;71:87-93.
164. Cao L, Zan M, Chen F, Kou X, Liu Y, Wang P, et al. Formation mechanism of carbon dots: From chemical structures to fluorescent behaviors. Carbon. 2022.194:42-51;
165. Li CH, Li RS, Li CM, Huang CZ, Zhen SJ. Precise ricin A-chain delivery by Golgi-targeting carbon dots. Chemical communications. 2019;55(45):6437-40.
166. Zhou N, Zhu S, Maharjan S, Hao Z, Song Y, Zhao X, et al. Elucidating the endocytosis, intracellular trafficking, and exocytosis of carbon dots in neural cells. RSC Advances. 2014;4(107):62086-95.
167. Sawalha S, Abdallah S, Barham A, Badawi H, Barham Z, Ghareeb A, et al. Green synthesis of fluorescent carbon nanodots from sage leaves for selective anticancer activity on 2D liver cancer cells and 3D multicellular tumor spheroids. Nanoscale Advances. 2023;5(21):5974-82.
168. Alibert C, Goud B, Manneville JB. Are cancer cells really softer than normal cells? Biology of the Cell. 2017;109.167-89:(5)
169. Assali M, Almasri M, Kittana N, Alsouqi D. Covalent functionalization of graphene sheets with different moieties and their effects on biological activities. ACS Biomaterials Science & Engineering. 2019;6(1):112-21.
170. Forman HJ, Maiorino M, Ursini F. Signaling functions of reactive oxygen species. Biochemistry. 2010;49(5):835-42.
171. Lam P-L, Wong R-M, Lam K-H, Hung L-K, Wong M-M, Yung L-H, et al. The role of reactive oxygen species in the biological activity of antimicrobial agents: An updated mini review. Chemico-Biological Interactions. 2020;320:109023.
172. Belovolova LV. Reactive oxygen species in aqueous media (a review). Optics and Spectroscopy. 2020;128:932-51.
173. Yang H, Villani RM, Wang H, Simpson MJ, Roberts MS, Tang M, et al. The role of cellular reactive oxygen species in cancer chemotherapy. Journal of Experimental & Clinical Cancer Research. 2018;37:1-10.

174. Nakamura H, Takada K. Reactive oxygen species in cancer: Current findings and future directions. Cancer Sci. 2021.3945-52:(10)112;
175. Huang R, Chen H, Liang J, Li Y, Yang J, Luo C, et al. Dual Role of Reactive Oxygen Species and their Application in Cancer Therapy. J Cancer. 2021;12(18):5543-61.
176. Kim SJ, Kim HS, Seo YR. Understanding of ROS-Inducing Strategy in Anticancer Therapy. Oxid Med Cell Longev. 2019;2019:5381692.
177. Starkov AA. The role of mitochondria in reactive oxygen species metabolism and signaling. Annals of the New York Academy of Sciences. 2008;1147(1):37-52.
178. Balaban RS, Nemoto S, Finkel T. Mitochondria, oxidants, and aging. cell. 2005;120(4):483-95.
179. Bystrom LM, Guzman ML, Rivella S. Iron and reactive oxygen species: friends or foes of cancer cells? Antioxidants & redox signaling. 2014;20(12):1917-24.
180. Liberti MV, Locasale JW. The Warburg Effect: How Does it Benefit Cancer Cells? Trends Biochem Sci. 2016;41(3):211-8.
181. Mao X, Liu K, Shen S, Meng L, Chen S. Ferroptosis, a new form of cell death: mechanisms, biology and role in gynecological malignant tumor. Am J Cancer Res. 202.2751-62:(7)13;3
182. Dixon SJ, Lemberg KM, Lamprecht MR, Skouta R, Zaitsev EM, Gleason CE, et al. Ferroptosis: an iron-dependent form of nonapoptotic cell death. cell. 2012;149 (5):1060-72.
183. Yao X, Li W, Fang D, Xiao C, Wu X, Li M, et al. Emerging roles of energy metabolism in ferroptosis regulation of tumor cells. Advanced Science. 2021;8 (22):2100997.
184. Xiong Y, Xiao C, Li Z, Yang X. Engineering nanomedicine for glutathione depletion-augmented cancer therapy. Chemical Society Reviews. 2021;50.6013-41:(10)
185. Zheng J, Conrad M. The metabolic underpinnings of ferroptosis. Cell metabolism. 2020;32(6):920-37.
186. Muri J, Kopf M. Redox regulation of immunometabolism. Nature Reviews Immunology. 2021;21(6):363-81.
187. Demuynck R, Efimova I, Naessens F, Krysko DV. Immunogenic ferroptosis and where to find it? Journal for Immunotherapy of Cancer. 2021;9.(12)
188. Zhang R, Kang R, Tang D. The STING1 network regulates autophagy and cell death. Signal transduction and targeted therapy. 2021;6(1):208.

189. Yao L, Zhao M-M, Luo Q-W, Zhang Y-C, Liu T-T, Yang Z, et al. Carbon quantum dots-based nanozyme from coffee induces cancer cell ferroptosis to activate antitumor immunity. ACS nano. 2022;16(6):9228-39.

جـامعـــة النجاح الوطنية

كليـــة الدراســـات العليـــا

تصنيع نقاط الكربون النانونية من أنواع مختلفة من السكريات للتطبيقات الطبية الحيوية

إعداد

سماح غازي قاسم

إشراف

د. محي الدين العسالي

د. شادي صوالحه

قدمت هذه الرسالة استكمالا لمتطلبات الحصول على درجة الماجستير في العلوم الصيدلانية، من كلية الدراسات العليا، في جامعة النجاح الوطنية، نابلس– فلسطين.

2025

تصنيع نقاط الكربون النانونية من أنواع مختلفة من السكريات للتطبيقات الطبية الحيوية

إعداد

سماح غازي قاسم

إشراف

د. محي الدين العسالي

د. شادي صوالحه

الملخص

يُعتبر السرطان ثاني أبرز سبب للوفاة عالميًا، مما يدفع العلماء إلى استكشاف طرق علاجية مختلفة مثل الجراحة، والعلاج الإشعاعي، والعلاج الكيميائي، والعلاج الجيني. ونظرًا للآثار الجانبية الكبيرة للعلاجات التقليدية، هناك طلب متزايد على العلاجات البديلة. في الآونة الأخيرة، لجأت الأبحاث الطبية إلى تقنيات النانوتكنولوجيا، لا سيما الجسيمات النانوية التي يتراوح حجمها بين 1–100 نانومتر، لتطوير علاجات جديدة للسرطان. وتبرز النقاط النانوية الكربونية نظرًا لخصائصها الفريدة الفيزيائية والكيميائية والكهربائية والميكانيكية والبصرية، مما يجعلها خيارًا واعدًا في علاج السرطان.

يهدف هذا المشروع إلى استخدام طريقة حرارية مائية خضراء وبسيطة كنهج تصنيعي من الأسفل إلى الأعلى لإنتاج النقاط النانوية الكربونية من أنواع مختلفة من السكريات (الجلوكوز، والجالاكتوز، والفركتوز، والسكروز، واللاكتوز، والمالتوز). يتم تحقيق عملية التخليق عن طريق كربنة السكريات داخل الأوتوكلاف (الفرن) عند درجة حرارة 200 درجة مئوية لمدة 24 ساعة.

تمت دراسة خصائص النقاط النانوية الكربونية باستخدام تقنيات مختلفة، بما في ذلك المجهر القوة الذرية (AFM)، مطيافية الأشعة تحت الحمراء بتحويل فورييه(FT–IR) ، مطيافية فوتوإلكترون الأشعة السينية (XPS)، مطيافية الامتصاص للأشعة فوق البنفسجية–المرئية(UV–Vis) ، ومطيافية التألق. أكدت نتائج التوصيف أن النقاط النانوية الكربونية قابلة للذوبان في الماء، وتتميز بحجم صغير جدًا وخصائص مضيئة.

وفقًا للنتائج، يبلغ متوسط حجم الجسيمات (4.8) نانومتر، بمتوسط كفاءة كمومية 2.35٪، ومتوسط نسبة الإنتاج (15٪)، كما أنها قابلة للذوبان في الماء مع متوسط جهد زيتا يبلغ −24.08 مللي فولت.

نتيجة لذلك، تم تعريض النقاط النانوية الكربونية المحضرة إلى نوعين من خطوط الخلايا: خلايا سرطان الكبد والخلايا الطبيعية وأظهرت النتائج نشاطًا مضادًا للسرطان ضد خلايا سرطان الكبد ، بينما لم تتأثر الخلايا الطبيعية ويرجع التفسير الداعم للنشاط المضاد للسرطان إلى تكوين أنواع الأكسجين التفاعلية، مما يشير إلى خصوصية النقاط النانوية الكربونية ضد الخلايا غير الطبيعية فقط.

الكلمات المفتاحية: نقاط الكربون النانوية(CNDs) ، سرطان الكبد (سرطان الخلايا الكبدية)، الجسيمات النانوية، الكربوهيدرات.